UNIVERSITY OF CALIFORNIA
SANTA CRUZ

MACROECONOMIC RESEARCH WITH INNOVATIVE METHODS

A dissertation submitted in partial satisfaction of the
requirements for the degree of

DOCTOR OF PHILOSOPHY

in

ECONOMICS

by

Ziyu He

March 2021

The Dissertation of Ziyu He
is approved:

Carl Walsh, Chair

Professor Kenneth Kletzer

Professor Hikaru Saijo

Quentin Williams
Interim Vice Provost and Dean of Graduate Studies

Table of Contents

List of Figures

List of Tables

Abstract

Macroeconomic Research with Innovative Methods

by

Ziyu He

This dissertation uses innovative methods to study different perspectives of macroeconomics. In particular, topics in this dissertation including macroeconomic modeling, computational technics, and empirical analysis.

In the first chapter, I propose a numerical routine to approximate the radius of convergence (ROC) for perturbation methods. The classical issue of solving dynamic stochastic models with perturbation methods is that the solution only converges (to the true solution) locally over the state space. Moreover, such a convergence range is usually undetectable under current existing numerical methods. The proposed algorithm, in the limit, can approximate this range both necessarily and sufficiently. It resolves the difficulty of assessing the appropriateness of perturbation solutions. This chapter makes two types of contributions. First, method-wise, the proposed algorithm is the first numerical routine on approximating the ROC of perturbation solutions. In addition, as shown in this chapter, the approximated ROC converges to the true value (no matter if it is analytically obtainable or not) as the order of the approximation increases. Second, modeling-wise, this algorithm provides two main insights on the real business cycle (RBC) model: (i) the perturbation method is capable of solving the standard RBC model; the ROC is large enough to cover most commonly used calibrations; (ii) models with recursive utility or stochastic volatility can not be solved appropriately by the perturbation method as the standard calibration for TFP volatility exceeds the ROC of value function on this dimension.

In the second chapter, I try to shed light on the frontier research discussions around

declining trends in business dynamism using a general equilibrium model structure with heterogeneous individuals. The key mechanism of the framework is the strategic technological innovation process of firms in response to an individual's wealth holding and lifetime value of being in different occupations. Such an endogenous TFP process accompanies by wealth inequality reflects a firm's relative technological position among other producers. The resulting "winner takes all" dynamics help the model jointly account for several observed empirical trends of the U.S. economy. To accomplish this analysis, I adept a two-stage approach in my structural model. In the first stage, I run a comparative analysis to numerically show that multiple structural shocks are unnecessary to create stylized facts of declining business dynamism. As a consequence, for the second stage, I introduce the "winner takes all" dynamics to the model and provide intuitions on the mechanism. I try to use both stages to emphasize the key role of the interactions between wealth inequality and firm-specific productivity growth in explaining the DBD facts during transitional dynamics.

In the third chapter, I investigate whether the series of President Trump's tweets had any effect on the stock market. In order to accomplish this, I divide this project into two separate parts. For the first part, I collect all president Donald Trump's tweets from his Twitter database. I then run sentiment analysis on those tweets which contain content related to a particular company that is in the S&P 500 index. For the other part, I create a new routine for obtaining the abnormal daily return of stock indexes by time series forecasting. Combining both parts together, I test the main hypothesis that a tweet from President Donald Trump will significantly affect the stock price of the mentioned company. This chapter suggests only tweets with positive sentiment have significant effects on stock price movement. Moreover, such an effect only lasts for about one trading day.

To myself,

Ziyu He,

my lovely wife, Jingwen

and my dog, Newton

Acknowledgments

The five years' Ph.D. study is an incredible journey for me. It shapes me from a young master's student who had almost nothing but the courage to move forward to a more mature young man ready to conquer tough challenges in the real world. Throughout this journey, I could not survive without helps from a group of people.

Foremost, I would like to express my sincere gratitude to my advisor Prof. Carl Walsh for the continuous support of my Ph.D. study and research, for his patience, motivation, enthusiasm, and immense knowledge. His guidance helped me in all the time of research and writing of this dissertation. I could not have imagined having a better advisor and mentor for my Ph.D. study.

Besides my advisor, I would like to thank the rest of my reading committee: Prof. Kenneth Kletzer, Prof. Hikaru Saijo, for their encouragement, insightful comments, and challenging questions.

My sincere thanks also go to Dr. Eric Aldrich for all of your inspirations, encouragements, and passions to keep pursuing career goals. Prof. Yongyang Cai, for your valuable suggestions on my research and all the other resources you brought to me. Prof. Kenneth Judd, for all of your generous help and offering me the RAship opportunities in your groups, and leading me to work on diverse, exciting projects.

I want to thank all other professors in the department for providing me with fruitful knowledge in economics and give great feedback on my works. I want to thank our program coordinator Sandra, who has always been there and providing all possible help she can. I want to thank my cohorts, who are pursuing the same goals together with me. I will miss the difficulties we face together, as well as the happiness we share.

Finally, I would like to thank my wife for supporting me on this journey and offering me spiritual aid throughout my life.

I hope this dissertation could be a good summary report for all people mentioned above and also myself.

Chapter 1

Approximating the Radius of Convergence of Dynamic Stochastic Models

1.1 Introduction

The complexity and dimensionality of dynamic stochastic general equilibrium (DSGE) models make them difficult and time-intensive to solve. Except for some special cases that yield analytical solutions, DSGE models are usually solved by two subcategories of numerical methods: global methods and local methods (see Table 1.1). The current "state of arts" of computational economics makes balancing the tradeoff between numerical accuracy and computational cost of a solution method very important. However, such a comparison is only relevant to the extent that (1) a global method can be obtained with much lower cost and (2) a local method is appropriate for the region under consideration. The classical way of addressing the first issue includes numerical tools innovation and computational power improvement. In comparison, the

second issue has not even been touched yet by the literature. Filling this gap is the primary motivation of this paper.

To make the exposition simpler, this paper treats the perturbation method and projection method as two representative examples of local and global solution methods, respectively. Briefly speaking, in economics, projection methods proposed by Judd (1992) and Gaspar and Judd (1997) are globally convergent for the entire domain of the approximated function. However, such solutions may be computationally demanding and even infeasible for nonlinear functions of many state variables. Perturbation methods suggested by Judd and Guu (1993), a Taylor expansion around the deterministic steady state of the original model typically requires far less computations but are only convergent for a certain domain of the state space around the point of approximation. This domain is known as the *radius of convergence* or *range of convergence* (ROC) and is determined by the objective function, deep parameters, and the point of approximation.

Table 1.1: Numerical methods for solving DSGE model

<table>
<tr><td colspan="2">Linear solution</td><td colspan="4">Non-linear solution</td></tr>
<tr><td colspan="2">Local method</td><td colspan="4">Global method</td></tr>
<tr><td colspan="2">Perturbation</td><td rowspan="2">Projection</td><td>Dynamic</td><td>Simulation</td><td>Certainty</td></tr>
<tr><td>Log-linearization</td><td>VF perturbation</td><td>Programming</td><td>Approach</td><td>Equivalence</td></tr>
<tr><td>1st Order</td><td>Optimal</td><td>Smolyak's Algorithm</td><td>VFI</td><td>GSSA</td><td rowspan="2">NLCEQ</td></tr>
<tr><td>Perturbation</td><td>change of variables</td><td>Chebyshev polynomial</td><td>PFI, FPI</td><td>EDS</td></tr>
<tr><td colspan="6">Hybrid Algorithm (e.g., Taylor projection)</td></tr>
</table>

For most current quantitive economic studies, the perturbation method is still extensively used for model solving and structural estimation purposes, despite having little knowledge of its localness and the desirable global properties of the projection solution. There are several

reasons for this. First and foremost, higher-order perturbation solutions often produce analytical approximations that reveal the essential dependence of the exact solution on model parameters in a manner that is clearer than other numerical methods, assisting in economic interpretation and model sensitivity analysis. For example, Collard and Juillard (2001) document that perturbation captures the distribution of shocks (e.g., skewness and kurtosis) more precisely than Chebychev polynomials in the asset pricing model of Burnside (1998). Second, as Aruoba et al. (2006) pointed out, perturbation strikes an excellent balance between computational cost and numerical accuracy relative to other numerical methods. More recently, Caldara et al. (2012) claimed that solving complex DSGE models with recursive preferences and stochastic volatility is computationally challenging, and perturbation is the only feasible approach with a reasonable computational burden. Moreover, the performance and versatility of the perturbation method have been improved a lot by later works[1]. Third, recent progress on the global method such as Smolyak's Algorithm and NLCEQ method is not satisfactory enough for competing with the perturbation method in terms of the implementability[2]. Fourth, the current way of detecting the appropriateness of the perturbation method is costly and *ex-post*, as it has to rely on the case study and cross validation comparison with the global solution on numerical errors. Stylized papers on this topic including, Swanson et al. (2006) and Swanson (2012), emphasize that in some circumstances, a high-order perturbation solution exhibits excellent global accuracy. Petrosky-Nadeau and Zhang (2017) shown that the perturbation method can produce severe Euler equation errors when solving the Diamond–Mortensen–Pissarides model. Similarly, Schumacher and Nikolai Graber (2019) argues that the perturbation-based solution method does not suffice whenever

[1]For improving the performance and versatility of perturbation method, see Judd (2003), Fernández-Villaverde and Rubio-Ramírez (2006) for change of variables, and Van Binsbergen et al. (2012) and Caldara et al. (2012) for value function perturbation.

[2]For example, the Smolyak's Algorithm developed by Judd et al. (2014) largely mitigates the computational cost of the projection method by reducing the total number of grids used for the approximation step. However, it's less efficient in terms of coding and can not be parallelized. The NLCEQ methods developed by Cai et al. (2017) can solve models with 400 state variables with no pressure. However, this method is a deterministic transformation of the original model and has only 2 or 3 digit accuracy for stochastic problems and cannot solve risky portfolio optimization or stochastic problems with recursive preferences.

the economy is exposed to risks with long-lasting effects, etc.

To sum up, in the current literature, verifying the appropriateness of perturbation solutions is computationally costly and case by case. There is no general and *ex-ante* numerical method for addressing this issue. As a result, knowing the theoretical limitation of the perturbation method does not contribute a lot to current economic research. For resolving such a difficulty, this paper deviates from the above mentioned classical wisdom and step back to the fundamentals of the perturbation method and the origin of its localness: the Taylor theorem and the *radius of convergence*.

In functional analysis, the Taylor expansion of a function is only valid within a local region around the point of expansion (inside of the ROC), regardless of the exact order of this approximation. The derivatives of the underlying function determine the size of the region at the point of approximation. Though the radius of convergence can be infinite in some cases, it is usually finite, with a magnitude that diminishes with curvature (non-linearity) and continuity of the underlying function. For economic models, as perturbation methods are Taylor expansions around the deterministic steady state, there is no guarantee they will provide an adequate approximation away from the fixed point (i.e., outside the ROC) of the unknown objective function, *even if they can be computed to an arbitrary high order*. Further, the inability to approximate the objective function over the *entire domain* is compounded, as perturbation solutions can only be computed to finite order in nearly all practical applications. As a consequence, the radius of convergence (to the extent that it is known) is the primary device for assessing the localness of a perturbation solution.

There are two approaches (described below) to analytically derive the ROC of a Taylor polynomial, both of which involve an infinite number of derivatives of the objective function. Unfortunately, in economic applications, such methods are impractical as the objective function (e.g., the policy function or value function) is usually unknown and, at best, its derivatives

can only be obtained up to a finite order. Historically, economists have resorted to *ex-post* evaluations for the appropriateness of their local solutions via Euler equation errors (Judd, 1992) (or χ^2 test (Den Haan and Marcet, 1994)) compared with global solutions. Nevertheless, in contrast with the projection method, where Euler equation errors provide a necessary and sufficient condition for their accuracy[3]. A small Euler equation error is only a necessary but not sufficient criteria for ensuring the appropriateness of perturbation solutions, as commented by Judd (1996). Until now, the ROCs for most DSGE models are unknown and even inaccessible for economists (Fernández-Villaverde et al., 2016).

In this paper, I develop a numerical routine on approximating the radius of convergence of an unknown objective function using only the coefficients of its finite perturbation solution. Given these Taylor coefficients and their corresponding orders in a polynomial approximation, the ROC can be approximated from a 2-stage optimization problem. Although, in practice, such a solution is simply an approximation of the ROC (as we only have finite order Taylor polynomial). It can be shown theoretically that, *in limit*, the optimized solution always results in a conservative convergent approximation. This algorithm has several desirable features: (i) theoretically, it provides a necessary and sufficient condition for characterizing the appropriateness of a perturbation solution (in the limit); (ii) the approximated ROC value is guaranteed to converge to the true ROC without knowing its value; (iii) there is relatively zero additional cost to implement this method once the perturbation solution is obtained; (iv) it preserves the dependency of the perturbation solution on the objective function, deep parameters, and the point of approximation; and (v) it is compatible with any existing routine on solving DSGE models with perturbation method.

I will now expand on the points above. First, the primary methodological contribution of this paper is a numerical algorithm for approximating the ROC with a finite-order perturbation

[3]The projection methods are basically solving for the minimization problem of global errors.

solution. Thus far, economists have typically assumed their perturbation solution is convergent in a small neighborhood of the deterministic steady state but have not rigorously determined how "*small*" the neighborhood should be. In most instances, researchers indirectly address this issue through using Euler equation errors, suggesting a solution is acceptable if the deviation between the model and the solution is small enough over a particular range. However, without knowing the ROC of the model, a small Euler equation error is *not sufficient* for a numerical solution to be highly reliable; similarly, a large Euler equation error is *not sufficient* to reject a valid solution. For example, we should accept a k-th order perturbation solution with acceptably small EEEs over some regions. However, without knowing the ROC, it is still possible for the EEEs of a $(k+1)$-th order perturbation solution to deteriorate in the same regions. Whenever this happens, it actually suggests the k-th order perturbation solution is numerically accurate but mathematically inappropriate, and the small EEEs is nothing but a coincidence. Alternatively, a linear perturbation solution may usually have large EEEs for dynamics far away from the point of approximation. However, it is not sufficient to reject this solution without knowing the ROC, because as long as the dynamics approximated by this solution is inside ROC, it is 100 percent capturing the first order effect of the original system. Hence it at least good enough for research that is targeting on the linearized economy. Overall, there is no guarantee on the appropriateness of the perturbation solution without knowing its necessary and sufficient answer: the *radius of convergence*.

Second, this algorithm is a direct transformation of d'Alembert's ratio test, hence guaranteeing that the approximated ROC will converge to the true ROC. In fact, I prove that the approximated ROC obtained by solving the 2-stage optimization problem is converging to its theoretical values as the order of perturbation solution increases. Additionally, from the applications of this paper, I also find the convergence rate is relatively faster when the order of perturbation solution is low. This feature makes the algorithm being even more useful for

various economic studies.

Third, computing Euler equation errors can be costly, as it requires simulation and numerical integration over the state space. In contrast, the proposed method only requires the optimal affine function fitting on the perturbation coefficients set, hence demanding essentially no additional computational cost as long as the perturbation solution is obtained.

Fourth, as Santos (2000) documents, changes in the curvature of the utility function and depreciation rate have an important influence on the localness of perturbation solutions. In such a case, Euler equation error is no longer able to further studying the sensitivity of perturbation solutions under various parameterizations as it is a pure numerical measurement of accuracy that has no interpretative meaning. However, as the ROC approximation uses the perturbation coefficients, which preserve the essential dependence of the exact solution on model parameters, it has natural advantages to study the mathematical property of perturbation solution.

Lastly, this algorithm is compatible with any existing perturbation-based routine on solving DSGE models. Specifically, the algorithm requires input nothing more than the Kronecker coefficient matrices of the perturbation polynomial, and it is independent of the exact procedure of deriving these coefficients. This means the algorithm can be coupled with the output of any standard perturbation package (e.g., Dynare, Dynare++, perturbationAIM, etc.).

This paper demonstrates the usefulness of the proposed ROC approximation routine through a number of numerical applications. First, I approximate the radius of convergence for univariate functions with known ROC. These examples allow me to evaluate the convergence of approximated ROC when extremely high-order solutions are feasible. Moreover, I show that the algorithm can also deliver a numerical approximation in cases where the ROC cannot be analytically derived. Second, I apply this method to a real business cycle model and a sequence of its variants. I start with the neoclassical growth model with log utility and full capital depreciation, which admits closed-form solutions and known ROC. This model has low-

dimensional state space and allows for high-order perturbation solutions as well. Subsequently, I apply the ROC approximation method on the standard RBC model with constant relative risk aversion (CRRA) utility and partial depreciation. I find that given most commonly used calibrations, perturbation solutions of this model have pretty large ROCs. The associate implication is that the perturbation solution is actually globally valid. Finally, I test this method with an RBC variant that features Epstein-Zin-Weill preferences, as considered by Van Binsbergen et al. (2012), Caldara et al. (2012), and Aldrich and Kung (2011). Using standard calibrations from the asset pricing literature, I find the value function has a much smaller ROC than the canonical RBC model in the total factor of production (TFP) volatility dimension. Consequently, these results suggest that, regardless of Euler equation errors, the perturbation method is inappropriate for solving RBC models with recursive utility. Also, from this practice, by running a cross-validation check with χ^2 test, I show that the Euler equation error fails to accept a valid solution with reasonable parameterization.

The paper is organized as follows. Section 2 introduces the two-stage interpolation – log-absolute difference algorithm on ROC approximation and a detailed practice on univariate function with analytical ROC. Section 3 further applies the proposed algorithm into macroeconomic models both with known ROCs (the neoclassical growth model with log utility and full depreciation) and unknown ROCs (the standard RBC model). Section 4 extends applications to DSGE models with more complex features and unknown ROCs, such as recursive utility and stochastic volatility. Section 5 concludes, and additional material is provided in the Technical appendix.

1.2 Numerical approximation for ROC

This section introduces the numerical algorithm for approximating the radius of convergence of an unknown objective function using its finite-order Taylor expansion. Mathematically, the

radius of convergence of an objective function centered on a point c is equal to the distance from c to the nearest point in the complex plane, where the objective function cannot be defined in a way that makes it holomorphic. Two approaches, the d'Alembert's ratio test and the Cauchy-Hadamard theorem can be used to arrive at an analytical expression for the ROC at an arbitrary point in the domain of the objective function. Additionally, for specific points in the domain, the ROC can be computed using the complex-plane approach (see, e.g. Judd and Jin, 2002). However, knowing the theoretical ROC requires information about the objective function and all its derivatives associate with the point of expansion. Since these requirements are rarely practically feasible, a numerical algorithm that approximates the ROC with a finite-order perturbation solution is an important methodological contribution to the literature.

1.2.1 An equivalent numerical specification of the theoretical ROC

Given Banach spaces X and Y, suppose $F : X \to Y$ is analytical (i.e., majorant series converges) and a C^{k+1} function (continuously differentiable up to order $k+1$) at domain $\mathbb{C} \in \mathbb{R}$. The k-th order Taylor expansion of $F(x)$ at point $c \in \mathbb{C}$ is defined as

$$T_k^c(x) = \sum_{n=0}^{k} t_n^c (x-c)^n \tag{1.1}$$

where the Taylor coefficient is defined to be

$$t_n^c = \frac{F^{(n)}(c)}{n!}, \qquad \forall n \in \mathbb{N} \tag{1.2}$$

By Taylor's theorem, the radius of convergence, R^c, is the region such that for $x \in (c - R^c, c + R^c)$,

$$F(x) = \lim_{k\to\infty} T_k^c(x) = \sum_{n=0}^{\infty} t_n^c (x-c)^n \tag{1.3}$$

That is, an infinite-order Taylor polynomial at point c converges to the objective function *only on the region* $(c - R^c, c + R^c)$; convergence is not guaranteed on other parts of the domain, even with an infinite expansion. Notice that by definition, the Taylor coefficients, $\{t_n^c\}_{n=0}^{\infty}$, only

depending on the functional form of objective function $F(x)$, its parameters, and the point of expansion c.

Given an infinite Taylor expansion, d'Alembert's ratio test defines the radius of convergence around point c to be

$$R^c = \lim_{k\to\infty} \left| \frac{t_k^c}{t_{k+1}^c} \right|, \left|t_{k+1}^c\right| \neq 0 \text{ for } k \text{ large} \tag{1.4}$$

In special cases, Equation (1.4) results in an analytic expression for the radius of convergence. However, in most economic applications, such an expression does not exist nor is it feasible. To arrive at a numerical approximation, I rewrite this equation as

$$\frac{1}{R^c} = \lim_{k\to\infty} \left| \frac{t_{k+1}^c}{t_k^c} \right| \tag{1.5a}$$

$$\Leftrightarrow -\ln R^c = \lim_{k\to\infty} \left[\ln\left|t_{k+1}^c\right| - \ln\left|t_k^c\right|\right] \tag{1.5b}$$

$$\Leftrightarrow B^\infty = \lim_{k\to\infty} \left[\frac{\ln\left|t_{k+1}^c\right| - \ln\left|t_k^c\right|}{(k+1)-k} \right] \tag{1.5c}$$

Notice that Equation (1.5b) implies, as $k \to \infty$, the difference between $\ln|t_k^c|$ and $\ln\left|t_{k+1}^c\right|$ of the Taylor expansion is converging to a constant number, $-\ln R^c$. Moreover, Equation (1.5c) suggests that this constant $B^\infty = -\ln R^c$ can also be understood as the slope of the affine function lies in-between points $(k, \ln|t_k^c|)$ and $\left(k+1, \ln\left|t_{k+1}^c\right|\right)$. In such a plane, the exponent index n can be thought as the x coordinates and the associated magnitude of $\ln|t_n^c|$ stands for the y coordinates (see Section 1.2.4). Writing it down in an informative way, the following Equation (1.6) presents the numerical specification of ROC approximation using d'Alembert's ratio test as

$$B^\infty = -\ln R^c = \lim_{k\to\infty} \left[\frac{\ln\left|t_{k+1}^c\right| - \ln\left|t_k^c\right|}{(k+1)-k} \right] \tag{1.6}$$

Alternatively, Cauchy-Hadamard theorem also allows us to compute the radius of convergence analytically with the form,

$$R^c = \frac{1}{\limsup_{n\to\infty} \sqrt[n]{|t_n^c|}} \tag{1.7}$$

However, I find it is tough to translate Equation (1.7) into a specification that has numerical meaning. Hence the ROC approximation routine in this paper is simply build upon Equation (1.6).

As a remark of this part, comparing adjacent terms in the series is easier to implement numerically than the Cauchy-Hadamard expression. Therefore, the key numerical inference of this section is that using the coefficients of the Taylor polynomial from set $\{(n, t_n^c)\}_{n=0}^{\infty}$, the radius of convergence at point c can be exactly computed by either reaching the limit of the set $\left\{\left[\ln\left|t_{n+1}^c\right| - \ln|t_n^c|\right]\right\}_{n=0}^{\infty}$ following Equation (1.5b), or solving the limit slope term from the set $\{(n, \ln|t_n^c|)\}_{n=0}^{\infty}$ following Equation (1.5c). Specifically, for the slope approach, solution B^{∞} from Equation (1.6) is uniquely determines the radius of convergence as

$$B^{\infty} = -\ln R^c \Leftrightarrow R^c = \exp\left(-B^{\infty}\right) \tag{1.8}$$

Equation (1.8) holds with exact equality whenever an infinite set of Taylor coefficients is available.

Corollary 1. *Under the same assumptions, as the order of Taylor expansion $k \to \infty$, the solution of numerical specification Equation (1.5b) and Equation (1.5c), B^{∞}, deliver the equivalent result to the theoretical ROC value, R^c, that is defined by Equation (1.4).*

Proof. The prove of the equivalency is directly from Equation (1.5) and the unique mapping from B^{∞} to R^c is captured by Equation (1.8) . □

1.2.2 A finite approximation for the numerical ROC

In practice, an infinite-order Taylor expansion is rarely available for objective function $F(x)$. Instead, under the same assumptions stated in the previous section, a finite Taylor

approximation is defined as

$$F(x) \approx T_k^c(x) = \sum_{n=0}^{k} t_n^c (x-c)^n \tag{1.9}$$

where k is a finite positive integer. Analogous to the transformation in Section 1.2.1, we can define the finite approximation for Equation (1.6) as

$$-\ln \hat{R}^{c,k} = B^k = \left[\frac{\ln |t_k^c| - \ln \left| t_{k-1}^c \right|}{k-(k-1)} \right] = \left| \ln t_k^c \right| - \left| \ln t_{k-1}^c \right|, \quad k < \infty \tag{1.10}$$

Notice that this finite approximation is well defined as long as $k \geq 1$. Lemma 1 illustrates the asymptotic convergence properties of the finite approximation proposed above.

Lemma 1. *Given the finite set of Taylor coefficients $\{(n, t_n^c)\}_{n=0}^k$ of objective function $F(x)$, the slope B^k solves the finite approximation of the d'Alembert's ratio test (1.10), and its associated ROC approximation, $\hat{R}^{c,k}$, converge to the true radius of convergence as $k \to \infty$.*

Proof. The result can be immediately derived from equation (1.10) by taking the limit of k on both sides

$$\lim_{k\to\infty} -\ln \hat{R}^{c,k} = \lim_{k\to\infty} B^k = \lim_{k\to\infty} \left[\ln |t_k^c| - \ln \left| t_{k-1}^c \right| \right]$$

by equation (1.6) (set $k = k+1$), the RHS is equal to

$$\lim_{k\to\infty} \left[\ln |t_k^c| - \ln \left| t_{k-1}^c \right| \right] = -\ln R^c = B^\infty$$

Therefore, the solution B^k and its corresponding ROC approximation $\hat{R}_R^{c,k}$ solved from the finite approximation (1.10) is converging to the true solution B^∞ and R^c as $k \to \infty$ by Corollary 1. □

Notice that although Lemma 1 can ensures an asymptotic convergent approximation in limit, there is no guarantee that the numerical performance of the finite approximation ROC is going to stable. For example, in practice, the set $\{(n, t_n^c)\}_{n=0}^k$ can be quite volatile before it converges to the slope B^∞. In such a case, the log-absolute difference between two Taylor coefficients, B^k, as computed by Equation (1.10), is going to have some degree of fluctuation as

well. However, as explained below, this issue can be mitigated by introducing several numerical refinements.

1.2.3 A two-stage routine on ROC approximation with finite Taylor expansion

Based on the results in Section 1.2.2, I will now present a two-stage numerical routine on the finite approximation of ROC that is easy to implement in practice. As a beforehand remark, this paper confines attention to developing a computationally efficient, parsimonious numerical method that can provide a convergent approximation for ROC rather than proposing the *most efficient* ROC approximation algorithm. Other possibilities of improving the algorithm are beyond its scope.

1.2.3.1 Domain Refinement

Let us begin by refining the set of inputs of the approximation procedure, $\{(n, t_n^c)\}_{n=0}^k$. The domain refinement proposed below can ensure the solution method is well-define and efficient (i.e., discard uninformative inputs). Given objective function $F(x)$, point of expansion c, and the associated k-th order Taylor polynomial specified in Equation (1.9). The active set of points for the finite approximation of the d'Alembert's ratio test (1.10) is defined as $\{(n^a, t_n^{c,a})\}_{n=0}^{k^a} \equiv \{(n, t_n^c) : t_n^c \neq 0\}_{n=0}^k$, where $k^a \leq k$ indexes the order of last non-zero coefficient, $\{t_n^{c,a} \neq 0\}_{n=0}^{k^a}$ is the non-zero subset of unnormalized Taylor coefficients ($\{(n, t_n^c)\}_{n=0}^k$), $n^a \in \{0, \dots k\}$ is the order index for non-zero terms. The intuition for the active set of points refinement is as follows. For most economic models, the set $\{(n, t_n^c)\}_{n=0}^k$ will comprise only non-zero values, where the active set of points is identical to the original set, $\{(n^a, t_n^{c,a})\}_{n=0}^{k^a} = \{(n, t_n^c)\}_{n=0}^k$. However, in certain cases, a subset of the Taylor coefficients may be coincidentally zero at the point of approximation, or because the objective function exhibits oscillatory behavior that causes the

Taylor coefficients to be periodically zero[4]. For these cases, the active set of points is simply a subset of the original set, hence still preserves the convergence properties of the numerical method as discussed in Section 1.2.2. Moreover, notice the theoretical definition of d'Alembert's ratio test (1.4) also requires non-zero coefficients as input. Hence, the active set refinement for the inputs is necessary.

Utilizing the active set refinement, we have the following useful lemma.

Lemma 2. *Given the active set of points* $\{(n^a, t_n^{c,a})\}_{n=0}^{k^a}$ *of objective function* $F(x)$*, the slope* B^{k^a} *solves the finite approximation of the d'Alembert's ratio test (1.10), and its associated ROC approximation,* $\hat{R}^{c,k^a}$*, is well defined and converge to the true radius of convergence as* $k \to \infty$*.*

Proof. I first show that B^k, defined in (1.10), is only well defined on the active set of Taylor coefficients. Suppose $t_n^c = 0$ for some n, then $\ln|t_n^c| = \ln|0|$, which is not well-defined, hence making the finite approximation of the d'Alembert's ratio test ill-conditioned.

To show convergence, I appeal to Corollary 1 and Lemma 1, which prove the B^k, using the full set of Taylor coefficients for $k < \infty$, converges to $B^\infty = -\ln(R^c)$. Since any subsequence of a convergence sequence converges, and because the active set $\{(n^a, t_n^{c,a})\}_{n=0}^{k^a}$ is a subsequence the of the full Taylor coefficients set $\{(n, t_n^c)\}_{n=0}^{k}$, they likewise converge to $B^\infty = -\ln(R^c)$ as $k \to \infty$. Therefore $B^\infty = \lim_{k\to\infty} B^{k^a}$. □

1.2.3.2 The first-stage approximation: a polynomial interpolation solution

As long as the active set of points behaves nicely (relatively linear), Equation (1.10) is still quite useful for ROC approximation, I then denote this solution (after domain refinement)

[4]An example of this type of functions is $\cos x$, whose Taylor expansion evaluated at $c = 0$ is

$$\cos x \approx \sum_{n=0}^{k} (-1)^n \frac{x^{2n}}{(2n)!} = 1 - \frac{x^2}{2!} + \frac{x^4}{4!} - \frac{x^6}{6!} + \cdots$$

In this case, coefficients of all odd terms are zero, whereas the even terms are nonzero.

by

$$B_{ld}^{k^a} = \ln\left|t_{k^a}^{a,c}\right| - \ln\left|t_{k_{-1}^a}^{a,c}\right| \tag{1.11}$$

where $k^a = \max\{n : t_n^{a,c} \neq 0\}$, and k_{-1}^a stands for the second-largest index for the active set. Notice solution $B_{ld}^{k^a}$ is literally the slope of the affine function that connects the last two Taylor coefficients of the active set.

However, whenever the stability issue (as mentioned in Section 1.2.2) exists, Equation (1.11) is no longer efficient. I am now introducing a polynomial interpolation solution to the d'Alembert's ratio test. Notice there are many possible numerical ways of addressing this issue, among which the polynomial interpolation method may not be the most efficient approach but is definitely the one that is straightforward and intuitive enough to go with.

To be specific, let us define the polynomial interpolation solution of the finite approximation of the d'Alembert's ratio test as

$$B_{Inter}^{k^a} = P\left(k^a + 1\right) - \ln\left|t_{k^a}^{a,c}\right| \tag{1.12a}$$

$$P(n) = \sum_{j=k_{-3}^a}^{k^a} \ln\left|t_j^{a,c}\right| P_j\left(n\right), \quad P_j\left(n\right) = \prod_{\substack{k=k_{-3}^a \\ k\neq j}}^{k^a} \left(\frac{n-k}{j-k}\right) \tag{1.12b}$$

where $k^a = \max\{n : t_n^{a,c} \neq 0\}$ and k_{-3}^a stands for the fourth-largest exponent index for the active set. Notice this interpolation solution requires four Taylor coefficients from the active set. There are two main reasons for selecting this number. First, the computational cost of getting four Taylor coefficients, or equivalently a third-order perturbation solution, is quite reasonable. Second, four points can be used to construct a cubic polynomial approximation that is capable of capturing most of the non-linearity of the active Taylor coefficients set, hence providing a more robust approximation for ROC. Consequently, it can largely smooth out the volatility of irregular Taylor coefficients while producing accurate approximation for the slope B^∞ when

the coefficients are well behaved. Simultaneously, it is efficient and not tends to over-fitting or under-fitting.

In the limit, the polynomial interpolation solution has the following property.

Proposition 1. *Given the active set of points* $\{(n^a, t_n^{c,a})\}_{n=0}^{k^a}$*, the polynomial interpolation solution* $B_{Inter}^{k^a}$ *from Equation (1.12) solves the finite approximation of the d'Alembert's ratio test (1.10). The solution* $B_{Inter}^{k^a}$ *converges to* $-\ln R^c$ *as* $k \to \infty$*.*

Proof. Since the solution of Equation (1.11) converges to the true ROC by Lemma 2, we only need to show the polynomial interpolation solution converges to $B_{ld}^{k^a}$ when $k \to \infty$. To see this, let's assume that the interpolation solution is not converging to $B_{ld}^{k^a}$. Without loss of generality, let's denote the cubic polynomial solution with the form $P(n) = \alpha_0 + \alpha_1 n + \alpha_2 n^2 + \alpha_3 n^3$. Now the value of $\ln |t_{k^a}^{a,c}|$ and the extrapolation value of $\ln \left|t_{k^a+1}^{a,c}\right|$ can be written as

$$P(k^a) = \alpha_0 + \alpha_1 k^a + \alpha_2 (k^a)^2 + \alpha_3 (k^a)^3$$

$$P(k^a + 1) = \alpha_0 + \alpha_1 (k^a + 1) + \alpha_2 (k^a + 1)^2 + \alpha_3 (k^a + 1)^3$$

simplifying we have

$$P(k^a + 1) = P(k^a) + \alpha_2 (2k^a + 1) + \alpha_3 \left[3 (k^a)^2 + 3k^a + 1\right]$$

Taking limit on both side

$$\lim_{k\to\infty} P(k^a + 1) = \lim_{k\to\infty} P(k^a) + \lim_{k\to\infty} \left\{\alpha_2 (2k^a + 1) + \alpha_3 \left[3 (k^a)^2 + 3k^a + 1\right]\right\} \Leftrightarrow$$

$$\lim_{k\to\infty} \ln \left|t_{k^a+1}^{a,c}\right| - \lim_{k\to\infty} \ln |t_{k^a}^{a,c}| = (\alpha_2 + \alpha_3) + \lim_{k\to\infty} \left\{3\alpha_3 (k^a)^2 + (2\alpha_2 + 3\alpha_3) k^a\right\}$$

By Lemma 2, the following identity must holds

$$\begin{aligned} -\ln R^c &= \lim_{k\to\infty} \left[\ln \left|t_{k^a+1}^{a,c}\right| - \ln |t_{k^a}^{a,c}|\right] \\ &= (\alpha_2 + \alpha_3) + \lim_{k\to\infty} \left\{3\alpha_3 (k^a)^2 + (2\alpha_2 + 3\alpha_3) k^a\right\} \end{aligned}$$

Shifting k^a back by one, i.e. let $k^a = k^a - 1$, we will end up with exactly the same expression as Equation (1.11) which contradicts to the original assumption. Therefore the solution $B^{k^a}_{Inter}$ converges to $-\ln R^c$ as $k \to \infty$. □

For conservative purposes, let us define the final first-stage approximation result as

$$\hat{R}^{c,k^a} = \min\left\{R^{c,k^a}_{Inter}, R^{c,k^a}_{ld}\right\} = \exp\left(-\max\left(B^{k^a}_{Inter}, B^{k^a}_{ld}\right)\right) \tag{1.13}$$

where $\hat{R}^{c,k^a}$ refers to be the first-stage approximation given k^a. The intuition for Equation (1.13) is as follows: given the same point of expansion c and the order of Taylor polynomial k (hence same k^a), the solution R^{c,k^a}_{Inter} and R^{c,k^a}_{ld} are not necessarily identical. However, for conservative purposes, one may always want to pick up the smaller approximated ROC value rather than the larger one, i.e., underestimation is always preferred in ROC approximations. The following proposition states the first-stage approximation converges.

Proposition 2. *Given solution $B^{k^a}_{Inter}$ and $B^{k^a}_{ld}$, the first-stage approximation $\hat{R}^{c,k^a}$ defined by (1.13) converges to R^c as $k \to \infty$.*

Proof. By equation (1.13), the first stage approximation can also be rewritten as

$$\begin{aligned}
\hat{R}^{c,k^a} &= \exp\left(-\max\left(B^{k^a}_{Inter}, B^{k^a}_{ld}\right)\right) \\
&= \max\left(\exp\left(-B^{k^a}_{Inter}\right), \exp\left(-B^{k^a}_{ld}\right)\right)
\end{aligned}$$

Taking limit on both side and by Lemma 2 and Preposition 1

$$\begin{aligned}
\lim_{k\to\infty} \hat{R}^{c,k^a} &= \lim_{k\to\infty}\left[\max\left(\exp\left(-B^{k^a}_{Inter}\right), \exp\left(-B^{k^a}_{ld}\right)\right)\right] \\
&= \max\left(\lim_{k\to\infty}\left[\exp\left(-B^{k^a}_{Inter}\right)\right], \lim_{k\to\infty}\left[\exp\left(-B^{k^a}_{ld}\right)\right]\right) \\
&= \max\left(\exp\left(-B^{\infty}\right), \exp\left(-B^{\infty}\right)\right) \\
&= \exp\left(-B^{\infty}\right) \\
&= R^c
\end{aligned}$$

which equality completes the proof. □

1.2.3.3 The second-stage approximation: a monotonic transformation

Regardless that the first-stage approximation $\hat{R}^{c,k^a}$ has been carefully selected, a restrictive finite set of points $\{(n, t_n^c)\}_{n=0}^{k}$ (from a Taylor polynomial with small k) is still the most challenging part of making the ROC approximation conservative. In fact, Proposition 2 only guarantees that $\hat{R}^{c,k}$ will converge to the true ROC in limit, but not in how it converges. For example, this value can monotonically decrease to the true R^c or the other way around. In the worst case, it may even oscillate while converging to the true R^c.

One way to avoid the aforementioned cases is to impose increasing monotonicity on the $\hat{R}^{c,k^a}$ sequence such that it increasingly converges to the true R^c from below as the degree of Taylor expansion rises. For example, given a k-th order Taylor expansion of $F(x)$, we should be able to get $(k^a - 1)$ numbers of first-stage approximation from $\{(n^a, t_n^{a,c})\}_{n=0}^{k^a}$ [5]. If the Taylor coefficients set is highly nonlinear, the first-stage approximations are going to oscillate correspondingly, i.e., the first-stage ROC approximation may either overestimated $\left(\hat{R}^{c,n} > R^c\right)$ or underestimated $\left(\hat{R}^{c,n} < R^c\right)$. Now, if we can use a trick to force all leading values to be uniformly smaller than the later approximation, i.e., $\hat{R}^{c,n} < \hat{R}^{c,n+1} < \hat{R}^{c,k^a}$ for $n < k^a$, then by Proposition 2, *in limit*, the ROC approximations are going to converge to the true ROC monotonically from below.

Considering the ROC is usually unknown, the best we can do to capture this idea is to impose increasing monotonicity on the first-stage approximations (up to a finite k) such that all leading values are uniformly smaller than the latest approximation $\hat{R}^{c,k^a}$. As a result, the ROC approximation after this monotonic transformation is, at least, always a conservative approximation for a k-th degree Taylor polynomial. Conceptually, such a property acts exactly

[5] Recall that a first-stage approximation only requires two Taylor coefficients (Equation (1.11)). Therefore we can get $(k^a - 1)$ number of $\hat{R}^{c,k^a}$s by repeating the first-stage procedure for n from 1 to k^a.

as the sufficient condition of the conservative ROC approximation as $k \to \infty$. Hence, the second-stage can also be thought of as an approximation for the sufficient condition of the Taylor theorem, and the appropriateness of the perturbation solution.

To illustrate the second-stage implementation, let us begin with obtaining $\left\{\hat{R}^{c,n}\right\}_{n=0}^{k^a}$ from a k-th order Taylor expansion of $F(x)$. To impose a monotonic transformation, first solve

$$\left(1-\frac{1}{n}\right)^{p_n}\hat{R}^{c,n} \leq \hat{R}^{c,k^a},\ \forall 0 \leq n \leq k^a \tag{1.14}$$
$$\Rightarrow p_n = \left\lceil \log\left(\frac{\hat{R}^{c,k^a}}{\hat{R}^{c,n}}\right) / \log\left(1-\frac{1}{n}\right)\right\rceil$$

where $\hat{R}^{c,k^a}$ is the latest approximation using full $\{(n^a, t_n^{a,c})\}_{n=0}^{k^a}$ set.

Notice that Equation (1.14) is essentially *ad-hoc* imposing a p_n-th[6] order penalty term on all of the (k^a-1) leading terms of $\hat{R}^{c,k^a}$. By imposing $(1-1/n)^{p^n}$, each of these terms is guaranteed to be smaller than the first-stage approximation $\hat{R}^{c,k^a}$. Now, defining $p^k = \max\{p_n\}_{n=0}^{k^a}$, let us then construct the second-stage monotonic transformed approximation by

$$\hat{\hat{R}}^{c,n} = \left(1-\frac{1}{n}\right)^{p^k}\hat{R}^{c,n},\ \forall 0 \leq n \leq k^a \tag{1.15}$$

where $\left\{\hat{\hat{R}}^{c,n}\right\}_{n=0}^{k^a}$ refers to the second-stage approximation sequence and $\hat{\hat{R}}^{c,k^a}$ is the final approximation result from the second-stage.

By Equation (1.15), $(1-1/k)^{p^k} \in (0,1)$. Hence, the way it penalizes the first-stage finite approximation $\left\{\hat{R}^{c,n}\right\}_{n=0}^{k^a}$ is, after obtaining the approximated value $\hat{R}^{c,n}$, the penalty term reduces this approximated range by $\left[1-(1-1/n)^{p^k}\right]\hat{R}^{c,n}$. Notice as $(1-1/k)^{p^k} \to 1$, the second-stage transformation procedure allows $\hat{R}^{c,k^a}$ converging to the true limit when $k \to \infty$. Moreover, each term of the second-stage sequence $\left\{\hat{\hat{R}}^{c,n}\right\}_{n=0}^{k^a}$ is guaranteed to be smaller than their following term. This property is summarized in proposition 3 below.

Proposition 3. *Given the first-stage approximation $\hat{R}^{c,k^a}$, the second-stage approximation $\hat{\hat{R}}^{c,k^a}$ converges to R^c monotonically from below as $k \to \infty$.*

[6] For simplicity reason, I set p_n to be always an integer.

Proof. By constructing Equation (1.15), we can compute the limit of $\left\{\hat{\hat{R}}^{c,n}\right\}_{n=0}^{k^a}$ as

$$\lim_{k\to\infty}\hat{\hat{R}}^{c,k^a}=\lim_{k\to\infty}\left(1-\frac{1}{n}\right)^{p^k}\hat{R}^{c,k^a}=\lim_{k\to\infty}\left(1-\frac{1}{n}\right)^{p^k}\cdot\lim_{k\to\infty}\hat{R}^{c,k^a}=R^c$$

which proves the second-stage approximation converges. By convention, it always true that

$$\left(1-\frac{1}{n}\right)^{p^k}\leq\left(1-\frac{1}{(n+1)}\right)^{p^k}\leq 1\Rightarrow\hat{\hat{R}}^{c,n}\leq\hat{\hat{R}}^{c,n+1}\leq R^c,\ \text{for } k\to\infty$$

Therefore, I conclude that in limit, the second-stage approximation $\left\{\hat{\hat{R}}^{c,n}\right\}_{n=0}^{k^a}$ converges to R^c monotonically from below. □

1.2.3.4 Algorithm

Combining subsection 1.2.3.1~1.2.3.3, Algorithm 1 summarized the two-stage interpolation – log-absolute difference routine for ROC approximation in steps.

We also have the asymptotical conservative convergent property for Algorithm 1. Given k-th order Taylor expansion T_k^c of the objective function $F(x)$ around point c, the numerical approximation of ROC from Algorithm 1 is conservative and converges to the theoretical ROC as $k\to\infty$.

Proof. The prove is an immediate result of Proposition (1)-(3). □

Notice Algorithm 1 is able to provide an approximation of ROC with finite Taylor expansion. Moreover, it also provides an approximation for the sufficiency condition of the Taylor theorem in the limit. The appropriateness of the perturbation solution becomes assessable.

Algorithm 1 The 2S-Inter-ld algorithm for ROC approximation.

Step 1. Given objective function $F(x)$, the point of expansion c, and the order of Taylor expansion k, derive the analytical form of finite Taylor expansion as defined in Equation (1.9).

Step 2. Collect the order index $n = 0, \dots k$ and its corresponding Taylor coefficient t_n^c, construct the original full Taylor coefficients set $\{(n, t_n^c)\}_{n=0}^{k}$ and its nonzero active subset $\{(n^a, t_n^{c,a})\}_{n^a=0}^{k^a}$.

Step 3. Get the first-stage approximation by

1. Solve $B_{ld}^{k^a}$ of the d'Alembert's ratio test (1.10) by log-absolute difference approximation (1.11).
2. Solve $B_{Inter}^{k^a}$ of the d'Alembert's ratio test by polynomial interpolation approximation (1.12).
3. Selecting the minimum of the approximations by Equation (1.13).

Step 4. Get the second-stage approximation by

1. For each $0 \leq n \leq k^a$, solve for p_n using Equation (1.14) and picking up the maximum value $p^k = \max\{p_n\}_{n=0}^{k^a}$.
2. Superimpose monotonic transformation on the first-stage sequence $\left\{\hat{R}^{c,n}\right\}_{n=0}^{k^a}$ using Equation (1.15) and formulate the second-stage approximation sequence $\left\{\hat{\hat{R}}^{c,n}\right\}_{n=0}^{k^a}$.
3. The final approximation for R^c is $\hat{\hat{R}}^{c,k^a}$.

1.2.4 An illustrative example

In order to finalize this section, I use a univariate function as a detailed example to illustrate how Algorithm 1 is executed. This includes a visualization of the active Taylor coefficient set $\{(n^a, t_n^{c,a})\}_{n=0}^{k^a}$, the theoretical slope B^{∞} for the d'Alembert's ratio test (1.10),

the polynomial interpolation solution, and the second-stage monotonic transformation.

Using the concept of slope B^{∞} from the d'Alembert's ratio test, Figure 1.1 plots the 2S-Inter-ld algorithm for approximating the radius of convergence of function $y = \sqrt{x}$ at $x = 0.7$. In this case, one can exactly compute $R^{0.7} = 0.7$, the associated $B^{\infty} = -\ln 0.7$, is captured by the slope of the solid red line in this plot. The blue dots in both panels 1.1a and 1.1b represent the Taylor coefficients of function $y = \sqrt{x}$ at $x = 0.7$ up to a 25-th order Taylor expansion (a 6-th order Taylor expansion in panel 1.1a and a 25-th order Taylor expansion in panel 1.1b). And notice for this case, $\{(n^a, t_n^{c,a})\}_{n=0}^{k^a} = \{(n, t_n^c)\}_{n=0}^{k}$, all Taylor coefficients are non-zero.

Figure 1.1: 2S-Inter-ld algorithm on $y = \sqrt{x}$ up to 25th order at $x = 0.7$ (B^{∞})

(a) $k = 6$ (b) $k = 25$

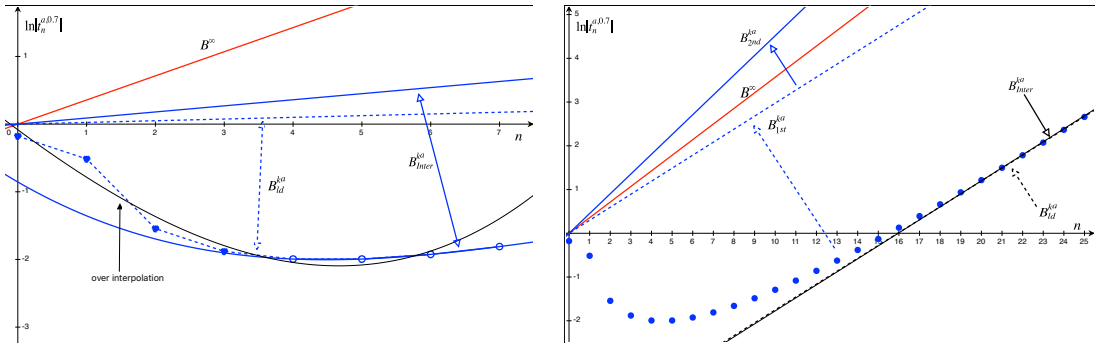

The main takeaway of Figure 1.1a is that the polynomial interpolation solution performed more robustly when Taylor coefficients are highly nonlinear. To be specific, the seven blue dots in the left panel represent the first seven Taylor coefficients of a 6-th order Taylor expansion of $y = \sqrt{x}$ at $x = 0.7$. The dashed blue curve that connects each two Taylor coefficients can be understood as a graphical representation for the log-absolute difference approach (1.11). The slope of the straight dashed blue line (above the horizontal axis) is B_{ld}^{6}. It is easy to see that the slopes are quite volatile before the Taylor coefficients converging to the theoretical trend

B^{∞}, hence deliver oscillatory and less efficient ROC approximations. Instead, the polynomial interpolation solution B^{6}_{Inter} captured by the solid blue lines approximate the theoretical trend B^{∞} in a much stable way as it smooths out the oscillations from the log-absolute difference approach, therefore able to provide more efficient approximations. The black curve describes one possible case of overfitting. It uses all seven coefficients to interpolate a cubic polynomial.

Figure 1.1b presents a big picture of Algorithm 1. The blue dots represent all 26 Taylor coefficients of a 25-th order Taylor expansion of $y = \sqrt{x}$ at $x = 0.7$. The solid black line captures the solution B^{25}_{Inter}, where the dashed black line representing the solution B^{25}_{ld}. Notice these two approaches are almost identical whenever Taylor coefficients are very well behaved. Selecting the minimum ROC approximation among these two, the first-stage approximation is $\hat{R}^{0.7,25} = \min\left[-\exp\left(B^{25}_{Inter}\right), -\exp\left(B^{25}_{ld}\right)\right]$ (slope of the dashed blue line).

Notice from Figure 1.1b, the slope $B^{25}_{1^{st}}$ is smaller than B^{∞}, suggesting that it overestimates the true ROC. However, following Step 4 of Algorithm 1, the maximum penalty exponent of first-stage sequence $\left\{\hat{R}^{0.7,n}\right\}_{n=0}^{k^a=25}$ is solved to be $p^{25} = 3$. Imposing this penalty, the last term of the second-stage sequence $\left\{\hat{\hat{R}}^{0.7,n}\right\}_{n=0}^{k^a=25}$ is $\hat{\hat{R}}^{0.7,25} = 0.6620$, this is also the final ROC approximation result conducted by Algorithm 1. Translating to the slope, it is represented by the solid blue line ($\hat{\hat{R}}^{0.7,25} = -\exp\left(B^{25}_{2^{nd}}\right)$). This result is numerically conservative because $\hat{\hat{R}}^{0.7,25} < R^{0.7}$. Thus, it provides a necessary and sufficient condition of the appropriateness of the Taylor expansion.

Figure 1.2 uses the radius of convergence R^c to further illustrate Algorithm 1, in which example I approximate $y = \sqrt{x}$ at $x = 0.7$ by a 100-th degree Taylor expansion. The first subsection of Figure 1.2 plots the approximated ROC values solved by both the polynomial interpolation ($\{B^{n}_{Inter}\}^{100}_{n=1}$) and the log-absolute difference ($\{B^{n}_{ld}\}^{100}_{n=1}$) method. Notice both approaches tend to overestimate the ROC at the first stage. In the second subsection, the

black star curve represents the first-stage sequence $\left\{\hat{R}^{0.7,n}\right\}_{n=0}^{k^a=100}$, which formulated by taking the minimum value among $R_{Inter}^{0.7,n}$ and $R_{ld}^{0.7,n}$ for each order n. After superimposing the penalty exponent $p^{100}=3$, the second-stage sequence ends up with $\left\{\hat{\hat{R}}^{0.7,n}\right\}_{n=0}^{k^a=100}$, which is represented by the blue hexagram curve. Clearly, the second-stage sequence converges to the true ROC from below after the monotonic transformation. Finally, the approximated ROC value is $\hat{\hat{R}}^{0.7,100}=0.6898$, which is closer to 0.7 than the 25-th order Taylor expansion case. Moreover, from the third subsection, the convergence rate of Algorithm 1 is quite fast for the early stage but gradually slows down as higher-order terms are added.

Figure 1.2: 2S-Inter-ld algorithm on $y=\sqrt{x}$ up to 100th order at $x=0.7$ (R^c)

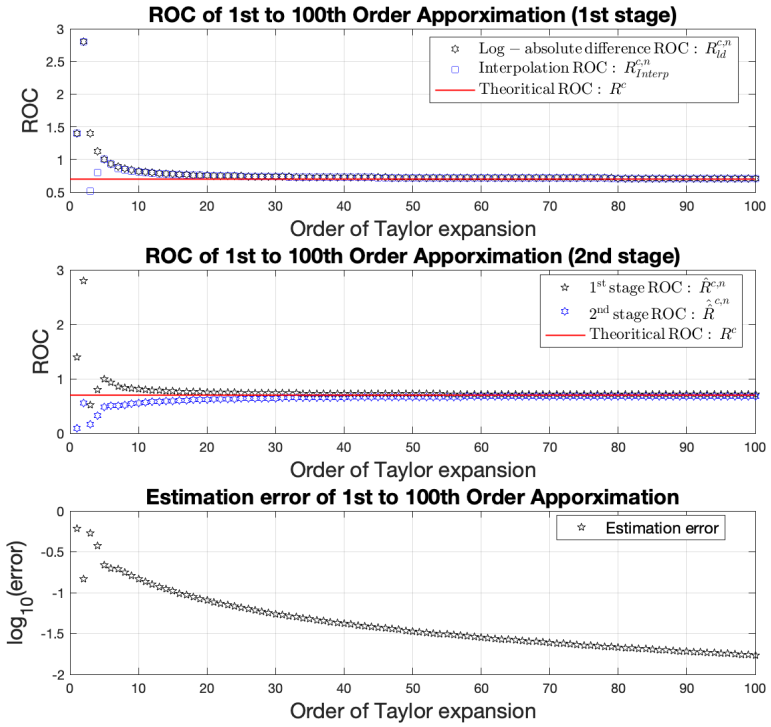

Overall, this example visualizes some of the essential numerical features of Algorithm

1 discussed in this section[7]. As shown, even with a finite Taylor polynomial, the proposed algorithm still exhibits good practical potentials on the numerical approximation for ROC and is ready to be unleashed to macroeconomic applications.

1.3 Numerical applications on benchmark macroeconomic models

The main purpose of this section is to use perturbation solutions of basic RBC models with and without analytical ROC to test whether Algorithm 1 can deliver a satisfactory performance. To accomplish this, I start with the neoclassical growth models with closed-form ROC and then relaxed the assumptions to a standard RBC model where the radius of convergence is uncomputable. As these practices show, the 2S-Inter-ld algorithm is able to assess the appropriateness of perturbation solutions of benchmark macroeconomic models.

1.3.1 Approximated ROC of the closed-form neoclassical growth models

For conservative reasons, the numerical application starts from models with analytical solutions. I pick the simple neoclassical growth model with log utility compounded with fully depreciated capital and the asset pricing model proposed by Burnside (1998) (see the Technical Appendix) as two benchmark tests for Algorithm 1.

Consider the economy with representative households decide consumption c_t and capital k_{t+1} at every time period to maximize their lifetime utility on

$$\max_{\{c_t,k_{t+1}\}_{t=0}^{\infty}} \mathbb{E}_0 \sum_{t=0}^{\infty} \beta^t u(c_t)$$

where $\mathbb{E}_0$ is the expectation operator at time 0, $\beta \in (0,1)$ is the discount factor, and the utility

[7]For the other two univariate function examples, see Appendix A.2.

function $u(c_t) = \log(c_t)$. For simplicity, I normalized the labor to one that drops the labor decision in this model setup. The production function takes Cobb-Douglas form

$$y_t = e^{z_t} k_t^{\alpha}$$

where z_t is the productivity shock and follows $AR(1)$ process

$$z_t = \rho z_{t-1} + \chi \sigma_z \epsilon_t, \quad \epsilon_t \sim \mathcal{N}(0,1)$$

with time consistency $|\rho| < 1$, scale parameter σ_z, and perturbation parameter χ. Assuming full depreciation $\delta = 1$, the law of motion of capital becomes

$$k_{t+1} = e^{z_t} k_t^{\alpha} - c_t$$

This is the well-known case of the neoclassical growth model with closed-form policy functions given by

$$k_{t+1} = \alpha\beta e^{z_t} k_t^{\alpha}$$

$$c_t = (1 - \alpha\beta)\, e^{z_t} k_t^{\alpha}$$

However, one can also use the perturbation solution to solve this model around the non-stochastic steady state. It can be shown that the perturbation solution[8] is identical to the Taylor expansions of these closed-form policy functions.

To see this, recall that the state space in this model is two dimensional. Hence, there are three interacting variables in the perturbation solution. Using policy function of capital as

[8]For all macroeconomic applications in this paper, I use Mathematica to obtain the perturbation solution. The symbolic computation feature of Mathematica provides high numerical efficiency on taking high dimensional derivatives. Moreover, this feature also allows me to get perturbation coefficients with an extremely simple transformation.

an example, the perturbation solution has the following form

$$\begin{aligned} k_{t+1}(k_t, z_t, \sigma_z; \chi) =& k_{ss} + k_k (k_t - k_{ss}) + k_z z_t + k_\chi \chi + k_{kz} (k_t - k_{ss}) z_t + k_{k\chi} (k_t - k_{ss}) \chi \\ &+ \frac{1}{2}\left[k_{kk} (k_t - k_{ss})^2 + k_{ss} z_t^2 + k_{\chi z} \chi z_t + k_{\chi^2} \chi^2 \sigma_z^2\right] \\ &+ \frac{1}{6}[\cdots] + \cdots \end{aligned} \tag{1.16}$$

Set $z_t = 0$ and $\chi = 1$, the right hand side of (1.16) will be the same as the Taylor expansion of policy function of capital for $z_t = 0 = z_{ss}$ (Same trick applies for deriving high order perturbation solution for the capital policy function when $k_t = k_{ss}$):

$$k_{t+1}(k_t, z_t = 0, \sigma_z) \approx \sum_{n=0}^{k} \frac{F^{(n)}(k_{ss}, 0, \sigma_z)}{n!} (k_t - k_{ss})^n$$

$$F(k_t, z_t, \sigma_z) = \alpha\beta e^{z_t} k_t^\alpha$$

As a numerical demonstration, Table 1.2 displays the first six coefficients of the Taylor expansion and the perturbation solution for policy function of capital (on k_t and z_t dimension).

Based on such interchangeability, in this application, I use the Taylor expansion of policy functions as a shortcut to approximate R^c. Same as the previous univariate examples, this equivalency saves enormous computational cost on deriving the perturbation solution, and at the same time, allows me to test the asymptotical performance of Algorithm 1, as a 100-th order Taylor expansion of policy function in readily available. In addition, for this closed-form neoclassical growth model, I show that (see the Technical Appendix) the ROC of the capital policy function is $(-k_{ss}, k_{ss})$ on k_t dimension and $(-\infty, +\infty)$ on z_t dimension (or equivalently σ_z in this model).

Table 1.2: Coefficients comparison between Taylor expansion and perturbation solution

(a) Coefficients for $K_{t+1}(k_t)$

Order	Perturbation method	Taylor expansion
0	0.18829	0.18829
1	0.33000	0.32999
2	-0.58709	-0.58709
3	1.73562	1.73561
4	-6.15257	-6.15252
5	23.98300	23.98277

(b) Coefficients for $K_{t+1}(z_t)$

Order	Perturbation method	Taylor expansion
0	0.18829	0.18829
1	0.18829	0.18829
2	0.09414	0.09414
3	0.03138	0.03138
4	0.00784	0.00784
5	0.00156	0.00156

Following the same logic as the square root example, Figure 1.3 plots the details of ROC approximations for the perturbation solution of the capital policy function on the k_t dimension. Again, the first subsection suggests the first-stage ROC approximation sequences are both overestimate R^{∞}. The second subsection states the importance of superimposing the

monotonic transformation at the second-stage. In this case, the approximated ROC for k_t dimension has around two-decimal accuracy using a 15-th order perturbation solution.

Figure 1.3: Closed-form neoclassical growth model (ROC approximation on k_t dimension)

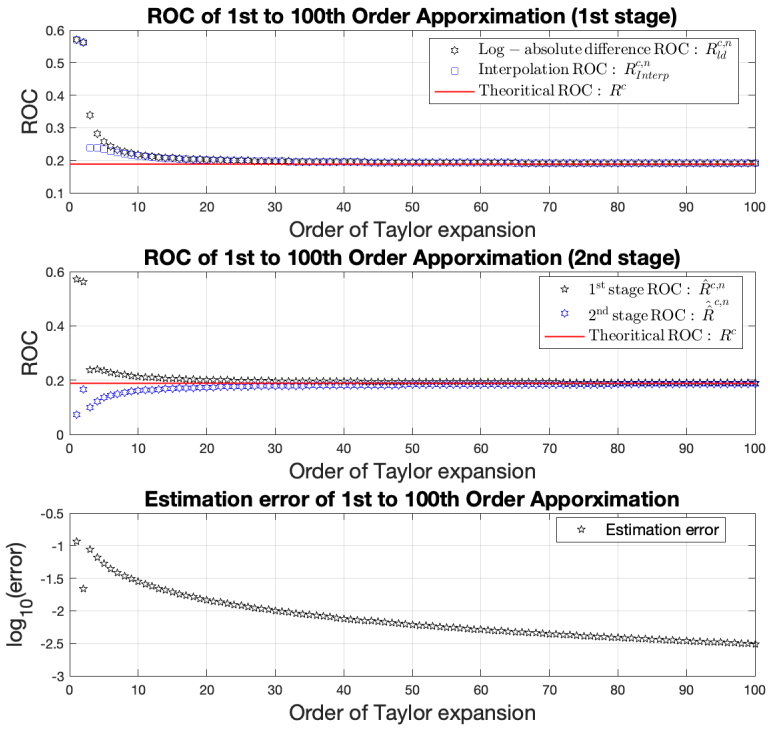

As a finish of the test, from Figure 1.4, the approximated ROC values for the perturbation solution of capital policy function on the z_t dimension are monotonically increasing. This matches with the fact that the true ROC is $R^c = \infty$. An economic interpretation for this infinity ROC is that the correction for risk is zero in a closed-form neoclassical growth model. Thus, any increment in risk generates two counterbalancing mechanisms: a desire to accumulate more capital to buffer future negative shocks and a desire to accumulate less capital to avoid the additional production risk. Therefore, the volatility of TFP shocks plays no role in policy function, i.e., the perturbation solution is globally appropriate on TFP dimension. However,

there is no way of approximating infinity. A monotonically increasing ROC approximations (as the number of coefficients growing) is the best that Algorithm 1 can do. For the same reason, there is no need for the second-stage penalty in this case.

Figure 1.4: Closed-form neoclassical growth model (ROC approximation on z_t dimension)

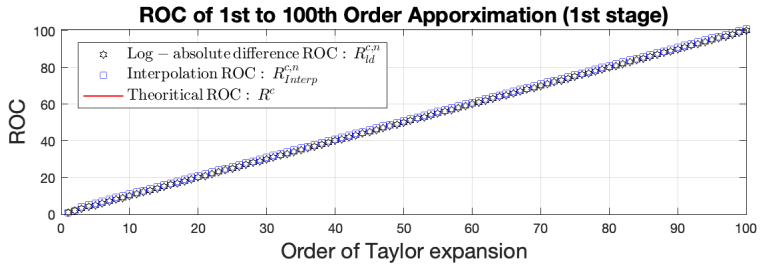

Overall, the numerical practices on the closed-form neoclassical growth model confirms further that the Algorithm 1 is reliable on economic applications. Moreover, it also confirms that, as Swanson et al. (2006) and Swanson (2012) point out, the policy functions of some DSGE models are globally supported by the perturbation solution.

1.3.2 Approximated ROC of the standard RBC model

For the first macroeconomic application with unknown ROC, I add the CRRA utility function that allows risk-aversion to take values other than 1. Meanwhile, the capital now partially depreciates at every period. Hence, the model used in this part can be reduced to a closed-form neoclassical model by only resetting values for δ, θ, and γ.

1.3.2.1 Model setup and equilibrium conditions

Consider the economy with representative households deciding consumption C_t, leisure $1 - L_t$ and capital K_{t+1} at every period to maximize their life time utility on

$$\max_{\{C_t, K_{t+1}\}_{t=0}^{\infty}} \mathbb{E}_0 \sum_{t=0}^{\infty} \beta^t \frac{\left(C_t^{\theta} (1 - L_t)^{1-\theta}\right)^{1-\gamma}}{1-\gamma}$$

where $\mathbb{E}_0$ is the expectation operator at time 0, $\beta \in (0,1)$ is the discount factor, γ stands for the risk aversion and θ is the weight between consumption and leisure.

The production function takes Cobb-Douglas form $Y_t = e^{z_t} K_t^{\alpha} L_t^{1-\alpha}$, where z_t is the productivity shock and follows the $AR(1)$ process $z_t = \rho z_{t-1} + \chi \sigma_z \epsilon_t, \quad \epsilon_t \sim \mathcal{N}(0,1)$ with time consistency $|\rho| < 1$, scale parameter σ_z, and perturbation parameter χ. The law of motion of capital has partial depreciation $\delta \neq 1$ and the household satisfies the budget constraint $Y_t = C_t + I_t$.

The equilibrium conditions for this model contain a Euler equation for consumption path, the first-order condition between consumption and labor, a budget constraint, and a low of motion of innovation. Mathematically, the system can be written as

$$\frac{\left(C_t^{\theta}\left(1-L_t\right)^{1-\theta}\right)^{1-\gamma}}{C_t} = \beta E_t \left\{ \frac{\left(C_{t+1}^{\theta}\left(1-L_{t+1}\right)^{1-\theta}\right)^{1-\gamma}}{C_{t+1}} \left(1 + \alpha e^{z_t} K_{t+1}^{\alpha-1} L_{t+1}^{1-\alpha} - \delta\right) \right\} \tag{1.17a}$$

$$(1-\theta)\frac{\left(C_t^{\theta}\left(1-L_t\right)^{1-\theta}\right)^{1-\gamma}}{1-L_t} = \theta \frac{\left(C_t^{\theta}\left(1-L_t\right)^{1-\theta}\right)^{1-\gamma}}{C_t} (1-\alpha) e^{z_t} K_t^{\alpha} L_t^{1-\alpha} \tag{1.17b}$$

$$C_t + K_{t+1} = e^{z_t} K_t^{\alpha} L_t^{1-\alpha} + (1-\delta) K_t \tag{1.17c}$$

$$z_t = \rho z_{t-1} + \epsilon_t \tag{1.17d}$$

1.3.2.2 ROC sensitivity on parameterizations

For simplicity, I only focus on the ROC of capital policy function on σ_z direction instead of enumerating all ROC approximations on nine dimensions (because each of three jumping variables in the system (1.17) will have three ROCs on each state variable dimension).

Following the standard perturbation procedure proposed by Judd and Guu (2001) and keeping the notation the same as Aruoba et al. (2006), the perturbation solutions of this model

are

$$C_t^p\left(K_t, z_t, \sigma_z\right) = \sum_{i,j,m} p_{ijm}^C \hat{K}_t^i \hat{z}_t^j \sigma_z^m,$$

$$K_{t+1}^p\left(K_t, z_t, \sigma_z\right) = \sum_{i,j,m} p_{ijm}^K \hat{K}_t^i \hat{z}_t^j \sigma_z^m,$$

$$L_t^p\left(K_t, z_t, \sigma_z\right) = \sum_{i,j,m} p_{ijm}^L \hat{K}_t^i \hat{z}_t^j \sigma_z^m$$

where $\hat{x}_t = (x_t - x_{ss})$ represents the deviation from steady states and

$$p_{ijm}^x = \left.\frac{\partial^{i+j+m} x_t\left(K_t, z_t, \sigma_z\right)}{\partial K_t^i \partial z_t^j \partial \sigma_z^m}\right|_{K_{ss}, z_{ss}, \sigma_z}, \quad x_t = \{C_t, K_{t+1}, L_t\}$$

Notice the perturbation coefficients p_{ijm}^x depend on the model's structure and calibrations, one set of parameterization decide an uniquely set of perturbation coefficients, therefore an unique ROC. This means, for Algorithm 1, which takes perturbation coefficients as its inputs, the approximated ROC totally preserves such dependencies. As an immediate implication, this advantage allows Algorithm 1 to be a general framework for a detailed study on the sensitivity of the localness of perturbation solution like mentioned by Santos (2000).

Example in Section 1.3.1 confirms the ROC of state variables like K_t and Z_t are quite large (this is a general fact for most DSGE models). However, experience in computational macroeconomics tells a different story for σ_z. The perturbation solution may easily explode given the large volatility of TFP. This fact potentially suggests that the RBC model may have a very tiny ROC on the dimension of the volatility of shocks. To confirm this, I decide to study the sensitivity of ROC of σ_z concerning risk aversion and capital depreciation. Actually, γ and δ should be the key factors when creating ROC variations. This result is indirectly confirmed by Santos (2000), who suggested that the curvature of utility functions and the depreciation are two critical determinants of the Euler equation errors. Given the advantage of Algorithm 1, it should be able to show that the ROC is sensitive to them as well. As an extra test for the 2S-Inter-ld routine, I decided to go with this route.

For this practice, the model is solved by a fifth-order perturbation polynomial. Besides γ and δ, I use the calibration from Aruoba et al. (2006)[9]. The values are shown in Table 1.3. Values of δ are taken from $(0, 1)$, where the value of γ covers the most-used calibrated value from $(0, 10)$.

Table 1.3: Calibration for sensitivity experiment of standard RBC model

β	θ	α	ρ	σ_z
0.9896	0.357	0.4	0.95	0.007˜0.03

Figure 1.5 plots some main results of this sensitivity experiment. Figure 1.5a plots the ROC approximations on (γ, δ) space (left panel) and the same plot with a zoomed vertical axis (right panel). There are two main observations from Figure 1.5a. First, the biggest spike is located at $(\gamma, \delta) = (1, 1)$. This confirms the numerical result from Section 1.3.1 that the ROC of σ_z is infinity for the closed-form neoclassical growth model (The approximated value is around 60. However, this approximation will increase as more higher-order terms are added. Further, considering there are only six Taylor coefficients in this practice, this is already a decent result). Second, from the right panel, there is another smaller spike in the(γ, δ) plane at $(\gamma, \delta) = (1, 0.0196)$. We can also see that the approximated ROCs are uniformly large when $\gamma = 1$ (in fact, the surface has a ridge at $\gamma = 1$). To study this ridge further, Figure 1.5b plots some slices of Figure 1.5a around critical values. For example, the right column plot slices when $\delta = 0.0196$ and $\gamma = 5$. It is easy to see that for classical parameterizations (the red horizontal line represents $\sigma_z = 0.007$ and the gray area stands for the range of 0.007˜0.03), the appropriate range of σ_z (around 0.015) is larger than the calibration proposed in Table 1.3. Fixed γ, the largest ROC achieved when capital depreciation equals 1, where another spike occurs when δ

[9]I use the same calibrations because the model setup in these two papers is exactly the same. Moreover, this makes the comparison between the ROC of σ_z and their estimation result for σ_z much easier.

takes the most commonly used calibrated values.

Figure 1.5: Sensitivity of ROC of $K_{t+1}(\sigma_z)$ with respect to γ and δ

(a) 3-D projection of ROC of $K_{t+1}(\sigma_z)$ on (γ, δ) space

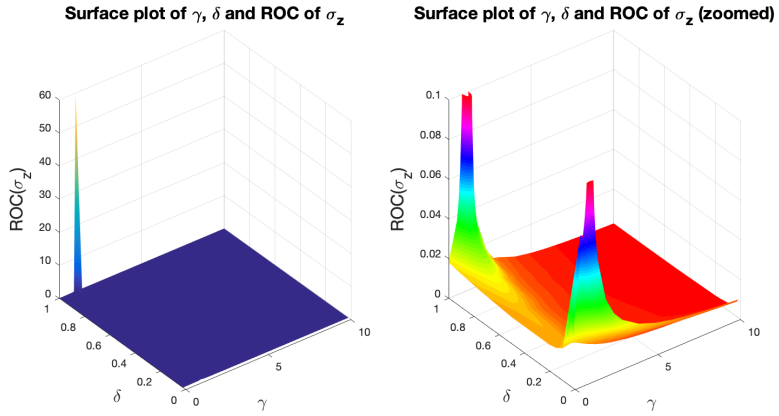

(b) 2-D slice of ROC of $K_{t+1}(\sigma_z)$ on γ and δ space

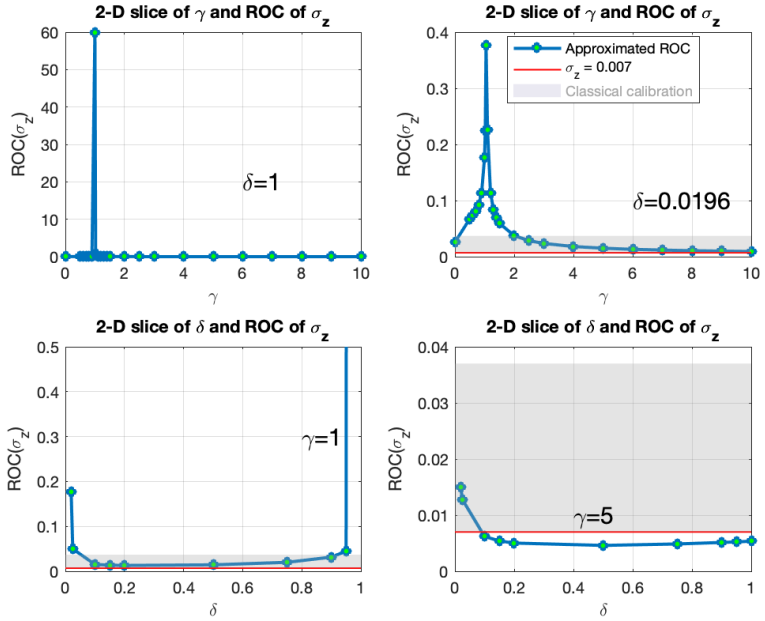

To sum up, the sensitivity analysis of ROC of σ_z in the standard RBC model suggests

the ROC is sensitive to the value of γ and δ, the ROC drastically falls from infinity to a small number when the parameterization deviates from the closed-form model ($\gamma = \delta = 1$). Yet, Algorithm 1 confirms that it is appropriate to solve a standard RBC model by perturbation method as the ROC is covering the most used calibration for σ_z.

1.4 Numerical Applications on complex model variants

This section studies perturbation solutions of models with more complex features, unknown ROC, and higher sensitivity on the localness. To be consistent with earlier numerical applications, I decide to stick with the RBC model and its variants. There are two advantages associate with this roadmap. First, the RBC model has the most stable structure that allows the practice to fully concentrate on continuing the sensitivity analysis rather than becoming distracted by other modeling issues. Second, the RBC variants in this section are built on previous setups, i.e., all complex features can collapse to the simpler setup by only adjusting the parameterization. Therefore, cross-validation checks can be executed conveniently.

1.4.1 Approximated ROC of RBC model with recursive utility and adjustment costs

I extend the standard RBC model by two extra features in this application: the Epstein-Zin-Weil utility and the adjustment costs. There are two motivations for adding recursive utility. First, recursive utility changes the dynamic a lot and makes the standard RBC model more sensitive to uncertainty shocks. Second, recursive utility separates IES and risk aversion. Therefore, the enlarged parametric space may change the calibrations, especially for γ and σ_z. For comprehensiveness, I also include the adjustment costs.

1.4.1.1 Model set up, equilibrium conditions, and solution strategy

I follow Kaltenbrunner and Lochstoer (2010) in specifying a basic RBC model with the Epstein-Zin-Weil utility. The economy admits a representative agent whose utility function follows Epstein and Zin (1989) and Weil (1990):

$$U(\bar{C}_t) = \left((1-\beta) C_t^{\frac{1-\gamma}{\theta}} + \beta \left(E_t \left[U\left(\bar{C}_{t+1}\right)^{1-\gamma} \right] \right)^{\frac{1}{\theta}} \right)^{\frac{\theta}{1-\gamma}} \tag{1.18}$$

$$\theta = \frac{1-\gamma}{1-\frac{1}{\psi}},\ \bar{C}_t = (C_t, C_{t+1}, \ldots)$$

where $\beta \in (0,1)$ is the subjective discount factor, $\mathbb{E}_t$ is the conditional expectations operator, C_t denotes aggregate consumption, γ denotes the agent's coefficient of relative risk aversion, and ψ denotes the agent's inter-temporal elasticity of substitution (IES).

A single firm owns the capital stock and produces a consumption good via Cobb-Douglass technology, using labor and capital as inputs:

$$Y_t = \left(Z_t L_t\right)^{1-\alpha} K_t^{\alpha}$$

with the log technology process $z_t = \ln Z_t$, which evolves exogenously according to

$$z_t = \mu t + \tilde{z}_t,$$

$$\tilde{z}_t = \varphi \tilde{z}_{t-1} + \chi \sigma_z \epsilon_t,$$

$$\epsilon_t \sim \mathcal{N}(0,1)$$

For the law of motion of capital with adjustment cost, I follow same construction as Jermann (1998), and the system is captured by

$$K_{t+1} = \phi\left(\frac{I_t}{K_t}\right) K_t + (1-\delta) K_t, \tag{1.19a}$$

$$\phi(x) = \frac{\alpha_1}{1-1/\xi} x^{1-1/\xi} + \alpha_2 \tag{1.19b}$$

where $\alpha_1 = \left(\exp(\mu) - 1 + \delta\right)^{1/\xi}$ and $\alpha_2 = \frac{1}{1-\xi}\left(\exp(\mu) - 1 + \delta\right)$. The parameter ξ governs the degree of concavity and capital stock grows deterministically at rate $\exp(\mu)$.

To solve the model, notice that L_t does not appear in the utility function. Hence, the maximized labor can be normalized to $\bar{H} = 1$, then the production function becomes

$$Y_t = Z_t^{1-\alpha} K_t^{\alpha} \tag{1.20}$$

For the technology process, I restrict the value of φ to be 1, as this helps reduce the dimension of state space. Thus, the log TFP is a random walk with drift parameter μ, and in this special case, shocks to technology are permanent, this returns the following process for innovation

$$Z_t = Z_{t-1} \exp\left(\mu + \sigma_z \epsilon_t\right), \quad \epsilon_t \sim \mathcal{N}(0,1) \tag{1.21}$$

The following normalized variables (by the level of the contemporaneous technology process) preserve the stationarity of the economy:

$$\left\{\hat{C}_t, \hat{K}_t, \hat{Z}_{t+1}, \hat{I}_t, \hat{Y}_t, \hat{V}_t\right\} = \frac{\{C_t, K_t, Z_{t+1}, I_t, Y_t, V_t\}}{Z_t} \tag{1.22}$$

Combining equation (1.18)-(1.22) with resource constraints, the normalized system of equilibrium conditions can then be expressed as[10] (the $\check{x}$ notation for optimal values of x)

$$\hat{V}\left(\hat{K}_t\right) = \left((1-\beta)\hat{C}_t^{\frac{1-\gamma}{\theta}} + \beta\left(\mathbb{E}_t\left[\hat{Z}_{t+1}^{1-\gamma}\hat{V}\left(\hat{K}_{t+1}\right)^{1-\gamma}\right]\right)^{\frac{1}{\theta}}\right)^{\frac{\theta}{1-\gamma}} \tag{1.23a}$$

$$1 = \mathbb{E}_t\left[M_{t+1}\phi'\left(\frac{\hat{I}_t}{\hat{K}_t}\right)\left(\frac{(\alpha-1)\hat{Y}_{t+1} + \hat{C}_{t+1}}{\hat{K}_{t+1}} + \frac{\phi\left(\frac{\hat{I}_{t+1}}{\hat{K}_{t+1}}\right) + 1 - \delta}{\phi'\left(\frac{\hat{I}_{t+1}}{\hat{K}_{t+1}}\right)}\right)\right] \tag{1.23b}$$

$$M_{t+1} = \beta\left(\frac{\check{C}_{t+1}}{\check{C}_t}\right)^{-\frac{1}{\psi}} \frac{\check{V}_{t+1}^{\frac{1}{\psi}-\gamma}}{\left(\mathbb{E}_t\left[\check{V}_{t+1}^{1-\gamma}\right]\right)^{1-\frac{1}{\theta}}} \tag{1.23c}$$

$$\hat{K}_{t+1} = \frac{\hat{K}_t}{\hat{Z}_{t+1}}\left((1-\delta) + \phi\left(\frac{\hat{I}_t}{\hat{K}_t}\right)\right) \tag{1.23d}$$

$$\hat{Z}_t = \exp\left(\mu + \chi\sigma_z\epsilon_t\right), \quad \epsilon_t \sim \mathcal{N}(0,1) \tag{1.23e}$$

For the numerical specification of equilibrium conditions (1.23), I follow Judd et al. (2014) to define the recursive dynamic system by deviation terms to avoid the convergence

[10] For details of deriving the equilibrium system, see A.5 and Aldrich and Kung (2011).

issue (see Technical Appendix). Also, it is easy to show that this model will collapse to the standard RBC model with a certain selection of parameters. This interchangeability feature ensures ROC sensitivity comparison between model specifications is consistent in this paper. For example, the ROC differences between the closed-form neoclassical growth model and the standard RBC model are induced by varying model parameterizations from Section 1.3.1 to Section 1.3.2. Similarly, the ROC differences between the standard RBC model and the RBC model with recursive utility result from adding new model features from Section 1.3.2 to this section.

1.4.1.2 ROC sensitivity on parameterizations

The appropriateness of a perturbation solution on a specific dimension depends on the smallest radius of convergence among value function and all policy functions. In the model with recursive utility, jumping variables (especially the value function and total welfare) are more sensitive to uncertainties than the standard RBC model. Hence, in this application, let us shift gear to the sensitivity analysis of ROC of value function on TFP volatility dimension.

Table 1.4: Calibration for RBC model with recursive utility and adjustment cost

β	ψ	δ	γ	α	μ	ξ	σ_z^L	σ_z^H
0.998	1.5	0.025	0˜80	0.36	0.004	13	0.01˜0.02	0.03˜0.04

As a motivative example, Figure 1.6 plots the ROC of capital policy function and value function on σ_z dimension, using calibrations from Table 1.4[11].

From Figure 1.6a, one can see the ROC of σ_z for capital policy function and value function are very different. The ROC of $\hat{K}_{t+1}(\cdot)$ is five times larger than $\hat{V}_t(\cdot)$ on σ_z dimension.

[11] I use calibrations from Aldrich and Kung (2011) as the models are identical, except for γ

As a graphical explanation, Figure 1.6b shows the perturbation solution (lower surface) of value function is curved while the "true" value function (upper surface) solved by the projection method is quite flat on σ_z dimension. Clearly, such a curvature difference indicates that the ROC of value function on the TFP volatility dimension is fairly small.

Figure 1.6: ROC of σ_z for $\hat{K}_{t+1}(\cdot)$ and $\hat{V}_t(\cdot)$

(a) ROC comparison

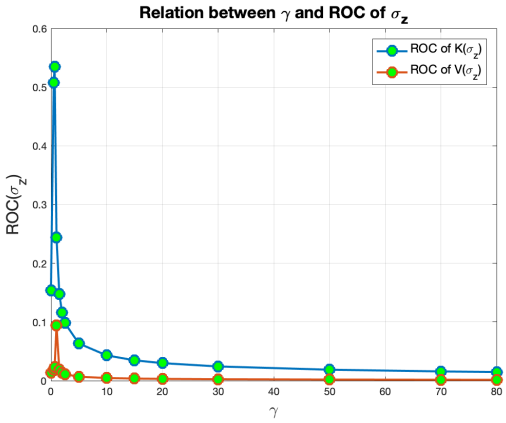

(b) 3-D plot of Value function

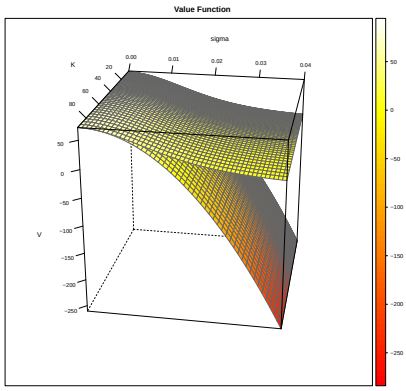

To display the sensitivity analysis, I stick with the 3-D surface plot as in Section 1.3.2. However, as the sensitivity of ROC is determined by three parameters in this case (because IES and risk aversion are two separate parameters in recursive utility), I use two figures to plot the approximated ROC surfaces when one of the three parameters is fixed, and the other two are freely adjustable.

Figure 1.7 shows the sensitivity of ROC of σ_z when δ is fixed and γ and ψ can change freely. The first panel is the smoothed surface for the ROC approximations, whereas the second and the third panel are two slices taken from the 3-D surface. The range for ψ and γ cover the most commonly used calibrations.

Figure 1.7: Sensitivity of ROC of $\hat{V}_t(\sigma_z)$ with respect to γ and ψ at $\delta = 0.0196$

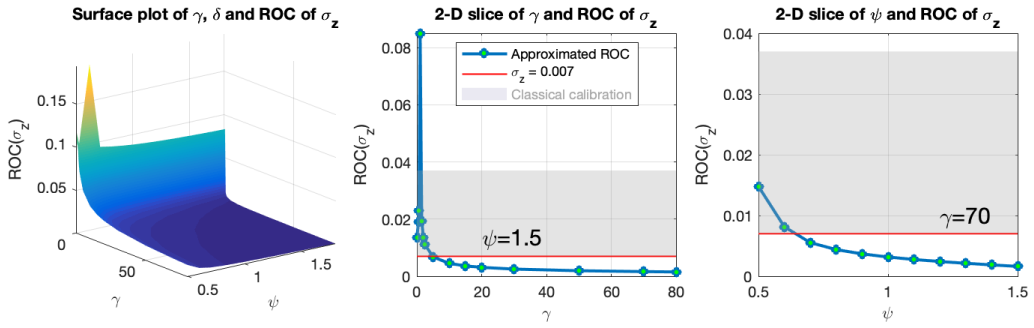

When depreciation takes a classical calibration, Figure 1.7 shows the ROC of σ_z behave exactly the same as the standard RBC model once ψ is fixed. The ROC achieves its peak when $\gamma = 1$ but sharply decreases as risk aversion deviating from it. Notice the ROC of σ_z is around 0.01 at $\psi = 1.5$ and $\delta = 0.0196$, which implies the perturbation method is only appropriate for solving the case when the volatility and risk aversion is low. Using the risk aversion estimation from Van Binsbergen et al. (2012), when γ takes a value of around 66, the ROC of σ_z is only approximated to be 0.002, which is much smaller than 0.007. As the third panel shows, the perturbation solution cannot capture the true dynamics when risk aversion is close to 70. The ROC of σ_z is only about 0.002 when $\psi = 1.5$. Hence, to conclude, the ROC of σ_z is extremely sensitive to of IES variations and risk aversion when the depreciation rate is set to be about two percent. Further, for most risk aversion values, the perturbation method is not appropriate for solving the RBC model with the recursive utility.

Figure 1.8 shows the sensitivity of ROC of σ_z when ψ is fixed and γ and δ can change freely. It has the same layout as Figure 1.7. The range for δ covers all possible values (i.e., from 0 to 1), the value of γ covers the most commonly used calibrations. When IES takes a classical value, the second panel suggests the ROC of σ_z is quite volatile once δ is fixed. In the opposite, ROC is relatively stable if γ is fixed while the depreciation moves around. The ROC of σ_z is at

its peak when $\gamma = 1$ but deteriorates to 0.0025 as it approaches 80. Again, this result implies the appropriateness of the perturbation solution is only restricted to low volatility states with a low risk aversion.

Figure 1.8: Sensitivity of ROC of $\hat{V}_t(\sigma_z)$ with respect to γ and δ at $\psi = 1.5$

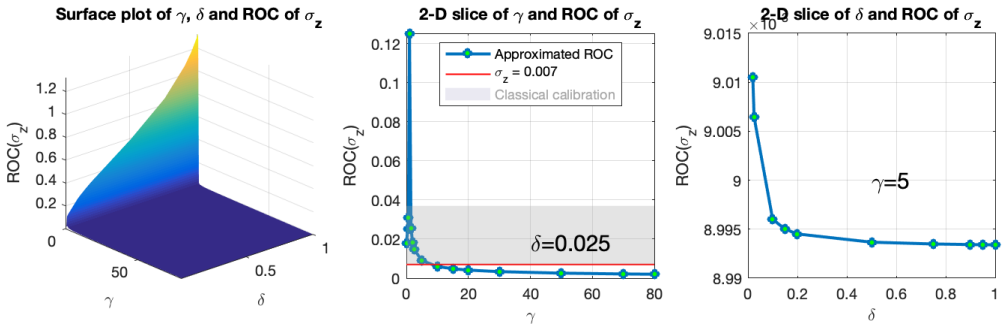

1.4.2 ROC VS. Euler equation error

As an extension of this application, I also compare the proposed algorithm with the Euler equation error on accessing the localness of the perturbation solutions. The comparison in this part shows the Euler equation error is insufficient for testing the appropriateness of the perturbation solution as it may rejects a valid approximation that associate with feasible parameterization.

Figure 1.9 plots some essential comparisons between the projection and the perturbation method. For this practice, I only focus on the first row of the figure. Fixing ψ, δ, and σ_z (I choose low volatility because previous application suggests the perturbation solution is only appropriate when $\sigma_z = 0.01$), I artificially select the value for γ to calculate the mean Euler equation error for different discount factors. The dashed red line corresponds to the third-order perturbation solution and the solid black line corresponds to the tenth-order Chebyshev projection solution. There are two observations from this plot. First, the Euler equation error accepts the perturbation solution for the case with low TFP volatilities and a low risk of aversion.

Second, the perturbation solution will be rejected by the Euler equation error for the cases with higher γ value and β closes to 1.

Figure 1.9: Mean $\log_{10}$ Euler equation errors, mean risk-free rate and mean log ratio of value function to consumption policy, plotted as functions of β for $\psi = 1.5$, $\delta = 0.025$, $\sigma_z = 0.01$ and different values of γ.

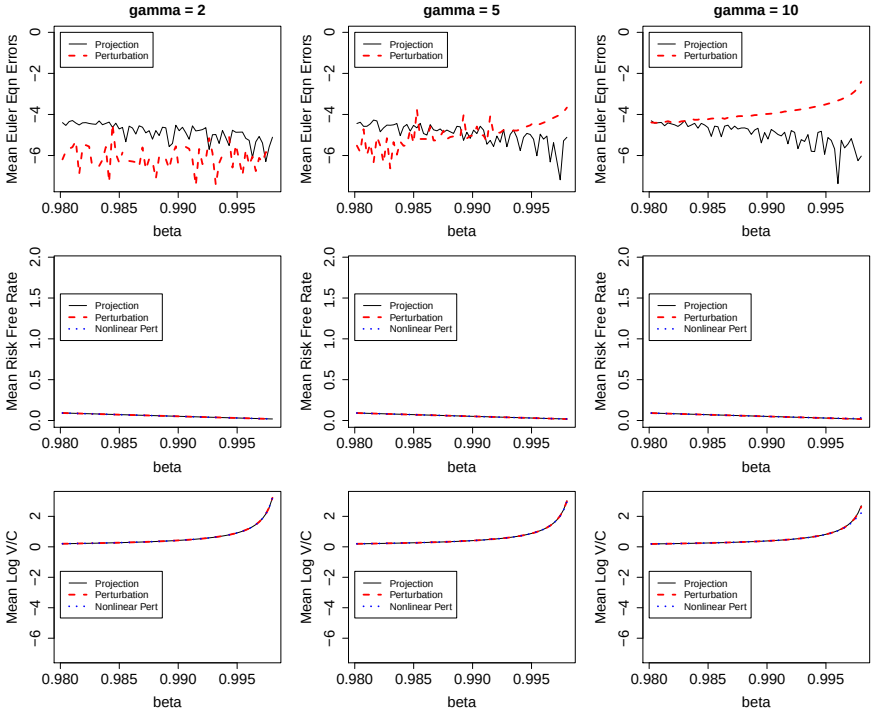

In fact, I double-check the reliability of these two conclusions by Den Haan-Marcet statistics (χ^2 test). As a summary, Table 1.5 displays the proportion of time that the Wald-type statistic is above or below the 5% points of the $\chi^2(11)$ density.

First, this test confirms that the perturbation solution can solve cases with low TFP volatilities and a low risk of aversion. Also, it rejects the perturbation solution for case $\gamma = 10$ (same as ROC and EEE). For the intermediate case with $\gamma = 5$, the χ^2 test provides us with confidence regarding the appropriateness of perturbation solution. Recall the approximated

ROC of the model with $\gamma = 5$ and $\delta = 0.025$ in the middle panel of Figure 1.8 is around 0.01, which means the perturbation solution is appropriate. However, by taking a close look at the middle panel of the first row of Figure 1.9, EEE rejects the approximation made by the perturbation method for $\beta = 0.998$, this result directly contradicts to results from both the ROC algorithm and the χ^2 test. Therefore, this practice can be thought of as a perfect example of demonstrating that a large Euler equation error is not sufficient to rule out valid parameterization and its associated perturbation solution. Rather, the better way of interoperating this contradiction is that, even thought ROC approximation confirms the appropriateness of the perturbation solution, the EEE suggests such an solution is only accurate up to the second order.

Table 1.5: Den Haan-Marcet statistics, computed for 500 simulations of $T = 3000$ quarterly observations. The numbers in the parentheses represent the proportion of times the statistic was below and above, respectively, the 5% and 95% percentage points of the $\chi^2(11)$ density. In all cases, $\beta = 0.998$.

	σ_z		
	$\gamma = 2$	$\gamma = 5$	$\gamma = 10$
Projection	$(0.052, 0.054)$	$(0.052, 0.052)$	$(0.050, 0.052)$
Perturbation	$(0.058, 0.052)$	$(0.050, 0.058)$	$(0.006, 0.338)$

To sum up, all current existing numerical methods are less efficient and *ex-post* on assessing the appropriateness of perturbation solution. However, with the 2S-Inter-ld algorithm, as long as the model is solved non-linearly (i.e., the perturbation order is higher than 1), the approximated dynamics, perturbation-based model estimations, and sensitivity analysis on model solutions can be better executed.

1.4.3 Adding stochastic volatility

For a comprehensive sensitivity analysis (in the asset-pricing literature) on the model solution with recursive utility, the model in this section inherits the same structure as in Section 1.4.1, with stochastic volatility added. The equilibrium system is identical to (1.23) with an additional equation for the stochastic process of TFP volatility. For the stochasticity of TFP variance, I follow Caldara et al. (2012), whose process is captured by the following equation

$$\sigma_{z,t} = (1-\rho)\,\bar{\sigma}_z + \rho\sigma_{z,t-1} + \eta\varepsilon_t, \quad \varepsilon_t \sim \mathcal{N}(0,1) \tag{1.24}$$

and for the calibration, I use 0.9 for ρ and 0.06 for η. Notice that equation (1.24) does not change the deterministic steady states of this model. However, it introduces one extra state $\sigma_{z,t}$, for which variable the steady state value is set to be 0.01 for conservative reasons. As a continuation of the sensitivity analysis, this practice will still concentrate on the sensitivity of ROC of $\sigma_{z,t}$ on different depreciation, IES, and risk aversion values.

Figure 1.10 plots the ROC approximations of the model with recursive utility and stochastic volatility. For $\delta = 0.0196$ (Figure 1.10a) and $\psi = 1.5$ (Figure 1.10b), all previous concluded properties of ROC are preserved when having stochastic volatility (the shape of the 3-D surface and 2-D slides are all behaved similarly as in Section 1.4.1). However, by comparing the transparent surface and blue curve (model with recursive utility only) with the darker surface and red curve (model with recursive utility and stochastic volatility), the approximated ROC of $\sigma_{z,t}$ from the latter model's structure is uniformly smaller than the former. Therefore, the perturbation solution is totally inappropriate on solving RBC model recursive utility and stochastic volatility over the entire parametric space (with the only exception when γ is closely around 1). This new finding is contradicting with Caldara et al. (2012). However, as the 2S-Inter-ld algorithm is more capable of assessing the appropriateness of perturbation solution, I appeal to the conclusion made here.

Figure 1.10: Comparison of ROC sensitivity between $\hat{V}_t(\sigma_z)$ and $\hat{V}_t(\sigma_{z,t})$

(a) 3-D projection on (γ, ψ) space with $\delta = 0.0196$

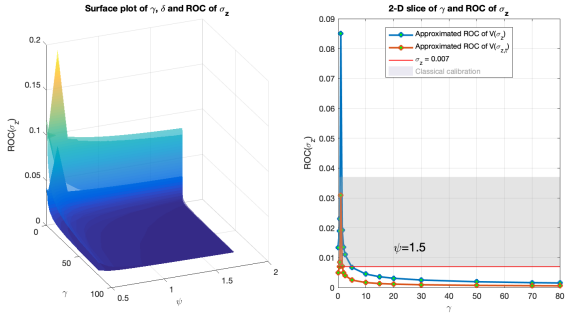

(b) 3-D projection on (γ, δ) space with $\psi = 1.5$

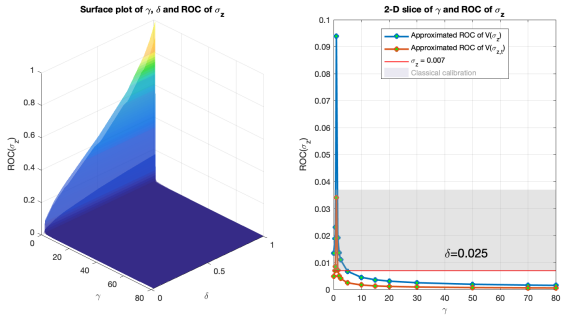

1.5 Conclusion

In which dimension and what degree the localness issue of perturbation method is going to influence the related economics study is unknown, and at best, we have little knowledge about this for some special cases. By step back to the original definition of the radius of convergence, this paper develops a numerical method that approximates the ROC of an objective function using a finite perturbation solution. It has two stages, where the first-stage solves an optimal function fitting problem with a polynomial interpolation solution and a log-absolute difference solution from a finite set of non-zero perturbation coefficients. In stage two, this algorithm

imposes increasing monotonicity onto the first stage approximation. This approximation preserves the dependency between the ROC, model structure, and deep parameters. In the limit, the solution is an equivalent transformation of the d'Alembert's ratio test. By Taylor theorem, it delivers a necessary and sufficient approximation for the localness of perturbation solutions.

The main methodology contribution of this paper is summarized into Algorithm 1. Section 1.2.4 uses a simple square root function as a representative example to show the exact implementation of Algorithm 1 in steps.

To test the reliability of the 2S-Inter-ld algorithm in economic applications, Section 1.3.1 conducts experiments on Algorithm 1 by two closed-form macro models. Results show that the proposed algorithm can access the appropriateness of perturbation solutions of economic models as it can replicate findings of previous case studies on the localness of perturbation method for specific model setup. Hence, Algorithm 1 is the first general and *ex-ante* numerical method on addressing the localness issue of the perturbation method.

In Section 1.4, I formulate a series of sensitivity analyses to address the classical puzzle of TFP volatility calibration in macroeconomics. I use the proposed method on the standard RBC model and its extensions to study the effect of different models' structure and parameterizations on ROC of TFP volatility.

The first case study confirms that the perturbation method is appropriate for solving the standard RBC model. Regardless that the closed-form neoclassical growth model has an infinity ROC for TFP shock, the ROC is extremely sensitive to calibration variations. Actually, this number will decrease drastically once it deviates from the log utility and full depreciation. Nevertheless, such a property does not prohibit the perturbation method from being a good choice for solving the RBC model with classical parameterization, as the ROCs are large enough to cover most of the commonly used calibrations. Consequently, the dynamics are well approximated.

As a continuation, I also test the sensitivity of the ROC of the RBC model with recursive utility, in which model setup the dynamics react to uncertainty a lot more. Using the ROC of TFP volatility for the value function as an example, I show the ROC is sensitive to different parameterizations. Moreover, the ROC of the value function is much smaller than other policy functions. To add, the ROCs of this model are uniformly (i.e., for all policy functions and the value function) smaller than the standard RBC model. Twisting IES, depreciation, and risk aversion around the classical calibrated values, I find the perturbation solution is only appropriate for cases with a low TFP volatility and low risk aversion. As a result, one may wants to use the perturbation method with cautions here.

For the extra extension, Section 1.4.2 is used to explain the insufficiency of the Euler equation error on assessing the appropriateness of perturbation solution. By running a cross-validation check between EEE, ROC, and χ^2 test, a main finding of this study is that the Euler equation error rejects the perturbation solution with feasible parameterization when both the ROC algorithm and the χ^2 test accept it. This contradiction proves the insufficiency of the EEE method.

As the last part of the sensitivity analysis, I use the RBC model with recursive utility and stochastic volatility. Motivated by previous results, one should expect to see the failure of perturbation method on solving the modeling economy. It turns out that the results indicates the perturbation method is totally inappropriate on handling the model setup of this section. Hence, any perturbation-based method is not able to provide adequate support for any research purposes for a model with recursive utility and stochastic volatility.

Chapter 2

Wealth Inequality, Production Heterogeneity and Declining Business Dynamism

2.1 Introduction

General equilibrium (GE) models with heterogeneity have received increasing attention and seen tremendous development in recent years. These models use the capability of homogenous general equilibrium models that allow one to study the steady state economy and transitional dynamics while keeping everything in a relatively manageable fashion and embedding it with heterogeneity to study the micro foundation of macroeconomic topics. Two types of model structure are particularly contributive in terms of better connecting macroeconomic theories with microeconomic evidence. They are the heterogenous household (or heterogenous agent) model and the heterogenous firm model. Most importantly, each type of model is associated with a set of fundamental questions that macroeconomists are trying to answer. General equilibrium

model with heterogenous households introduced by Bewley (1977) and Krusell and Smith (1998) provide a profound way to study how movements in the distribution of income and wealth affect the macroeconomy. GE models with firm heterogeneity introduced by Khan and Thomas (2008), are able to uncover the mechanism on how idiosyncratic shocks and firm-specific investment decisions can affect the aggregate dynamics.

In this paper, inspired by the work of Buera and Shin (2013), I build a heterogenous individual GE model by introducing endogenous TFP growth and endogenous firm entry and exit to study the interactions between heterogenous households and heterogenous firms. The model economy features a continuum of individuals with heterogeneous entrepreneurial abilities and assets. Each individual face two occupational choices in every period, i.e., to be a worker or an entrepreneur. The TFP distribution (the aggregation between an individual's entrepreneurial ability and the aggregate TFP of the economy) of firms ranges endogenously. Every entrepreneur's capital input is subject to a collateral borrowing constraint based on the firm's value. A credit crunch in the model acts as an unexpected reduction of the maximum capital that entrepreneurs can borrow from financial markets. Therefore, a dynamic threshold on wealth holdings always distinguishes entrepreneurs from workers.

This paper aims to connect heterogenous households with heterogenous firms, and use it to address challenging topics. The motivations for this paper are threefold. First and foremost, many recent studies have highlighted the limitations of a model that only contains one source of heterogeneity. For instance, when trying to study the source of aggregate fluctuations, Buera and Moll (2015) found that different variants of heterogenous firm models always resulted in an undistorted Euler equation for the aggregate of firm owners; therefore it indicates the limitation of using representative agent models to identify sources of business cycle fluctuations. On the other hand, as De Nardi and Fella (2017) pointed out in their survey paper on heterogenous household models, allowing for heterogeneity in entrepreneurial production functions in a workhorse

model such as Marco and Mariacristina (2009) is essential for a number of questions, including the effects of taxation and government support programs on various types of entrepreneurs. Since all of these papers are built upon a neoclassical growth model, an attempt to build GE model with individual heterogeneity will help conquer the above mentioned limitations.

Secondly, one particular set of observations – a number of striking trends that indicate a rising market concentration and a slowdown in business dynamism – draws a lot of attention. To be specific, throughout this paper, I will use stylized facts summarized by Akcigit and Ates (2020a,b) as my main background references for declining business dynamism (DBD)[1]. Among the ten stylized facts listed in these works[2], I focus on seven of them (Fact 1 - Fact 7[3] from Akcigit and Ates (2020a)) since the other three facts (Fact 8 - Fact 10) are closely related to models on firm competition and beyond the horizon of this paper. DBD raises many challenges to macroeconomists, because some of the facts are closely connected to models with heterogenous firm (e.g., Fact 1, 2, 3), while some others are requiring models featuring heterogenous agents (e.g., Fact 7). An advantage of applying my model to the DBD literature is that with a heterogenous individual GE model, the stylized DBD facts can be studied jointly; the interactions between different facts may provide us with better understanding of the economic insights. Hence, it leads the focus of this paper toward the literature on DBD.

Last but not least, computational technics have improved a lot in the past few years, which opens the possibility of solving a fully heterogenous model. Two papers are beneficial for my model. Winberry (2018) created a brand new routine on solving and estimating heterogeneous agent macro models with aggregate shocks. He showed the method could be easily applied in

[1]The reason I decide to stick with these two papers are twofold. First, there are less common agreement among researchers on the "stylized facts" of DBD. Among of which, Akcigit's papers are one of the most representative and comprehensive series of works, hence I take those as the most updated references for the literature background of this study. Second, the stylized facts list in these works contain motivations for heterogenous individual GE model, and is naturally a good place to apply my model.

[2]I have list all ten stylized DBD facts in Appendix B.1 for referential purpose.

[3]These 7 stylized facts are, (1) increasing on market concentration , (2) increasing on average markups, (3) increasing on the profit share of GDP, (4) decreasing labor share of output , (5) fact (1) and (4) are positively associated, (6) increasing on productivity dispersion, (7) declining firm entry rate.

`Dynare` with advantages such as it is fast, general, and accurate for models like Krusell and Smith (1998) and Khan and Thomas (2008). Moreover, as he points out, his method can be extended to solve a fully heterogenous model. In the study of the labor wedge in a DSGE model with collateral borrowing constraint. Zhang (2018) finds that a credit crunch can affect the labor wedge through a mechanism different from an exogenous TFP shock when there are endogenous entry and exit of production. The model she used is a fully heterogenous individual neoclassical growth model, where each individual can decide to become an entrepreneur or a worker. Both papers not only bring confidence to the motivations of this paper but also provide valuable technical foundations for the numerical part of this study.

My model is able to connect the individual's wealth holding decision with the firm-specific technological innovation process. Under negative structural changes, the interactions between wealth inequality and productivity heterogeneity in this model can lead the dynamics to a steady state, in which process, the declining business dynamism such as market concentration and declining firm entry occurs (I name this mechanism as "winner takes all" dynamics, and will explain it in detail in a later section). Among the seven stylized facts I work with, my GE model is silent for endogenizing facts such as decreasing labor share and increasing productivity gap. Comparing to facts that could be matched with the model's transitional dynamics, I find they are more fit into a role such as exogenous changes of this model. As a result, I decided to treat both facts as exogenous variations, which cause the transitional dynamics to happen.

To better illustrate the capability of the model and its potentials to match with stylized DBD facts, Table 2.1 highlights the connections between the model's key features with stylized DBD facts[4]. Notice that the endogenous TFP growth feature of firms (heterogenous firm) is able to create transitional dynamics with divergent individual productivity. Over time, firms

[4]I dropped Fact 5 since if an exogenous labor share drop can trigger increasing market concentration, it immediately satisfied by convention.

with better productivity can scale up their production, ending with a higher total production share. As a result, market concentration increased. Since firm with better productivity becomes more competitive than others, their markup will increase during the transitional dynamics, so as their profit. On the other hand, the heterogenous individual setup has a natural result whenever an individual decides to switch her role – the firm entry and exit (i.e., entrepreneur to worker or worker to entrepreneur). This property, in particular, will spilt firms with lower productivity and wealth holding from the producer side. Furthermore, over time, lower division of the production side will gradually leave the market; meanwhile, due to the inflated threshold on productivity level and asset holding for running a new business, the entry rate also declines. As a result, the market is more concentrated on firm with better productivity. With such an advantage, firms at the upper division raise their markup. Throughout this whole process, wealth inequality will be amplified, and productivity dispersion will also be deepened.

Table 2.1: Match DBD facts with model's key features

Stylized Facts	Endogenous TFP growth	Endogenous Firm Entry & Exit
Fact 1. Increasing Market Concentration	✓	✓
Fact 2. Increasing markup	✓	✓
Fact 3. Increasing profit	✓	
Fact 6. Divergent Productivity	✓	
Fact 7. Declining Firm Entry Rate		✓

With everything mention above, I summarized the main hypothesis of this paper as follows: *structural changes* (such as productivity dispersion or decreasing labor share) trigger the transitional dynamics between two stationary equilibriums. A fully heterogenous individual

model, including firms-specific technological innovation process and endogenous firm entry & exit, allows interactions between *Wealth inequality* and *Productivity dispersion*. With negative structural changes, such a "winner takes all" dynamics in a heterogenous individual GE model can (ideally) replicate some of the observed stylized facts of declining business dynamism.

The main object I use to test the hypothesis is the joint distribution of firm's productivity and wealth. Conceptually speaking, if the heterogenous individual GE model and the "winner takes all" dynamics work well, the joint distribution should variate accordingly. In order to accomplish this, I decide to use a *two stages architecture* for this paper. In the first stage, I simplified the full model and run a comparative static analysis to show that wealth inequality can interact with individual productivity. By imposing different exogenous variations into the model, I show that the stationary joint distribution is not always distorted. This practice implies that my model with only structural changes cannot create both wealth inequality and productivity dispersion. Instead, introducing other sources of distortionary dynamics (e.g., the "winner takes all" dynamics) is necessary. Currently, in my stage two study, I built the full model and derived associated equilibrium conditions. Accompany with this, I also provide intuitive explanations for the "winner takes all" dynamics and how it can contribute to study the stylized DBD facts.

Finally, this paper is related to three sets of literature. It first related to the literature on declining business dynamism. Here I will only cite some representative works on the stylized facts I discussed in this paper. For the exogenous changes used by my model, Andrews et al. (2019) discuss their finding on the connection between weaker productivity and stronger divergence among frontier and laggard firms (Fact 6). In the paper demonstrating the steady decline in the labor share of output in the United States since the early 1980s, Karabarbounis and Neiman (2014) highlighted this trend also has an international nature (Fact 4). For the facts that the "winner takes all" dynamics is try to match, Autor et al. (2017, 2019) show that the degree of market concentration measured by the Herfindahl-Hirschman index (for largest 4 and 20 firms)

are increased over time. This result also aligns with the general conclusion on increasing market concentration in most U.S. industries in the post-2000 era (Fact 1). As Hall (2018) and others described, there is a global rise in markups (driven by firms in the top decile of the markup distribution) and a widening average markup gap between digitally-intensive and other sectors (Fact 2). Aghion et al. (2019) explain the link between innovation and top income inequality in the United States and show evidence of the tight association between innovative activity per capita and profit share of output (Fact3). In Autor et al. (2017), the authors provide suggestive evidence on new technological advances that favor more productive companies, namely, a positive association between industry-level productivity (measured by output per worker, patents per worker, etc.) and concentration (measured by the fraction of sales accrued by 20 largest firms) (Fact 5). Consistent with the work from Gourio et al. (2016), I consider the falling firm entry rate from Business Dynamics Statistics data as evidence on output losses (Fact 7).

The construction of my model is based upon the literature on wealth inequality, endogenous TFP growth and Heterogenous RBC models. For the first key feature of this paper, the firm-specific technological innovation process takes similar forms as modeled by Greenwood et al. (1997) and Cooper and Johri (2002), where the individual productivity takes Cobb-Douglas form between the firm's specific productivity investment and its productivity level of the current period. For the wealth inequality and individual heterogeneity, I borrow the idea from Marco and Mariacristina (2009); De Nardi and Fella (2017), and Wolff (2017). In the model, each individual has a certain amount of asset holding for both precautionary saving and personal investment (on their entrepreneur ability) purposes. The main difference is, in my model, an individual can switch her role between worker and entrepreneur. In order to connect both features, I build up the model parallel to Khan and Thomas (2008) and Buera and Shin (2013). One specialty of my model is, by twisting some parameters, the system can be reduced to their specifications.

Lastly, I use the following works from the numerical method literature for solving my model. I use Winberry (2018) on solving the heterogenous agent model as the cornerstone. At the same time, I also borrow the idea from Aiyagari (1994) and Krusell and Smith (1998) on Kolmogorov forward equation; Den Haan et al. (2010) on steady-state transitions. With these works, I am able to solve my heterogenous individual GE model, running the comparative static analysis and study transitional dynamics.

The rest of the paper is organized as follows. Section 2 describes the full model (Stage 1 and 2 combined). Section 3 presents the comparative static study on the stationary joint distribution of the simplified model. Section 4 illustrates the connection between the full model and the "winner takes all" dynamics. Section 5 summarizes and discusses future extensions.

2.2 The Full Model (Stage 1 and 2 combined)

In this paper, I propose a heterogenous individual general equilibrium model with endogenous individual-specific technology innovations (determined by individual's wealth holding and idiosyncratic individual productivity shock) and endogenous firm entry and exit to study the stylized facts of declining business dynamism (DBD) documented by Akcigit and Ates (2020a,b). In this model, the decreasing labor share and divergent productivity are treated as exogenous variations. This paper has two stages. In the first stage, I will work with a simplified model, and in the second stage, I will work with the full mode. For exposition purpose, I will start with the full model in this section.

2.2.1 Heterogeneity and demographics

Borrowing the idea of home production economy from Buera and Shin (2013), I build my model with discrete time and assume that the economy is populated by a continuum of

individuals indexed by $i \in [0,1]$. Each individual is endowed with one unit of time to divide between labor n_t and leisure $1 - n_t$. Individuals live indefinitely and can save using risk-free assets (or wealth) a_t.

Individuals are heterogeneous with respect to their wealth holdings and individual-specific productivity A_I (or entrepreneurial ability). Entrepreneurial productivity evolves according to an exogenous AR(1) process in the Stage 1 model but grows endogenously in the Stage 2 model. At each period, in the Stage 2 model, individuals choose either to operate a firm with individual-specific technology (i.e., to become an entrepreneur) or to work for a wage. However, they are not allowed to make occupational decisions in the Stage 1 model[5].

At the beginning of a period, each individual draws a random fixed cost ξ in units of consumption good from a uniform distribution $\mu(\xi)$, where $\xi \in \left[0, \bar{\xi}\right]$. After the fixed cost ξ is realized, each individual chooses whether to pay the realized fixed cost to change her occupation or simply maintain her current role and pay nothing. By making an occupational decision, entrepreneurs can endogenously enter and exit the production. Let $\mathbb{OD}$ denotes the occupational decision of an individual from the previous period. Since the idiosyncratic random fixed cost is only paid when an individual changes occupation, keeping track of the occupational history for one period is sufficient for the analysis. Then, we can define occupational decision as

$$\mathbb{OD} = \begin{cases} 1, & if\ previouly\ is\ entrepreneur \\ 0, & if\ previouly\ is\ worker \end{cases} \tag{2.1}$$

Throughout the dynamics, I will use $G_t(A_I, a, \mathbb{OD})$ to denote the time variate joint distribution of individual productivity, wealth and occupational decision. After period 0, the dynamics of A_I , a, $\mathbb{OD}$ and $G_t(A_I, a, \mathbb{OD})$ follow the individual's optimal decision rules. Notice that for the Stage 1 model, the occupational decision channel can be easily shut down by replace

[5]Both Stage 1 and Stage 2 model can be written into a generalized (unified) model framework, they can be derived by assigning different parametric values to the full model.

$\mu(\xi) = \bar{\xi} = \infty$.

2.2.2 Preference

Each individual shares the same utility function from consumption and leisure using the same discount factor β. The individual's utility function at period s takes the form

$$\mathbb{E}_0 \sum_{t=s}^{\infty} \beta^{s-t} u(c_s, 1-n_s)$$

$$\text{where } u(c_s, 1-n_s) = \frac{\left(c_s^{\tau}(1-n_s)^{(1-\tau)}\right)^{1-\sigma} - 1}{1-\sigma}, n_s \in \{n_s^w, n_s^e\} \tag{2.2}$$

where n_s^w stands for the working hours of worker and n_s^e for entrepreneur. For simplicity, in the Stage 2 model, I assume individuals will work $\tilde{n}$ hours as long as their occupational choice is entrepreneurs, i.e., $n^e = \tilde{n}$ is a constant. Whereas in the Stage 1 model, an individual can freely adjust her consumption-leisure allocation, i.e., n_s is a choice variable.

2.2.3 Individual-specific technological innovation process

In any given period, firm produces with capital and labor according to the following production technology

$$f(A_A, A_I, k, l) = A_A A_I \left(k^{\alpha}(n+l)^{\theta}\right)^{1-v} \tag{2.3}$$

where A_A is aggregate productivity of the economy, A_I is the individual-specific productivity (or equivalently, entrepreneurial ability), k is capital input. For the Stage 1 model, $(n+l)$ represents the aggregate labor supply. And for the Stage 2 model, individuals can choose either to work for a wage or to operate an firm with its individual-specific technology level. For the latter case, an entrepreneur works $n^e = \tilde{n}$ unit of time for herself. Parameter $1-v$ represents the share of output going to the input factors, α is capital share and θ is labor share. The

aggregate productivity follows a mean zero log AR(1) process

$$\log A_A^{'} = \rho_A \log A_A + \varepsilon_{A_A}, \text{where } \varepsilon_{A_A} \sim \left(0, \sigma_{A_A}^2\right) \tag{2.4}$$

For individual-specific productivity, I assume the technological innovation process takes Cobb-Douglas form as proposed by Cooper and Johri (2002)

$$A_I^{'} = A_I^{\gamma} i_{A_I}^{\eta} \exp\left(\varepsilon_{A_I}\right), \text{where } i_{A_I} = s_{A_I} f\left(A_A, A_I, k, l\right) \tag{2.5}$$

or equivalently the specification similar to Greenwood et al. (1997)

$$\log A_I^{'} = (\gamma + \eta) \log A_I + \eta \left[\log s_{A_I} + \log f\left(A_A, 1, k, l\right)\right] + \varepsilon_{A_I} \tag{2.6a}$$

$$\varepsilon_{A_I} \sim \left((1 - \gamma - \eta) \log \mu_A, \sigma_{A_I}^2\right) \tag{2.6b}$$

where s_{A_I} represents the investment rate on individual-specific productivity A_I for the Stage 2 model (for simplicity, I set it as a constant now). Equation (2.5) and (2.6) combined emphasize that the current individual-specific productivity A_I and the baseline productivity $f\left(A_A, 1, k, l\right)$ are two driven forces of the evolutional process of $A_I^{'}$. To be specific, a firm with better A_I tends to have higher expected individual-specific productivity $\mathbb{E}\left(A_I^{'}\right)$ tomorrow. Similarly, a productive firm also results in higher $\mathbb{E}\left(A_I^{'}\right)$ for future. There are two advantages associated with this specification. (i) It ensures all individuals will have enough motivation to be an entrepreneur if they are wealthy enough. Moreover, an entrepreneur will also have the motivation to invest in individual-specific productivity A_I as it is an increasing function of i_{A_I}; (ii) The path of individual-specific productivity A_I among individuals are going to diverge over time as $\mathbb{E}\left(A_{I_i}^{'}\right) \geq \mathbb{E}\left(A_{I_j}^{'}\right)$ whenever $A_{I_i} > A_{I_j}$ or $f_i\left(A_A, 1, k, l\right) > f_j\left(A_A, 1, k, l\right)$.

For the Stage 1 model, I just set $\eta = 0$, which will give me the standard log AR(1) process for individual-specific productivity without endogenous law of motion.

Throughout the paper, I also assume the labor market is perfectly competitive and frictionless. All individuals in the economy share the same real wage w_t and real return rate on

asset r_t. Therefore individual occupational choices, investment decisions, and labor supply do not affect prices.

2.2.4 Financial markets

Follow the simple linear collateral constraint used by Buera and Shin (2013) and Moll (2014) in studying the financial frictions and resource misallocation. The financial intermediaries are perfectly competitive in this economy. Each entrepreneur can rent capital from financial intermediaries using her deposit asset a_t as collateral. The return to the capital is r_t and the depreciation rate is δ. This implies the effective capital rental rate is $r_t + \delta$.

The collateral constraint limits the entrepreneur's borrowing power with the form

$$k_t \leq \lambda a_t, 1 \leq \lambda \leq \infty \text{ and } a_t \geq 0 \tag{2.7}$$

where parameter λ measures the degree of financial market incompleteness, $\lambda = \infty$ means capital market is perfect. To ensure financial markets allow an individual to smooth consumption via intra-temporal borrowing of capital for production but not inter-temporal borrowing, I impose $a_t \geq 0$.

2.2.5 Time scheme

The time scheme of the economy is as follows:

For the Stage 1 model, everything is parallel to standard heterogenous RBC models, such as Khan and Thomas (2008) and Buera and Shin (2013).

For the Stage 2 model. First, aggregate productivity and individual productivity are realized and known by all. Second, individuals draw random fixed costs and make occupational decisions. Third, individuals deposit assets in the financial market. Entrepreneurs rent capital, hire labor, invest in individual productivity and carry out productions. Finally, workers get

paid, entrepreneurs take the profits, individuals trade and consume final goods.

2.2.6 The individual's problem

The aggregate state in the economy can be denoted by $S = (A_A, G(A_I, a, \mathbb{OD}))$. I will start with defining the worker's problem and the entrepreneur's problem separately. Then I will present a unified way of defining the individual's problem for the model.

The worker's problem

Taking the real wage w and interest rates r as given, a worker solves the following problem in every period:

$$V^w(a, A_I, S) = \max_{\{c, 0 \le n^w \le 1, a' \ge 0\}} \left\{ u(c, 1 - n^w) + \beta \mathbb{E}\left[V'\left(a', A_I', S'\right)\right]\right\} \tag{2.8a}$$

$$\text{s.t. } c + a' \le w n^w + (1 + r)\, a - \xi \mathbb{OD} \tag{2.8b}$$

where $V^w(\cdot)$ is the life-time value of being a worker.

The entrepreneur's problem

Taking the real wage w and interest rates r as given, an entrepreneur solves the following problem in every period:

$$V^e(a, A_I, S) = \max_{\{c, n^e = \tilde{n}, a' \ge 0, k \ge 0, l \ge 0\}} \left\{ u(c, 1 - n^e) + \beta \mathbb{E}\left[V'\left(a', A_I', S'\right)\right]\right\} \tag{2.9a}$$

$$\text{s.t. } c + i_{A_I} + a' \le f(A_A, A_I, k, l) - (\delta + r)\, k - wl + (1 + r)\, a - \xi(1 - \mathbb{OD}) \tag{2.9b}$$

$$i_{A_I} = s_{A_I} f(A_A, A_I, k, l) \tag{2.9c}$$

$$k \le \lambda a \tag{2.9d}$$

where $V^e(\cdot)$ is the life-time value of being a worker.

The Value function

Given that the aggregate state of the economy is S, individual's asset holding a, and individual-specific productivity A_I. A rational behavior will makes her occupational decision that has larger life-time value among the value of being a worker V^w and the value of running an individual-specific technology firm V^e. Which is,

$$V^O(a, A_I, S) = \max\{V^w(a, A_I, S), V^e(a, A_I, S)\} \tag{2.10}$$

where V^O stand for the value function associated with individual's optimal decision. Define $V(a, A_I, S)$ as the beginning of period expected value of an individual prior to the realization of its fixed cost, but after the determination of (a, A_I, S). Then

$$V(a, A_I, S) = \int_0^{\bar{\xi}} V^O(a, A_I, S)\,\mu(d\xi) \tag{2.11}$$

2.2.7 The unified individual's problem

A critical observation from equation (2.8) and (2.9) is that, in the Stage 2 model, the budget constraint is the only difference between the worker's problem and the entrepreneur's problem. However, equation (2.10) and (2.11) allow me to write down the whole model compactly into a single individual's optimization problem. Moreover, since the Stage 2 model can be easily reduced to Stage 1 model by manipulating some parameters, I am actually able to write down a unified individual's problem for both Stage 1 and 2. To be specific, follow the same logic as Buera and Shin (2013) and Moll (2014), taking the real wage w and interest rates r as given,

an individual solves the following problem in every period:

$$V(a, A_I, S) = \max_{\{c, \{n^e = \tilde{n} \text{ or } 0 \leq n^w \leq 1\}, a' \geq 0\}} \left\{ u(c, 1-n) + \beta \mathbb{E}\left[V'\left(a', A_I', S'\right)\right]\right\} \tag{2.12a}$$

$$\text{s.t. } c + a' \leq \max\left\{\pi(a, A_I, S) - \xi(1 - \mathbb{OD}), w n^w - \xi \mathbb{OD}\right\} + (1+r)a \tag{2.12b}$$

$$\pi(a, A_I, S) = \max_{\{0 \leq k \leq \lambda a, l \geq 0\}} \left\{(1 - s_{A_I}) f(A_A, A_I, k, l) - (\delta + r)k - wl\right\} \tag{2.12c}$$

$$\xi \sim \mu(\xi) = \begin{cases} U\left(0, \bar{\xi}\right) & if\ Stage\ 2 \\ \infty & if\ Stage\ 1 \end{cases} \tag{2.12d}$$

where I use $V(\cdot)$ to denote the individual's value function, inside of which the $\pi(a, A_I, S)$ represents the profit of an individual-specific technology firm if individual's occupational choice is entrepreneur.

2.2.8 Competitive equilibrium

I am now defining the competitive equilibrium for the Stage 2 model[6]. Given initial condition $G_0(a, A_I)$, a competitive equilibrium consists of the value function $V(a, A_I, S)$; Worker's allocations $c^w(a, A_I, S)$, $a^w(a, A_I, S)$ and $n^w(a, A_I, S)$; Entrepreneur's allocation $c^e(a, A_I, S)$, $a^e(a, A_I, S)$, $l(a, A_I, S)$, $k(a, A_I, S)$ and $n^e = \tilde{n}$; the evolution of joint distribution of individual-specific productivity and wealth $G(a, A_I)$, and prices (w, r) such that

1. Value function $V(a, A_I, S)$ solves the individual's problem (2.12)

   (a) Allocation $c^w(a, A_I, S)$, $a^w(a, A_I, S)$ and $n^w(a, A_I, S)$ are the associated policy functions to the worker's problem (2.8)

   (b) Allocation $c^e(a, A_I, S)$, $a^e(a, A_I, S)$, $l(a, A_I, S)$, $k(a, A_I, S)$ and $n^e = \tilde{n}$ are the associated policy functions to the entrepreneur's problem (2.9)

[6] I skip to define the CE for Stage 1 model since it is literally the same as the standard heterogenous firm RBC model.

(c) The labor, capital, and goods markets are all clear:

- The labor market clears so that the total demand of labor from entrepreneurs is equal to the total labor supply from workers

$$\iint_{a,A_I}\int_0^{\bar{\xi}} l\left(a,A_I,S\right)\mu\left(d\xi\right)G\left(d\left[a\times A_I\right]\right)=\iint_{a,A_I}\int_0^{\bar{\xi}} n^w\left(a,A_I,S\right)\mu\left(d\xi\right)G\left(d\left[a\times A_I\right]\right)$$

- The capital market clears so that the aggregate demand of capital equals to the total deposited assets in the economy

$$\begin{aligned}\iint_{a,A_I}\int_0^{\bar{\xi}} k\left(a,A_I,S\right)\mu\left(d\xi\right)G\left(d\left[a\times A_I\right]\right)=&\iint_{a,A_I}\int_0^{\bar{\xi}} a^e G\left(d\left[a\times A_I\right]\right)\\&+\iint_{a,A_I} a^w\mu\left(d\xi\right)G\left(d\left[a\times A_I\right]\right)\end{aligned}$$

- The good market clears so that aggregate output Y is equal to the sum of aggregate consumption C, aggregate investment on capital I_k and aggregate investment on individual-specific productivity level I_{A_I}, i.e., $Y=C+I_k+I_{A_I}+\Lambda$, where

$$\begin{aligned}Y=&\iint_{a,A_I}\int_0^{\bar{\xi}} f\left(A_A,A_I,k,l\right)\mu\left(d\xi\right)G\left(d\left[a\times A_I\right]\right)\\C=&\iint_{a,A_I}\int_0^{\bar{\xi}} c^w\left(a,A_I,S\right)\mu\left(d\xi\right)G\left(d\left[a\times A_I\right]\right)\\&+\iint_{a,A_I}\int_0^{\bar{\xi}} c^e\left(a,A_I,S\right)\mu\left(d\xi\right)G\left(d\left[a\times A_I\right]\right)\\I=&I_k+I_{A_I}=K^{'}-(1-\delta)K+I_{A_I}=K^{'}-(1-\delta)K+s_{A_I}Y\\=&\iint_{a,A_I}\int_0^{\bar{\xi}} a^e\mu\left(d\xi\right)G\left(d\left[a\times A_I\right]\right)+\iint_{a,A_I}\int_0^{\bar{\xi}} a^w\mu\left(d\xi\right)G\left(d\left[a\times A_I\right]\right)\\&-(1-\delta)\iint_{a,A_I} a\int_0^{\bar{\xi}}\mu\left(d\xi\right)G\left(d\left[a\times A_I\right]\right)\\&+s_{A_I}\iint_{a,A_I}\int_0^{\bar{\xi}} f\left(A_A,A_I,k,l\right)\mu\left(d\xi\right)G\left(d\left[a\times A_I\right]\right)\end{aligned}$$

and Λ stands for the aggregate fixed cost

$$\Lambda=\iint_{a,A_I}\int_0^{\bar{\xi}}\xi\mu\left(d\xi\right)G\left(d\left[a\times A_I\right]\right)$$

- The joint distribution of individual-specific productivity and wealth $G(a, A_I)$ according to the equilibrium mapping

$$G^{'}(a \mid A_I) = \int_i \mathbb{E}_{A_I^{'}} \left[\int_{u \leq a} \int_{a^{'}(A_I^{'}, v) = u} G\left(dv \mid A_I^{'}\right) du \right] di$$

2.3 Comparative static analysis on the stationary distribution (Stage 1)

In this section, I am conducting a comparative static analysis on the joint distribution of wealth and individual productivity of the simplified model (Stage 1). The key point of this section is, before I introduce the full "winner takes all" dynamics, to test if the key innovation of this paper (functionally) works, i.e., whether the interactions between the endogenous TFP growth and the wealth accumulation process amplify the productivity gap and the wealth inequality overtime *under the exogenous variations* (in particular, divergent productivity distribution and decreasing Labor Share).

Figure 2.1: Key channel on "winner takes all" dynamics

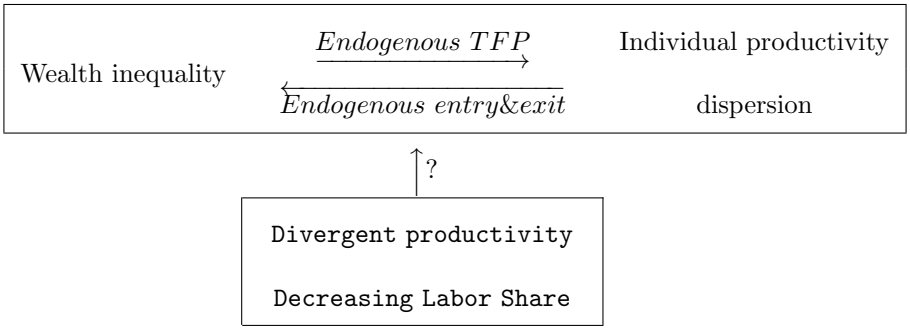

As Figure 2.1 shows, on the one hand, wealth inequality can affect firms' individual productivity growth through equation (2.6). The wealthier the entrepreneur, the more she can invest in accumulating individual productivity, and vise versa. Over time, the productivity gap

gets amplified. On the other hand, the individual's occupational decision is able to propagate the effect of productivity dispersion to their wealth holding by entering or exiting from the production. For any firm, the lower the productivity, the less profit it may obtain. Constrained by the limited credibility, these firms adept relatively slower productivity growth, and therefore, featuring less wealth accumulation, and vice versa.

The main question that this section tries to answer is whether divergent productivity or decreasing labor share can trigger the interactions between wealth inequality and productivity dispersion. If the answer is yes, can we still apply the conclusion to the case where the economy hit by both structural changes simultaneously?

2.3.1 The simplified model (Stage 1 model)

To answer the questions posted above, I use a simplified model and experiment with different sources of structural changes. I compare their stationary joint distributions to see if they are distinct. The model I use for this stage is a heterogenous firm model with a homogenous household; it is a simplified version of the full model introduced in the last section. There are two reasons for me to use this approach. First, the computational burden in solving a fully heterogenous model is huge, and I need to solve the model multiple times to compare the stationary joint distributions. A feasible simplification definitely helps a lot here. Secondly, a heterogenous firm model is adequate to test the hypothesis as it still allows the heterogeneity on productivity while maintaining wealth inequality among firm owners.

The model setup in this section is similar to the standard RBC model with heterogenous firms. The time is discrete and there is a continuum of firms indexed by $i \in I[0,1]$. The model features a representative household endowed with one unit of time to divide between labor and leisure. The household owns all the firms in the economy and markets are complete.

HHs share the same utility from consumption and leisure using the discount factor β.

$$\mathbb{E}_0 \sum_{t=s}^{\infty} \beta^{s-t} u\left(c_s, 1-n_s\right)$$

$$\text{where } u\left(c_s, 1-n_s\right) = \frac{\left(c_s^{\tau}\left(1-n_s\right)^{(1-\tau)}\right)^{1-\sigma} - 1}{1-\sigma}$$

For production, firm i produce output y_{it} according to the production function

$$f\left(A_A, A_I, k, l\right) = A_A A_I \left[k_{it}^{\alpha}\left(n_{it}\right)^{\theta}\right],\ \alpha + \theta < 1$$

The aggregate productivity and individual productivity follows a mean zero log AR(1) process respectively[7]

$$\log A_A^{'} = \rho_A \log A_A + \varepsilon_{A_A}, \text{where } \varepsilon_{A_A} \sim \left(0, \sigma_{A_A}^2\right)$$

$$\log A_I^{'} = \rho_I \log A_I + \varepsilon_{A_I}, \text{where } \varepsilon_{A_I} \sim \left(0, \sigma_{A_I}^2\right)$$

With the simplifications, the associated joint distribution for the Stage 1 model will becomes to $G_t\left(A_I, a\right)$, which denotes the time variant joint distribution of individual productivity and wealth among firms. After period 0, the given the dynamics of A_I , a and $G_t\left(A_I, a\right)$ follow the individual's optimal decision rules.

2.3.2 Computations

For the experiments in this part, I only need to solve the steady state of the economy since the stationary distribution is the main object of the comparative static analysis. I follow Tauchen (1986) on discretization and use the approximation from Zhang (2018) on the Markov matrix for individual productivity.

In particular, the steady state is solved by finding the market clearing real interest rate and real wage. To be specific, the steady state is solved by (i) Guess the p-th generation of real

[7]Here I use an exogenous process for individual productivity growth in order to simplify the comparative static analysis. Under this version, to get a structural change on productivity, I only need to impose different standard deviation to the ε_{A_I}.

interest rate r^p; (ii) Given r^p, guess wage rate $w^{p,s}$ and solve the individual's problem given r^p and $w^{p,s}$. After obtaining occupational decisions, asset decision rules and value functions, find the fixed point of household distribution. Then check whether the labor market clears. If the labor market does not clear, update wage to a new guess $w^{p,s+1}$ and repeat (ii); (iii) If the labor market clears, check if the credit market condition has been satisfied. If not, update the real interest rate to a new guess r^{p+1} and repeat (ii); (iv)The steady state is solved when all markets clear.

Table 2.2: Parameterization for Stage 1 model

Parameter	Description	Value	
		Baseline	Comparison
β	Discount factor	0.961	
τ	average working hour	0.33	
σ	Utility curvature	1.5	
α	Capital share	0.256	
θ	Labor share	0.67	0.61
δ	Capital depreciation	0.085	
ρ_A	Aggregate TFP $AR(1)$	0.859	
ρ_I	Idiosyncratic TFP $AR(1)$	0.859	
σ_{A_A}	Aggregate TFP std.	0.014	
σ_{A_I}	Idiosyncratic TFP std.	0.015	0.02

For current stage, I mainly use parameterization as Khan and Thomas (2013), Buera and Shin (2013), and Zhang (2018) as my source. For the simplified model, the baseline parameterization showed in Table 2.2 is able to generate moments well match the corresponding

moments in the U.S. data. In addition, for comparative static analysis, to mimic the exogenous change, I will use $\theta = 0.61$ for decreased labor share, and $\sigma_{A_I} = 0.02$ for diverged productivity, then see how stationary distribution reacts to these changes.

2.3.3 Comparative static analysis

In this subsection, I run three experiments to accomplish the comparative static analysis. In the first experiment, I exogenously impose different values for labor share. In the second experiment, I assign two different values to the standard deviation of the productivity distribution. Finally, I combine both changes simultaneously. After these, I compare the stationary joint distributions under these three scenarios.

Exogenous change on labor share

In this experiment, I solve steady states for two economies, the state with higher labor share and the state with lower labor share. I compare the stationary distributions for both cases to see if decreasing labor share can generate productivity divergence and wealth inequality.

Figure 2.2 below visualizes the results. The first subplot is the 3-D surfaces for the density of the joint distribution on wealth and productivity. Throughout this comparative static analysis, I use red color to represent the economy before changes, blue color for the economy after changes. The second subplot displays the productivity distribution among firms. It was calculated based on the column sum of firms located at the same productivity grid. The third subplot is for illustrating the wealth distribution. Again, the density was calculated based on the column sum of firms located at the same grid on capital holdings.

There are two main observations from Figure 2.2. First, the productivity at the steady state becomes more diverse. This is a direct result of the model. In this model economy, when the labor share decreases, the relative share of capital increases. As a consequence, the interest

Figure 2.2: Exogenous change on Labor share

(a) 3-D plot

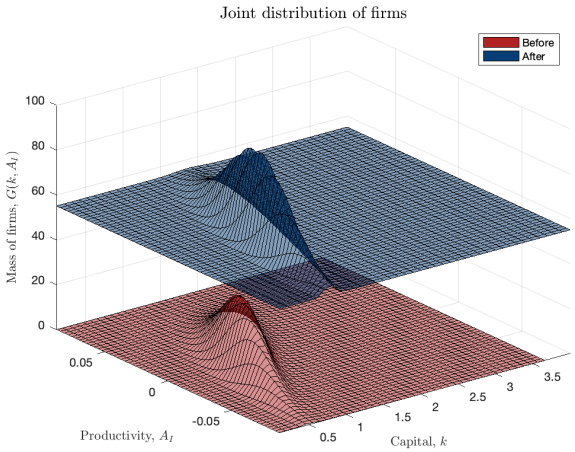

(b) Productivity distribution

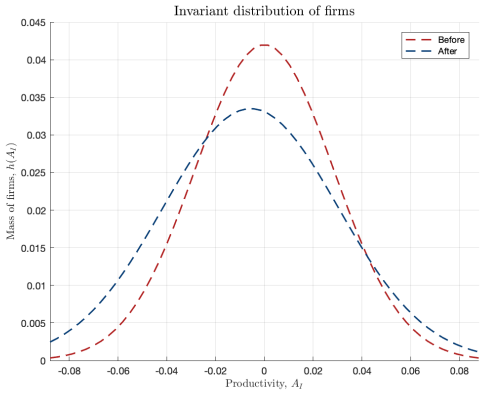

(c) Wealth distribution

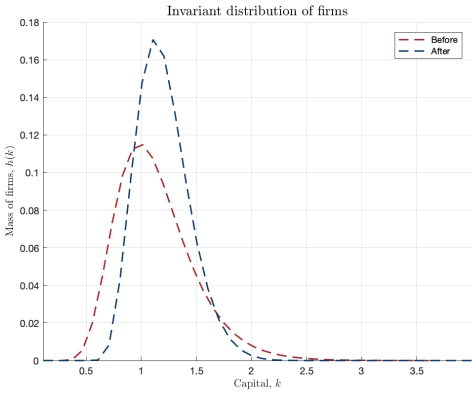

rate rises and there is a reallocation process where the higher productivity firm will end up with higher capital holdings and hence higher production level, and vice versa. The outcome of such a reallocation process diverges the productivity compared to the economy before the reduction of labor share. Second, the wealth distribution becomes more centralized and less spread out. Again, since the relative share of capital increases, capital flows toward the wealthier firm, therefore, the distribution shift to the right and become more centralized than the economy with higher labor share.

Exogenous change on productivity distribution

In this experiment, I solve steady state for two economies with different degrees of productivity dispersion. Specifically, I solve one model with a larger standard deviation on productivity distribution and another model with a smaller standard deviation. I then compare the associate joint distributions on wealth and productivity of firms.

Figure 2.3 visualizes the results. The subplots are formulated in the same way as Figure 2.2. There are two main observations from Figure 2.3. First, the productivity at the steady state becomes more diverse. This is a direct result of I exogenously increase the standard deviation of the productivity distribution. Second, the wealth distribution became more spread out and skewed to the left. The mechanism is as follows. The inflated productivity dispersion artificially imposes emphasis on individual TFP. The enlarged productivity gap enables firms with better TFP to be more competitive; thus, these firms will increase their profit and accumulate more capital stock. The model's dynamics produce a right-shifted threshold that creates a left-shifted center of the wealth distribution. Therefore, the wealth distribution has a fat right tail.

Figure 2.3: Exogenous change on Productivity

(a) 3-D plot

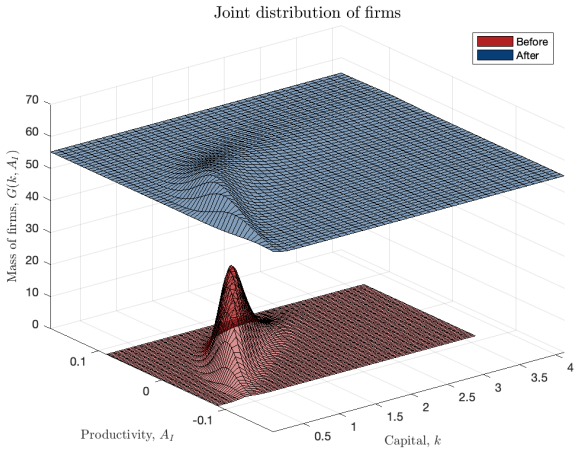

(b) Productivity distribution

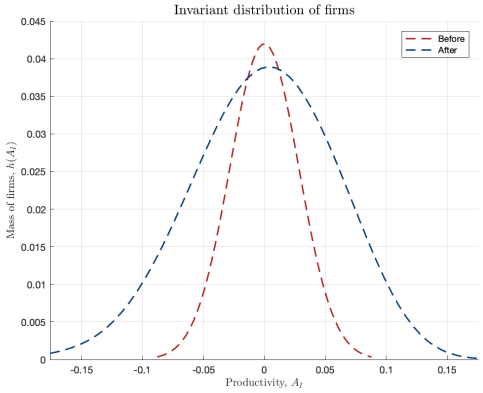

(c) Wealth distribution

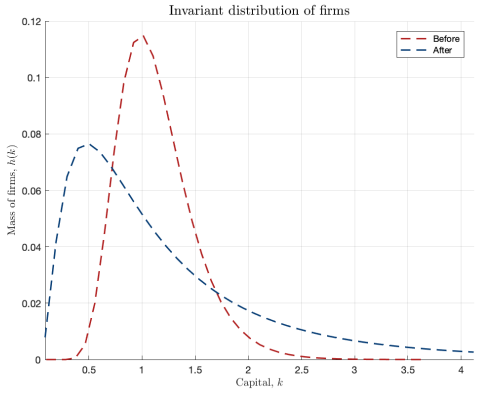

Exogenous changes on both

In this experiment, I solve the steady state for two economies, an economy with larger productivity differences and lower labor share, another economy with smaller productivity differences and higher labor share.

Figure 2.4: Exogenous change on both shocks

(a) 3-D plot

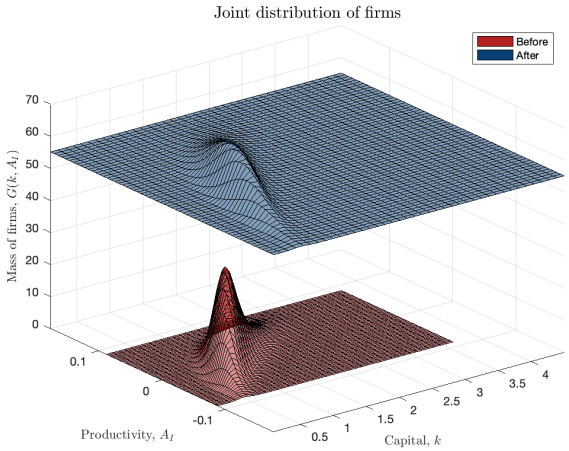

(b) Productivity distribution

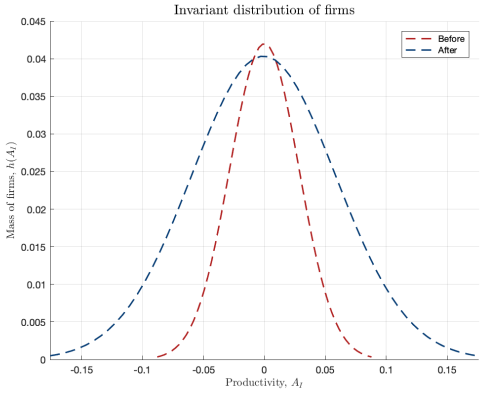

(c) Wealth distribution

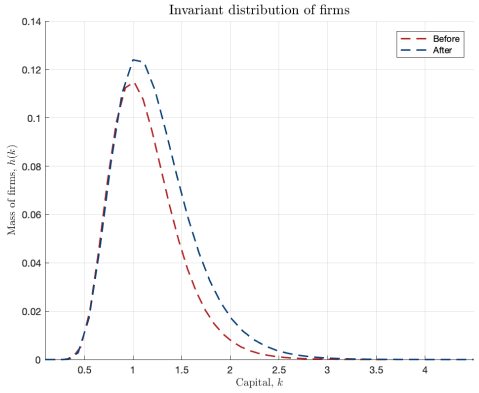

Figure 2.4 visualizes the results. There are two main observations from it. First, the productivity at the steady state becomes more spread out. This is, again, a direct result of the exogenous change imposed on the standard deviation of productivity. However, the distributions before and after the change are both symmetrical. Second, the wealth distribution is roughly unchanged. It does not shift or skewed as what the previous two experiments behaved. This

finding is interesting since both structural changes can distort the wealth distribution when they are hitting the economy individually. Nevertheless, when they are jointly disturbing the economy, the effects are canceling out each other, therefore have literally no net impact on the stationary distribution. This result makes sense, recall that the decreasing labor share tends to reduce the wealth inequality, whereas the productivity dispersion can amplify the capital holding differences from the previous experiments. As a result, when both shocks hit the economy, two counterproductive channels jointly ineffective in reshaping the stationary distributions.

The comparative static analysis in this section suggests that, in an RBC framework, the economy's stationary distribution is unchanged under the joint interruptions of decreasing labor share and divergent productivity. Hence structural changes alone are not sufficient to match multiple stylized DBD facts. Rather, introducing other sources of dynamics is critical.

2.4 The "Winner Takes All" dynamics

Figure 2.5 provides a graphical illustration for the core idea of Stage 2. To be specific, with fact 4 (decreasing labor share) and 6 (increasing productivity dispersion) simultaneously imposed on the heterogenous firm model, the Stage 1 model can not successfully match the stylized DBD facts. As an improvement, I will introduce the "winner takes all dynamics" into the model. As shown in the highlighted area, the proposed "winner takes all" dynamics is built upon two key features: endogenous TFP growth and endogenous firm entry and exit. The former can amplify the differences created by the interactions between wealth inequality and divergent productivity. The latter allows individuals to choose occupations. These channels add extra sources of variational dynamics to the model that are able to push the economy to a new steady state under structural changes. And intuitively, such a mechanism can results in dynamics that better match with stylized DBD facts.

Figure 2.5: Key ideas of Stage 2

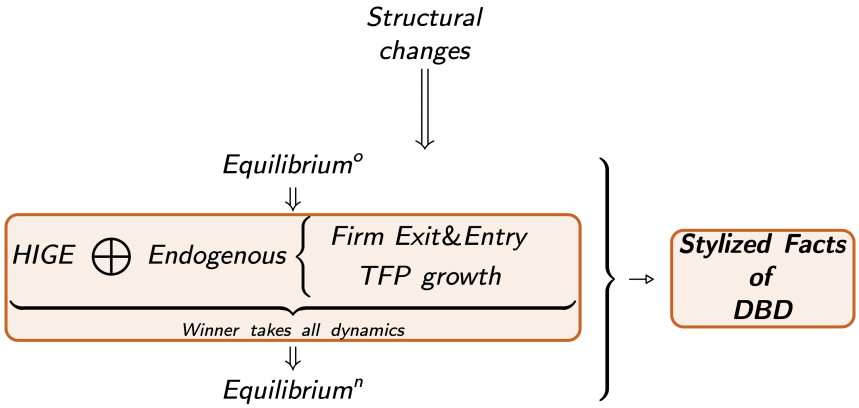

2.4.1 The mechanism

The model has not been numerically solved yet. Instead, I use this subsection to illustrate how intuitively the "winner takes all" dynamics can contribute to the study of declining business dynamism. Basically, triggered by structural shocks, the "winner takes all" dynamics activated. During the transitions between the two steady states, the stylized declining business dynamism facts can be generated throughout which process.

The whole dynamics are as shown in Figure 2.6. In this model, structural changes are the initial cause of the mechanism. Under shocks, the economy deviates from its original steady state $G_o\left(A_I^o, a_o, \mathbb{OD}^o\right)$. Since then, individuals make their occupational decision at every period. They will choose to become an entrepreneur whenever the associated lifetime value is larger. For an entrepreneur, they should make optimal decision to balance investment on capital holdings a_t and firm-specific technology accumulation A_I; what is more, their ability to borrow is constrained by limit credibility. Since the richer firm has more flexibility on individual technological accumulation, the growth paths for A_Is will become divergent. As a result, the joint distribution $G_t\left(A_I^t, a_t, \mathbb{OD}^t\right)$ is more skewed than previous. Since wealth holdings and

individual productivity are differentiated, production and the relative share among firms start to change. Due to the shift of joint distribution, a new set of benchmarks on wealth holdings and individual productivity yield at the end of each period. These benchmarks impose new criteria for the optimal decision of an individual's problem for the next period. On the other hand, individuals who decide to become workers will receive their labor income and capital rental at each period. At meanwhile, there will be a randomly revealed fixed cost for role switching and individual productivity shock. Once the lifetime value of the entrepreneur is dominating, firm entry happens. Overtimes, the above stated process will push the dynamics to a new steady state and end up with $G_n\left(A_I^n, a_n, \mathbb{OD}^n\right)$.

Figure 2.6: "Winner Takes All" dynamics

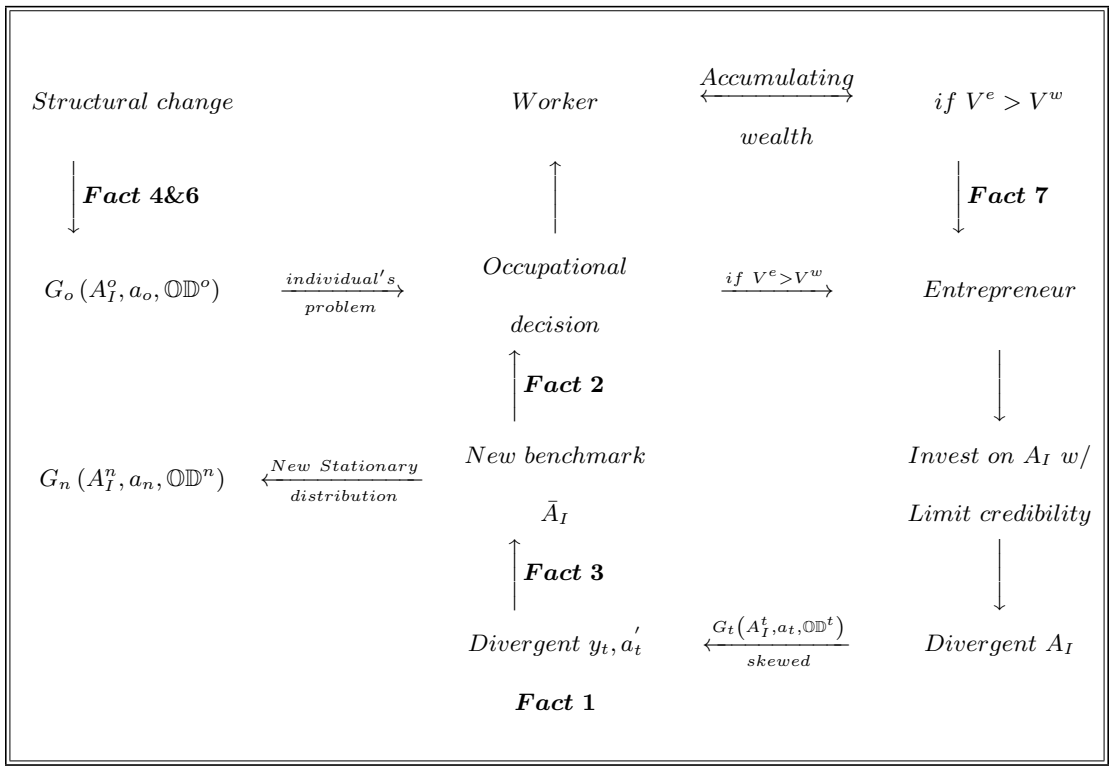

2.4.2 Matching stylized facts with model's mechanism

I will use this subsection to illustrate how the proposed mechanism can potentially help to explain the stylized facts in declining business dynamism. In particular, I will follow the logic presented in Figure 2.6.

Fact 1. Market Concentration

In the model, the proposed mechanism can increase market concentration through a direct and an indirect channel. First, limited credibility reduces followers' ability to catch the leaders; hence, market concentration increases. Second, firm's investment-specific technological innovation process increases the return to being the market leader. Leading firms are much closer to becoming a leader than a laggard who needs more innovations to become a leader. Therefore, this innovation process gives a bigger incentive to frontier firms, which in turn expands the share of unleveled industries, hence, the market concentration.

Fact 2. Increasing on Average Markups

The individual-specific technological progress set up allows firms that better adapt to new technologies can gain a relatively more advantageous position than their competitors and can capture outsized market power. Hence, these firms will raise their markups to earn more profit, build up better technology, and have advantages in the competition.

Fact 3. Increasing on the profit share of GDP

As a direct result of market concentration, firm with better productivity will increase their markup, accumulation on capital holding and technology. The profits in the model are mainly coming from the frontier firms with higher markup and productivity. Hence, the majority share of the profit in GDP has account toward these firms.

Fact 4. The Labor Share Has Declined

Since the labor share is treated as an exogenous variation in this model, this fact is automatically satisfied.

Fact 5. Market Concentration and Labor Share Are Negatively Associated

The model can generate increasing market concentration overtime if the labor share declines. Hence the negative correlation is guaranteed by the aggregate dynamics.

Fact 6. Divergent Productivity

This fact can be explained by another interesting feature of my model, the linkage between relative productivities and investment-specific technological innovation. To see this, recall from equation (2.5), the dynamic relative productivities (between firm i and j) can be written as

$$\begin{aligned}
\mathbb{E}\left(\frac{A_i^{'}}{A_j^{'}}\right) &= \mathbb{E}\left(\frac{\left(A_I^i\right)^{\gamma}\left(i_{A_I}^i\right)^{\eta}\exp\left(\varepsilon_{A_I}\right)}{\left(A_I^j\right)^{\gamma}\left(i_{A_I}^j\right)^{\eta}\exp\left(\varepsilon_{A_I}\right)}\right) = \mathbb{E}\left[\left(\frac{A_I^i}{A_I^j}\right)^{\gamma}\left(\frac{i_{A_I}^i}{i_{A_I}^j}\right)^{\eta}\right] = \mathbb{E}\left[\left(\frac{A_I^i}{A_I^j}\right)^{\gamma}\left(\frac{y_i}{y_j}\right)^{\eta}\right] \\
&= \mathbb{E}\left(\left(\frac{A_I^i}{A_I^j}\right)^{\gamma}\left(\frac{A_A A_I^i\left(k_i^{\alpha}\left(\tilde{n}+l_i\right)^{1-\alpha}\right)^{1-\upsilon}}{A_A A_I^j\left(k_j^{\alpha}\left(\tilde{n}+l_j\right)^{1-\alpha}\right)^{1-\upsilon}}\right)^{\eta}\right) \\
&= \mathbb{E}\left(\left(\frac{A_I^i}{A_I^j}\right)^{\gamma+\eta}\left(\frac{k_i^{\alpha}\left(\tilde{n}+l_i\right)^{1-\alpha}}{k_j^{\alpha}\left(\tilde{n}+l_j\right)^{1-\alpha}}\right)^{\eta(1-\nu)}\right)
\end{aligned}$$

expanding ratio A_I^i/A_I^j iteratively over time

$$\begin{aligned}
\mathbb{E}\left(\frac{A_i^{'}}{A_j^{'}}\right) =& \mathbb{E}\left(\left[\left(\frac{A_I^{i,-1}}{A_I^{j,t-1}}\right)^{\gamma+\eta}\left(\frac{k_{i,-1}^{\alpha}\left(\tilde{n}+l_{i,-1}\right)^{1-\alpha}}{k_{j-1}^{\alpha}\left(\tilde{n}+l_{j,-1}\right)^{1-\alpha}}\right)^{\eta(1-\nu)}\right]^{\gamma+\eta}\left(\frac{k_i^{\alpha}\left(\tilde{n}+l_i\right)^{1-\alpha}}{k_j^{\alpha}\left(\tilde{n}+l_j\right)^{1-\alpha}}\right)^{\eta(1-\nu)}\right) \\
=& \mathbb{E}\left(\left(\frac{A_I^{i,-1}}{A_I^{j,t-1}}\right)^{(\gamma+\eta)^2}\left[\left(\frac{k_{i,-1}^{\alpha}\left(\tilde{n}+l_{i,-1}\right)^{1-\alpha}}{k_{j,-1}^{\alpha}\left(\tilde{n}+l_{j,-1}\right)^{1-\alpha}}\right)^{(\gamma+\eta)}\left(\frac{k_i^{\alpha}\left(\tilde{n}+l_i\right)^{1-\alpha}}{k_j^{\alpha}\left(\tilde{n}+l_j\right)^{1-\alpha}}\right)\right]^{\eta(1-\nu)}\right)
\end{aligned}$$

$$\mathbb{E}\left(\frac{A_i^{'}}{A_j^{'}}\right)=\cdots$$

$$=\mathbb{E}\left\{\left(\frac{A_I^{i,0}}{A_I^{j,0}}\right)^{(\gamma+\eta)^{(T+1)}}\left[\left(\frac{k_{i,0}^{\alpha}\left(\tilde{n}+l_{i,0}\right)^{1-\alpha}}{k_{j,0}^{\alpha}\left(\tilde{n}+l_{j,0}\right)^{1-\alpha}}\right)^{(\gamma+\eta)^{T}}\left(\frac{k_{i,1}^{\alpha}\left(\tilde{n}+l_{i,1}\right)^{1-\alpha}}{k_{j,1}^{\alpha}\left(\tilde{n}+l_{j,1}\right)^{1-\alpha}}\right)^{(\gamma+\eta)^{(T-1)}}\right.\right.$$

$$\left.\left.\cdots\left(\frac{k_{i,-1}^{\alpha}\left(\tilde{n}+l_{i,-1}\right)^{1-\alpha}}{k_{j,-1}^{\alpha}\left(\tilde{n}+l_{j,-1}\right)^{1-\alpha}}\right)^{(\gamma+\eta)}\left(\frac{k_i^{\alpha}\left(\tilde{n}+l_i\right)^{1-\alpha}}{k_j^{\alpha}\left(\tilde{n}+l_j\right)^{1-\alpha}}\right)\right]^{\eta(1-\nu)}\right\}$$

at each period the optimal solution is to make collateral constraint (2.7) binding, therefore using the assumption that each individual starts from same individual-specific technology, we have

$$\mathbb{E}\left(\frac{A_i^{'}}{A_j^{'}}\right)\propto\left(\frac{A_I^{i,0}}{A_I^{j,0}}\right)^{(\gamma+\eta)^{(T+1)}}\mathbb{E}\left(\left[\prod_t\frac{\left(a_{i,t}^{\alpha}\left(\tilde{n}+l_{i,t}\right)^{1-\alpha}\right)}{\left(a_{j,t}^{\alpha}\left(\tilde{n}+l_{j,t}\right)^{1-\alpha}\right)}\right]^{\eta(1-\nu)}\right)$$

The above equation indicates that the evolutional process of firms' investment-specific technological innovation is a function of wealth path, i.e., wealth inequality can create further individual productivity divergence by model dynamics.

Fact 7. Declining Firm Entry Rate (& Exit rate)

Since an individual's occupational decision is forward looking, they would directly be influenced by those forces that impact the market concentration. In particular, the implication of increased market concentration implies that a new entrant is much more likely to compete against a top firm, which would discourage new firm creation. This would also imply that the fixed cost (total cost of investment-specific technological innovation) for a new entrant to survive is very big. Therefore, the average possibility of having a larger lifetime value to be an entrepreneur for a worker is declining over time. So as for the firm entry rate.

2.5 Conclusion and extensions

In this paper, I try to shed light on the frontier research discussions around declining trends in business dynamism using a general equilibrium model structure with heterogenous

individuals. The key mechanism of the framework is the strategic technological innovation process of firms in response to individual's wealth holding and life time value of being different occupations. Such an endogenous TFP process accompanied by wealth inequality reflects a firm's relative technological position. The resulting "winner takes all" dynamics can help the model to account for several observed empirical trends of U.S. economy jointly. To accomplish this analysis, I adept a two stages approach to my structural model. In the first stage, I conduct a comparative static analysis to numerically show that multiple structural shocks are not sufficient to create DBD facts. As a consequence, for my current second stage, I introduce the "winner takes all" dynamics to the model and provide intuitions on the mechanism. I try to use both stages to emphasize the key role of the interactions between wealth inequality and firm-specific productivity growth in explaining the DBD facts during transitional dynamics.

In the first stage, I simplify the model to a heterogenous firm model with a representative household. I then study the behaviors of stationary distributions of the economy under different sources of exogenous changes. I find that for the economy under single exogenous change such as decreasing labor share or divergent productivity, the stationary distribution is either shifted or skewed. Moreover, the effects from both channels are counter-directional. After this, I try to impose both changes simultaneously and observe that the effects are roughly canceling out each other, hence producing no change on the stationary distribution. Since the goal is to account for multiple DBD facts jointly, I claim that, in the model, only have structural changes is not able to accomplish such a purpose.

In my current second stage, I introduce the "winner takes all" dynamics to the model to create an extra source of variations for the transitional dynamics. Once the structural changes hit the economy, the composite transitional dynamics will bring the economy to a different equilibrium. Instead of numerically solving the model and simulating the transitional dynamics, in this chapter, I describe the intuitions behind the proposed mechanism and illustrate how

potentially the model can match the multiple DBD facts.

There are two main extensions for the next step of this research. Firstly, The full model (the Stage 2 model) should be numerically solved in order to quantitively assess whether the transitional dynamics are behaving as expected. Regrading this extension, further exploration and modifications on Winberry (2018) and Zhang (2018) will be the focus for next step. Secondly, the specification of the endogenous TFP growth process deserves more attention. To be accurate, the firm specific technological innovation process is the key feature of the "winner takes all" dynamics. There are many perspectives related to this process, including globalization, regulations, the changing nature of production, etc. A better adaptive formulation should be based on border examinations on various sources of micro data on these channels. Extension on this direction will be the key challenge for the Stage 2 study.

Finally, this work starts with constructing a GE framework with heterogenous individuals that allows one to study border topics related to interactions between heterogenous households and firms. In order to demonstrate the capability of this model, I apply it to the literature of declining business dynamism. In this two-stage study, I highlight the potential drawbacks of study DBD facts with only exogenous changes in the first stage. As a new attempt, I uncover the "winner takes all" dynamics from my full model and try to deliver the point that DBD facts may closely related to endogenous interactions between heterogenous households and firms. The project still requires many extensional works. However, the current results provide confidence in its promising future.

Chapter 3

Can Social Media Affect Stock Market? – A Case Study of Trump's Tweets

3.1 Introduction

The US president can have a significant influence on the US economy (Brans and Scholtens (2020)). Classical studies already provide profound understandings from both political and economic perspectives. I am curious if there is any new channel that I can dive into and then contribute to this broad topic.

By observing the reality, two facts drew my attention and eventually led me to the research question. In the first place, I noticed that President Trump is the first president to communicate with the public in a personal and informal manner using social media extensively. This fact leads my research to use social media to evaluate the presidential influence on the US economy. The second fact that inspired me is the increasing popularity of research that focuses on the linkage between media and stock returns. Results from these works allow me to analyze the effect of social media on the US stock market. Combining both observations, I eventually

decide to use this project to answer the following research question, "Does President Trump move the markets with his tweets?".

I will use an event study approach to examine the question proposed above. A key assumption of this study is the event has to be unexpected. I argue that this is the case with President Trump's tweets, as they relate to the President's mood and feelings about companies, which are difficult to predict. Another prerequisite with event studies is that the information has to available to market participants. As tweets can be freely accessed and, assuming market analysts monitor President Trump's Twitter account and his comments on publicly traded companies, investors may react to the tweets as if they were public news event releases (Chan (2003)). Within the window of this event study, I investigate if Trump's tweets affect stock market returns during his presidency and whether the sentiment of the tweet is influential.

This project is based upon four main areas of study. They are (i) event study on stock market; (ii) stock market reacts to media; (iii) efficient market hypothesis and (iv) study on the connection between President Trump's tweets and stock market movement. For the logic of event study, I follow research conducted by Brown and Warner (1980, 1985). Their papers introduced modifications to the event study methodologies, including applications of daily and even intraday data instead of monthly data. All these technics guarantee a fairly accurate measurement for abnormal returns and their reaction to new information. Paper such as S.P. Kothari and Warner (2006) provides the foundation for using complex methods to estimate abnormal returns. Their contributive works allow me to examine Trump's tweet using daily data, thus evaluating its short-term impact on stock prices.

The research on stock market reactions to media such as Mackinlay (1997); Campbell et al. (2010) is extremely helpful in data filtering, conducting concrete statistical testing, and decide estimation window for daily return data (window of study).

In terms of constructing a good measure of daily market movement and connecting

with social-media-based event studies, Schneider and Spalt (2016), Ge and Wolfe (2017), and other papers proposed and modified methodologies on EMH (efficient market hypothesis) for Trump's tweets. These works exam the impact of tweets with the most negative and positive sentiments regarding several publicly traded firms. Follow their logic, I build up my own data set with a lot more observations on tweets and daily return data on stock prices. By doing so, I expect my work can further refine their conclusions.

Lastly, a number of studies analyze the short-term effect of Trump's tweets on the stock market movement. For example, Aziz (2020) tests EMH using Donald Trump's company-specific tweets. He found that EMH is violated as stock markets were not efficient at incorporating new information into their stock prices. Brans and Scholtens (2020) analyze the effect of President Trump's Twitter messages that specifically mention a company name on its stock market returns. This paper suggests that tweets from the president that reveal strong negative sentiment are followed by the reduced market value of the mentioned company, whereas supportive tweets do not significantly affect.

To sum up, in this project, I run an event study on President Donald Trump's tweets. By combining data on the stock price movement of mentioned companies, I test the hypothesis that President Trump's tweets can trigger the company's stock price to move. To be specific, this paper tries to test if the average abnormal daily return before Trump post a Twitter (with a particular type of sentiment) is statistically significant different than the average abnormal daily return after its posting.

3.2 The Architecture and contribution of this project

The project is built upon two main pillars. For President Trump's tweets, I use sentiment analysis to classify each of his tweets. For stock market price data, I implement

time series forecasting routine to construct the abnormal daily returns.

Figure 3.1 presents a graphical illustration for the conceptual skeleton of this project. To be specific, let's consider the way that each pillar works as a mathematical function. From this sense, the orange rectangle on the left-hand side uses President Trump's original tweets as its input and creates tags for sentiment classification as its output. In between, I processed everything with sentiment analysis packages which I will discuss in detail in a later section.

Figure 3.1: Architecture of the project

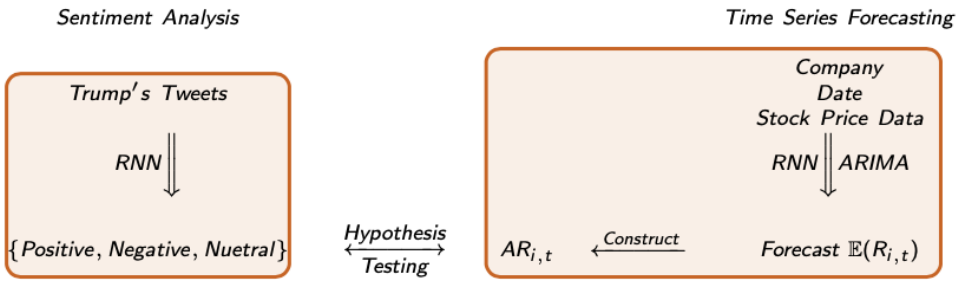

Similarly, the rectangle on the right-hand side first extracts information such as company name (index i), the date of the tweet (index t) and time series data on stock price from each of President Trump's tweets as its input. Then, it generates expected daily return ($\mathbb{E}(R_{i,t}|x_{i,t})$) by incorporating with either classical methods or data mining technics. Follow the definition from finance literature, I then construct abnormal daily return $AR_{i,t}$ for each firm i at time t.

Here the time series forecasting section is the main novelty of this project. For previous research, the most popular ways of constructing abnormal daily return are through the constant-mean return model (CMR), the market model, or the capital asset pricing model (CAPM). However, the main drawbacks of these models are either their theoretical limitations, or the researcher has to impose strong assumptions[1] in order to use it. Considering these facts, I

[1]For example, the market model assumes the relationship between the market returns and stock returns is stable and linear.

decided to directly forecast the close price for stock indexes and construct the abnormal daily return data afterward. The advantage of my approach is obvious. First, it doesn't require any assumption or theory, hence no limitations from this sense. Second, the accuracy of the predicted value is guaranteed by the method I am using. Hence it is transparent and well-controlled at a given accuracy level. As a result, I argue that the abnormal daily return data constructed under this approach should provide better confidence for my study than other previous research. Therefore, it becomes the critical contribution of this project.

Finally, combining two pillars together, I conduct several sets of hypothesis testing in order to provide a robust conclusion to the main question that this project is trying to answer.

3.3 Data and methodologies

In this section, I will describe the data sets I am using in this project. In addition, I will also present the methodologies I used to arrive at the pre-setup for hypothesis testing.

3.3.1 Sentiment analysis

3.3.1.1 Data on tweets

As mentioned before, I will be running an event study on president Trump's tweets. This specific event study examines tweets posted by President Trump that mention a publicly-traded company. Twitter data are collected from Trump Twitter Archive, which in total contains 55,886 tweets up to November 2020.

I then started to filter the data set and extract only tweets that can provide me with unbiased hypothesis testing results. There are four main steps of this data filtering process. First, in this paper, I only pay attention to President Trump's tweets posted before COVID-

19[2]. The main reason for this is, COVID-19 has significantly changed our life. That said, the patterns that the model is mining (i.e., the way that tweets can affect the stock market) may be different before and after COVID-19 pandemic. As a result, including data after pandemic will potentially bias the analysis. By doing so, the data size is reduced to around 47,000 tweets.

At the next step of data filtering, I pick tweets that directly mentioned a particular company. The reason for doing so is straightforward; as a conservative study, I have to make sure the hypothesis testing runs on a data set that may provide a significant result. That said, tweets that directly mentioned a specific company's name (I name it as "direct effect") should definitely fit into this requirement, but not vice versa. Hence, I decides to start with only the tweets that clearly mentioned a particular company. In this step, I also removed companies involved in merger and acquisition activity (like stock split, gave a profit warning, or saw a change in their top management team). The reason for removing companies involved in merger and acquisition activity is that the literature usually finds a stock market response after this type of news (Mackinlay (1997)). If the president tweets about this news and I would keep this tweet in my sample, it is impossible to determine whether the market response results from the event as such or from the president's tweet. After this step, the data size shirks to 186.

In the third step, I remove tweets that mentioned a company but are not part of the S&P 500 index. The S&P 500 is a stock market index based on the market capitalization of 500 large companies listed on the NYSE, NASDAQ, or CBOE. There are two main advantages of working with it. First, a large company may have a significant stock price movement after President Trump's tweet. Therefore it is easier for me to detect. Such a property is a potential guarantee for the conservativeness of a study like this project. Second, due to strict requirements, the S&P 500 index is one of the most accurate indicators of the stock market of the United States.

[2]To be specific, I drop tweets posted after April. In this step, I consider April as a benchmark date when the COVID pandemic started to spread all over the US.

Therefore, I decided to use the S&P500 as the market index for the sentiment analysis. This step shrinks the number of tweets to 112.

Finally, I select tweets posted after Donald Trump's presidency, which happened on a trading day. The reason for doing so is, for a research which focusing on evaluating Trump's presidential power on stock market movements, including data from before his presidency is going to bias the result. Additionally, I need to construct the actual daily return data for the date of tweet posting in order to run the hypothesis testing. As a result, any tweets post at a date that is not a trading day will be considered an observation with a variable value that is not available; therefore, it dropped out from the data set.

All these steps filtered the data set to 64 tweets in total, and I will use this data set as the starting point of my sentiment analysis. The Appendix C.1 list all tweets from President Donald Trump up to the second step of the above-mentioned data filtering process (which contains 186 tweets). In the appendix, for further extensional works, I also keep observations from companies not in the S&P 500 and tweets before his presidency.

3.3.1.2 Sentiment analysis

I divide the data set into subsamples (according to their sentiment) to perform the sentiment analysis regarding particular sentiment of the tweets. The subgroups categorization is mainly based on `SentiStrength`, which extracts sentiment strength from the informal English text. As Thelwall et al. (2010, 2011) point out, `SentiStrength` is a highly accurate sentiment analysis tool specified for short social web texts. It is produced as a part of the CyberEmotions project which is supported by the EU FP7; This tool is able to detect social media grammar and misspellings. `SentiStrength` gives all tweets a score from -5 (very strong negative attitude) to +5 (very strong positive attitude). Each tweet that gets a positive sentiment score between 0 and 5 will be classified as a positive tweet; a negative tweet has a sentiment score between 0

and -5, a neutral tweet has zero sentiment score.

Table 3.1: Overview of sentiment data set

Company	Date	Tweet	Other features	Nature of Tweet
Ford	1/9/2017	'...'	...	Positive
Walmart	1/17/2017	'...'	...	Positive
General Motors	1/17/2017	'...'	...	Positive
Lockheed Martin	1/18/2017	'...'	...	Neutral
⋮	⋮	⋮	⋮	⋮

The adjusted balanced accuracy of `SentiStrength` is tested for around 75% in this particular practice. After the classification by `SentiStrength`, I also manually checked all tweets and corrected all 7 tweets that were wrongly assigned. As a summary of this part, the result ends up with 34 positive tweets, 21 negative tweets, and 7 neutral tweets. Table 3.1 shows a glimpse of the outcomes from the sentiment analysis. For each tweet (each row of the table), I collect information about each mentioned company and also attached the manually checked sentiment classification for it[3].

3.3.2 Time series forecasting

3.3.2.1 Data on abnormal daily return

I have shown how I build my data set for event study in the previous section, and in order to evaluate their economic impact, let's now shift gear to the measurement of the market.

[3]I also apply the same process to other tweets listed in Appendix C.1 for further use.

In this paper, I decided to focus on the financial market to serve the research purpose better. Compared to other markets, financial data can react to social media at a relatively faster path while providing data that are easier to capture. Therefore, I will use an approach similar to Brown and Warner (1985) to measure the economic impact of an event over a short time period with stock prices.

Next, I decide the window of the event study to be *three trading days* for two considerations. First, this window includes one trading day before the tweet posting, the day of the tweet and the next trading day after the tweet. Such a window allows me to evaluate the short-term effect before and after President Trump posts his tweet. Second, my experiment suggests that the effect does not last long, and hence there is no need to include a longer window of study. For further details, see Aziz (2020) and Brans and Scholtens (2020).

Lastly, I decide to use abnormal daily return as the key variable for hypothesis testing. The abnormal return is the actual ex-post return of the security over the event study window minus the firm's normal return over the same time window, whereas the normal return is defined as the expected return without conditioning on the event taking place. Therefore I think this index is a good fit for the event study conduct in this paper. I use daily data as the data frequency due to the fact that EMH for stock market is violated, so this task doesn't require high-frequency data.

By definition, the abnormal return is defined by subtracting the expected normal return from the actual return

$$AR_{i,t} = R_{i,t} - \mathbb{E}\left(R_{i,t}|X_{i,t}\right) \tag{3.1}$$

where $AR_{i,t}$, $R_{i,t}$, and $\mathbb{E}\left(R_{i,t}|X_{i,t}\right)$ represent abnormal daily return, actual daily return and expected daily return of company i at time t. In this project, I use the following equations to

construct $R_{i,t}$, and $\mathbb{E}\left(R_{i,t}|X_{i,t}\right)$, respectively.

$$R_{i,t} = \frac{P_{i,t}^{Close} - P_{i,t}^{Open}}{P_{i,t}^{Open}} \tag{3.2a}$$

$$\mathbb{E}\left(R_{i,t}|X_{i,t}\right) = \frac{\hat{P}_{i,t}^{Close} - P_{i,t}^{Open}}{P_{i,t}^{Open}} \tag{3.2b}$$

where the $\hat{P}_{i,t}^{Close}$ stands for predicted close price of firm i at time t.

Applying equation (3.1) and (3.2) into this study, I first retrieve data on open and close price of company i for the past 6 years head of time t[4]. Then I construct the corresponding actual daily return and expected daily return by equation (3.2). With these two components, I calculate the abnormal daily return by equation (3.1). That said, in this time series forecasting step, for each tweet, there are 3 trading days in the window of study $t = T-1, T, T+1$ where T represents the actual date of tweet posting. For each of the trading days, I am running a time series forecasting based on data from the previous 6 years ahead of t. These sum up to around 180 time series forecasting in total.

Figure 3.2 displays the routine of constructing data for time series forecasting of the close price for each of the three trading days in the event study window.

Figure 3.2: Time schema for time series forecasting

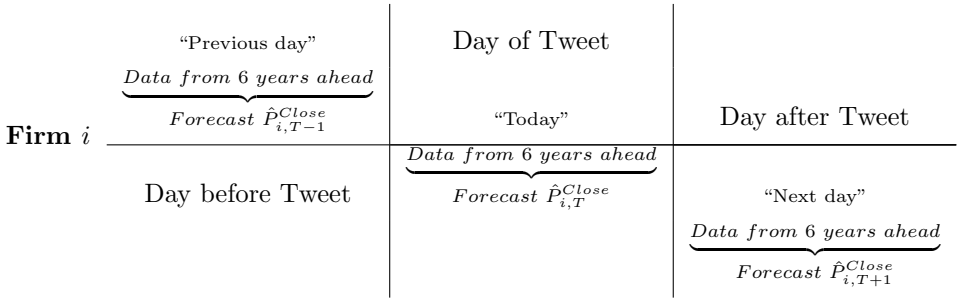

[4]The reason for me to set the time series with 6 years horizon is quite ad hoc. First, I need enough information to train the model. Second, I want to keep the computational cost and memory as efficient as possible. I find 6 years is a good balance between these two criteria.

3.3.2.2 Time series forecasting

I use two methods to accomplish the task. One of them is the ARIMA model, a classic model that is intensively used by the literature related to time series forecasting of the stock price. The other one is RNN. To be accurate, I use the long short term memory (LSTM) model as a representative method for data mining techniques. Many studies are comparing these two methods in terms of their accuracy on a task like time series forecasting of the stock price. In this project, I did the same thing on both methods with optimized hyperparameters, and I didn't find any significant difference in their performance (the MSE of both methods are almost identical in this practice). In other words, the results and conclusions are robust to the selection of methods. Therefore, for the rest of this paper, I decide to use LSTM as the benchmark method for time series forecasting practice due to its higher flexibility.

Algorithm 2 The RNN for time series forecasting on closed price

Step 1. For each tweet event study (out of the 64 filtered set of tweets), identify the date of trading (T), one trading day before ($T-1$) and after ($T+1$).

Step 2. For each date $t = \{T-1, T, T+1\}$, extract closed prices for the company mentioned in this tweet for 6 years head of t, i.e. for T, the time series data would be

$$\underbrace{P_{i,1}^{Close}, \cdots P_{i,T}^{Close}}_{Trading\ days\ for\ previous\ 6\ years}$$

Step 3. Use training set to train the LSTM model and validation set to predict, where the date of interest t should be the last prediction on the validation set.

$$\underbrace{P_{i,1}^{Close}, \cdots P_{i,Train}^{Close}}_{Training\ set}, \underbrace{\widehat{P_{i,Train+1}^{Close}}, \cdots \widehat{P_{i,t}^{Close}}}_{Validation\ set}$$

Step 4. Use $P_{i,t}^{Close}$ and $\widehat{P_{i,t}^{Close}}$ to construct expected abnormal daily return by equation (3.2).

Figure 3.3: Illustrative example of LSTM for 1 tweet event on 3 trading days

(a) $T-1$

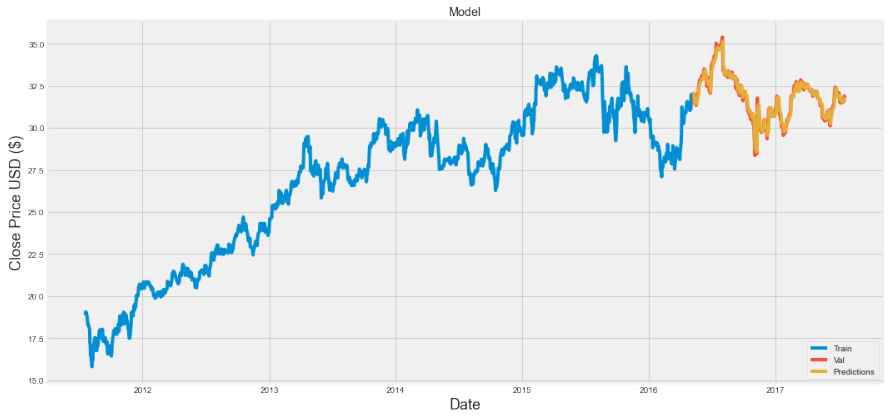

(b) T

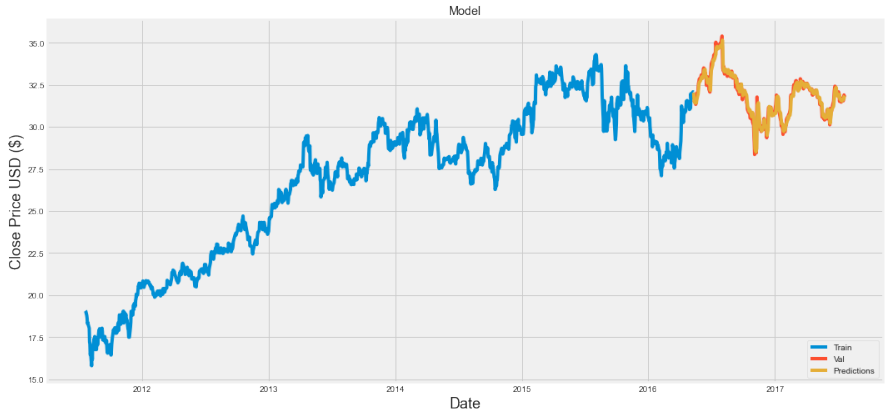

(c) $T+1$

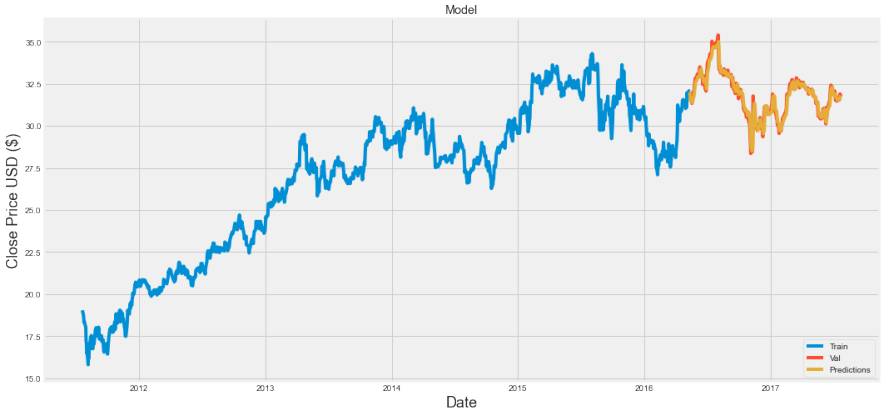

In the window of each tweet event study, I collect time series data from the previous 6 years on the close price of the company mentioned in the tweet for each trading day. I use a training set (blue curve) to train the model. The entire machine learning algorithm tries to minimize the deviation between the validation set (red curve) and the predictions (yellow curve). I set the date that I want to predict as the last day of the study window (the last point on the yellow curve). Therefore the last predicted value of the prediction set is the object of interest, $\hat{P}_{i,t}^{Close}$. As a detailed exposition, Algorithm 2 describes the whole process.

For the RNN model, I define it as a neural network with 4 layers where the first and second layers have 50 nodes and the third layer has 25 nodes. During the training process, I use 'adam' as the optimizer and mean squared error as the objective loss function. For the training process of each series, I use 10 batches with 20 epochs for each. As an illustrative example, Figure 3.3 shows time series forecasting results of 1 out of 64 tweet events; thus, it associated with 3 time series forecasting plots ($\widehat{P_{i,T-1}^{Close}}$, $\widehat{P_{i,T}^{Close}}$ and $\widehat{P_{i,T+1}^{Close}}$).

3.4 Hypothesis testing

In this section, I conduct two sets of hypothesis testings. For the first type of hypothesis testing, I try to test the hypothesis that tweets with different sentiments can create distinct ways of stock movement. For the second type of hypothesis testing, I try to unravel the exact pattern that each sentiment type can influence the stock market.

3.4.1 Hypothesis testing I

In this section, I try to use both sentiment data set for president Trump's tweets and time series data for each mentioned company's abnormal daily return to test if tweets with different sentiments can affect the stock market differently.

For this part, I divide the tweets data set into three subgroups. They are a subgroup of tweets with only positive sentiment, a subgroup of tweets with only negative sentiment, and a subgroup of tweets with only neutral sentiment. Then I compute the average abnormal daily return (AAR) for each subgroup per trading day. To be specific, the AARs are calculated by

$$AAR_t^{\{Positive,Negative,Neutral\}} = \frac{1}{N}\sum_{i=1}^{N} AR_{i,t}^{\{Positive,Negative,Neutral\}}$$
$$t \in \{T-1, T, T+1\} \tag{3.3}$$

where T corresponding to the date of tweet on company i. Therefore, $AAR_T^{Positive}$ can be interpreted as the average abnormal daily return for tweets with positive sentiment at the tweet's day.

With equation (3.3), the hypothesis "On average, Tweets with positive sentiment can influence the stock market movement in a different way than Tweets with other types of sentiment" can be written in a formal way as[5]:

Hypothesis: Overall, the Tweets from President Trump with positive sentiment and negative sentiment will have a different impact on abnormal daily return for the mentioned company.

$$H_0 : AAR_T^{Positive} = AAR_T^{Negative}$$
$$H_1 : AAR_T^{Positive} \neq AAR_T^{Negative}$$

It is obvious that for a hypothesis like the one stated above, two sample unpaired t-test[6] would be appropriate to use. In particular, the t-statistics for the above test are calculated in the following way,

$$t_{statistics} = \frac{AAR_T^{Positive} - AAR_T^{Negative}}{\sqrt{s^2\left(\frac{1}{N_1}+\frac{1}{N_2}\right)}} \tag{3.4}$$

[5]This part conducts multiple hypothesis testings, and however, for exposition purposes, I only use the hypothesis on positive tweets as a representative example here. Full testing results are shown in Table 3.2.

[6]I am using two sample t-test here because the data size is various for different subgroups of tweets.

where the N_1 and N_2 are the sample size of positive and negative subgroup respectively. s^2 is the adjusted standard error which is defined as

$$s^2 = \frac{\sum_{i=1}^{N_1} \left(AR_{i,T}^P - AAR_T^P\right)^2 + \sum_{i=1}^{N_2} \left(AR_{i,T}^N - AAR_T^N\right)^2}{N_1 + N_2 - 2} \tag{3.5}$$

Applying the equation (3.3)-(3.5) to the abnormal daily return data, I obtained the t-statistics and their associated p-values.

Table 3.2 shows the p-values for hypothesis testings on the average abnormal daily return of tweets with different sentiments within the study window. As a robustness check, the result from the first column of the table suggests that there is no statistically significant difference between tweets with any sentiment on the day before tweet posting. This makes sense since no tweet has been posted yet at $T-1$, so one should not expect any statistically significant difference to show up on these tests.

Table 3.2: Hypothesis testing I

	Hypothesis	$T-1$	T	$T+1$
P-value	Positive vs. Negative	0.7968	0.0253	0.7095
	Positive vs. Neutral	0.6771	0.0083	0.4843
	Negative vs. Neutral	0.6595	0.1285	0.6636

On the other hand, for tests on the date after a tweet was posted, the result suggests that the difference between positive and negative tweets only significant at the date of tweet (T) but not significant at one day after it ($T+1$). Thus, based on the data we have, the influence of tweet on stock market movement only persist for about one trading day. The same conclusion holds for the test on positive vs. neutral tweets. On the date of tweet posting, the effect of a

positive tweet is significantly different from tweets with neutral sentiment. But neither on the day before nor the day after. However, I didn't see any statistical significance between tweets with negative and neutral sentiment. Interestingly, there is no statistically significant impact of a tweet on a stock price move at $T+1$ regardless of the type of sentiment it has.

Figure 3.4 plots the abnormal returns of hypothesis testings conducted in this part. For 3.4a, the data dots with blue color are ARs for negative tweets, where the data dots with red color are for positive tweets. The red horizontal line stands for the AAR of tweets with positive sentiment; the blue line stands for the AAR of tweets with negative sentiment. The p-value from the first cell in the second column of Table 3.2 suggests the gap between the red line and the blue line is statistically different from zero. Similarly, For Figure 3.4b, the data dots with blue color are ARs for neutral tweets, where the data with red color are for positive tweets. The red horizontal line stands for the AAR of tweets with positive sentiment; the blue line stands for the AAR of tweets with neutral sentiment. The p-value from the second cell in the second column of Table 3.2 suggests the gap between the red line and the blue line is statistically different from zero.

The takeaways from this section are twofold. First of all, at the date of tweet posting, different sentiments create significant different effects on the stock market, especially the tweet with positive sentiment. Second, such an influence only lasts for one trading day and quickly vanishes.

3.4.2 Hypothesis testing II

In this section, I will use both sentiment data set for president Trump's tweets and time series data for abnormal daily return of each mentioned company to uncover the exact pattern of tweet with a particular sentiment on affecting the stock market movements.

For this part, I also divide the tweets data set into three subgroups in the same way

Figure 3.4: AAR difference for tweets with different sentiment

(a) Positive vs. Negative tweets

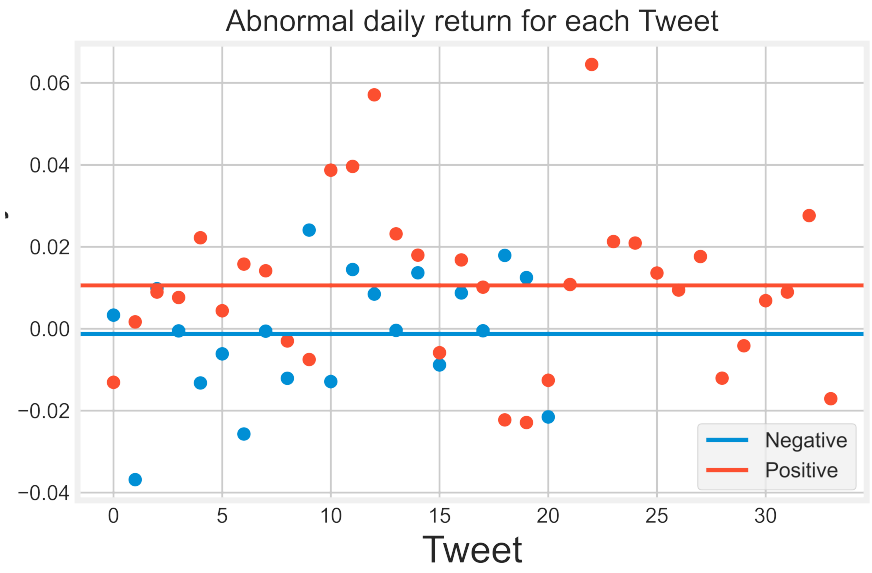

(b) Positive vs. Neutral tweets

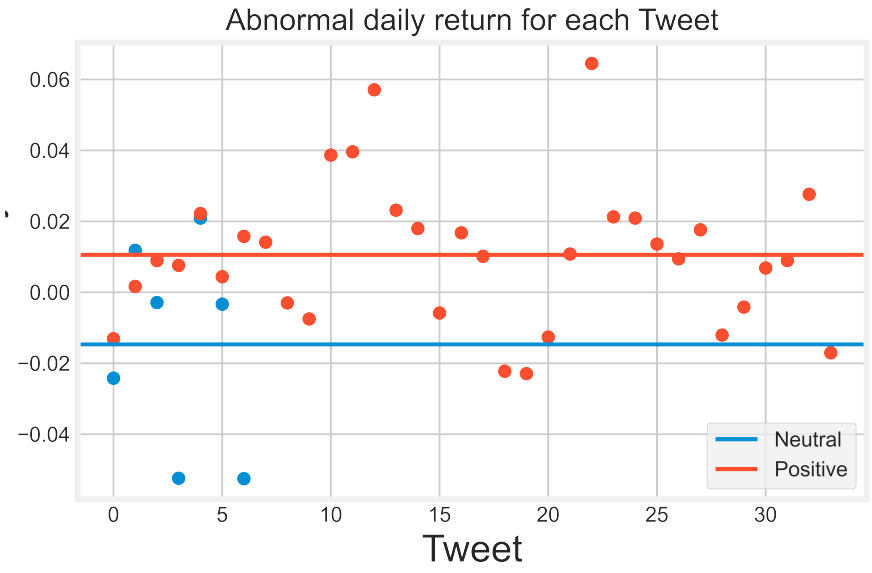

as I did in the last section. Then I compute the average abnormal daily return (AAR) for each subgroup per trading day. The whole process is actually parallel to equation (3.3).

In this section, I will focus on the intra-group difference rather than the inter-group difference. That said, one example[7] of the hypothesis I am testing in this part can be stated as "Overall, the average abnormal daily return of Tweets with positive sentiment will tend to deviate from the original trend after the date of tweet". More rigorously, it can be written as the following way:

Hypothesis: Overall, the Tweets from President Trump with positive sentiment will significantly influence abnormal daily returns for the mentioned company after it was posted.

$$H_0 : AAR_{T-1}^{Positive} = AAR_{T}^{Positive}$$

$$H_1 : AAR_{T-1}^{Positive} \neq AAR_{T}^{Positive}$$

For this intra-group hypothesis testing, I will use two sample t-test with equal sample size as my approach for this section. In particular, the t-statistics for the above test are calculated in the following way,

$$t_{statistics} = \frac{AAR_{T}^{Positive} - AAR_{T-1}^{Positive}}{\sqrt{s^2\left(\frac{2}{N}\right)}} \tag{3.6}$$

where the N are the sample size of tweets with positive sentiment. s^2 is the adjusted standard error which is defined as

$$s^2 = \frac{\sum_{i=1}^{N}\left[\left(AR_{i,T}^{P} - AAR_{T}^{P}\right)^2 + \left(AR_{i,T-1}^{P} - AAR_{T-1}^{P}\right)^2\right]}{2\left(N-2\right)} \tag{3.7}$$

Applying the equation (3.3), (3.6) and (3.7) to the abnormal daily return data, I obtained the t-statistics and their associated p-values.

Table 3.3 shows the p-values for hypothesis testings on the average abnormal daily return of positive, negative, and neutral tweets for the window of study. To be specific, it tests

[7] Again, I will use positive tweets as an example of the hypothesis testings in this part.

if the AAR of tweets with each type of sentiment are statistically different before and after they were posted. For each sentiment, I am testing whether the AAR is statistically significantly different between the day before the tweet $(T-1)$, the day of the tweet (T), and one day after the tweet $(T+1)$. Therefore, in total, I am running 9 hypothesis testings in this practice, and most of them are obviously not statistically significant at all.

Table 3.3: Hypothesis testing I

	Hypothesis	Positive	Negative	Neutral
P-value	$T-1$ vs. T	0.0998	0.5307	0.3916
	$T-1$ vs. $T+1$	0.2929	0.8512	0.8067
	T vs. $T+1$	0.5486	0.2148	0.3550

By taking a close look at the table, as a robustness check, testings on neutral tweets suggest no statistical evidence for a significant effect of neutral tweets on stock price movements. For testings on tweets with positive sentiment, the results suggest that the difference before and after a tweet was posted is only significant at 90% confidence level, based the comparison between the date of tweet (T) and the day before it $(T-1)$. That said, based on the data we have, only the tweet with positive sentiment has an influence on the stock market, and moreover, consistent with previous results, it only persists for about one trading day. Interestingly, for positive tweets, neither the differences between $T-1$ vs. $T+1$ nor the differences between T vs. $T+1$ are significant. This seems a little contradictory with the conclusion on positive tweets. An explanation would be the 90% confidence level is not restricted enough to get a consistent conclusion in this part. Thus, from this sense, one can reject the null by imposing a smaller

significant level.

Surprisingly, negative tweets are not able to affect the stock market. This result contradicts previous research such as Brans and Scholtens (2020).

Figure 3.5 plots the abnormal returns of hypothesis testings conducted in this part. The data dots with blue color are ARs for positive tweet before its posting, where the data dots with red color are for positive tweet after its posting. The red horizontal line stands for the AAR of tweets with positive sentiment before its posting, the blue line stands for the AAR of tweets with positive sentiment after its posting. The p-value from the first cell in the first column of Table 3.3 suggests the gap between the red line and the blue line is statistically different from zero at 90% confidence level. Moreover, the implication here is that, on average, president Trump's tweet with positive sentiment tends to increase the AAR for mentioned company.

Figure 3.5: AAR difference for tweets with different sentiment

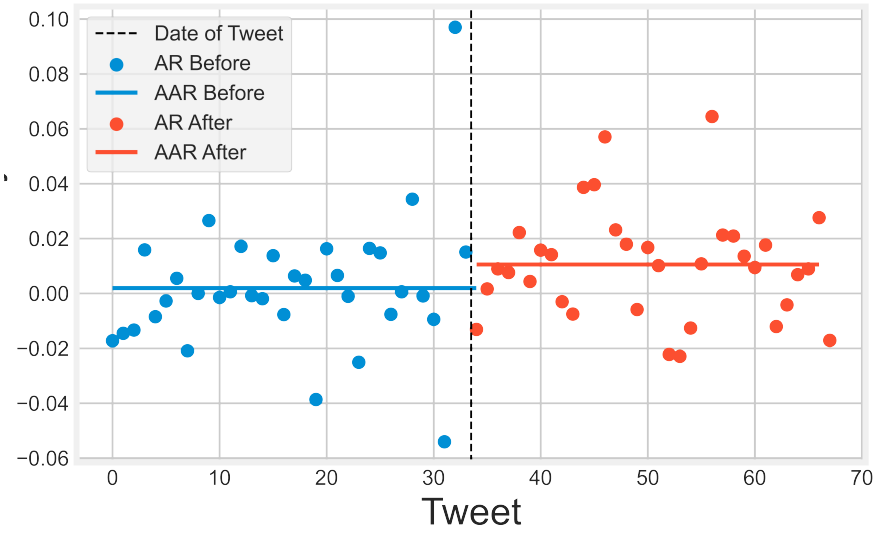

Combining hypothesis testing results from this section, we end up with a very interesting conclusion. That is, the positive tweets had a more significant impact than their negative

counterpart (and of course those neutral tweets) for the period when Donald Trump became US president. Moreover, the influence of the positive tweet was immediately effective (on the day of posting) but quickly vanished (on the following trading day). A possible explanation as to why positive tweets had a larger impact would be because Trump was synonymous with negative and controversial statements in his efforts to generate publicity for his presidential power. Therefore, even there are more positive company-specific tweets in the data set I am using, when count overall Tump's tweets, positive tweet still came rarely, thus leading to increased returns.

3.5 Conclusion

This paper studies the impact of President Trump's Twitter messages on the stock market. I investigate 60 of his tweets that include the name of a publicly listed company over the years of his presidency. I also carry out an analysis of the sentiment of the tweets by using textual analysis. Overall, the president's tweets did not yield a significant response from the stock market. However, when considering the tweets' sentiment, I find that especially tweets with a (strong) positive sentiment render a significant positive response from the investment community in an economically meaningful way. This contradicts previous research such as Juma'h and Alnsour (2018); Brans and Scholtens (2020), and instead, my result implies that investors are happier to react to good news than bad news. I feel that my systematic sampling approach, the substantially larger number of events, the inclusion of non-parametric testing, and relying on textual analysis regarding the sentiment of the tweets, contributes to a better understanding of the economic impact of communications from president Trump.

Methodological speaking, this paper features a brand new way of constructing abnormal daily returns for the stock price. Before my work, people usually follow the traditional econometric approach, which involves few drawbacks. In this research, the abnormal daily returns are

constructed based directly on its definition. Machine learning, especially RNN allows me to accurately forecast the expected daily return (hence abnormal daily return) while maintaining the flexibility (assumption-free) of the whole algorithm.

There are few limitations to this event study. First, the tweets are selected if the tweet was directly mentioned a company's name. This could lead to exclusion and inclusion from incorrect events in the dataset. One way to improve the result in the future is to include a tweet that "indirectly" mentioned a company and significantly influences its stock price.

Further, this study only uses tweets that mentioned companies in S&P 500. This may also potentially bias my evaluation result. Imagine that the effect of President Trump's tweet is totally in the opposite direction and larger in magnitude for stock indexes other than S&P 500. If so, the direction of my conclusion may get flipped when combining them with my current data set. For future research, including a stock index outside of the S&P 500 is definitely critical.

Finally, many variables are also useful to evaluate the stock market changes. For example, trading volume. Intuitively, if a positive tweet is indeed creating positive movement on stock price, the market will become more active as well. That said, it is highly likely that the trading volume of the mentioned company also increases. If such a piece of evidence can be captured and proved significant, the main finding in this paper can be further confirmed.

Bibliography

Aghion, P., Akcigit, U., Bergeaud, A., Blundell, R., and Hemous, D. (2019), "Innovation and Top Income Inequality," *Review of Economic Studies*, 86, 1–45.

Aiyagari, S. R. (1994), "Uninsured idiosyncratic risk and aggregate saving," *Quarterly Journal of Economics*, 109, 659–684.

Akcigit, U. and Ates, S. T. (2020a), "What Happened to U.S. Business Dynamism?" *FEDS Notes*, 2020.

— (2020b), "What Happened to U.S. Business Dynamism?" *FEDS Notes*, 2020.

Aldrich, E. M. and Kung, H. (2011), "Computational Methods for Production-Based Asset Pricing Models with Recursive Utility," .

Andrews, D., Criscuolo, C., and Gal, P. (2019), "The Best versus the Rest: The Global Productivity slowdown, Divergence across Firms and the Role of Public Policy," *OECD Going Digital Policy Note*, 8.

Aruoba, S. B., Fernández-Villaverde, J., and Rubio-Ramírez, J. F. (2006), "Comparing solution methods for dynamic equilibrium economies," *Journal of Economic Dynamics and Control*, 30, 2477–2508.

Autor, D., Dorn, D., Katz, L. F., Patterson, C., and Reenen, J. V. (2019), "The Fall of the Labor Share and the Rise of Superstar Firms," *The Quarterly Journal of Economics*.

Autor, D., Dorn, D., Katz, L. F., Patterson, C., and Van Reenen, J. (2017), "Concentrating on the fall of the labor share," *American Economic Review*, 107, 180–185.

Aziz, A. A. (2020), "Trump ' s Twitter-nomics : An Empirical Analysis of Trump ' s Tweets and Its Impact on the Stock Market," Ph.D. thesis.

Bewley, T. (1977), "The permanent income hypothesis: A theoretical formulation," *Journal of Economic Theory*, 16, 252–292.

Brans, H. and Scholtens, B. (2020), "Under his thumb the effect of president Donald Trump's Twitter messages on the US stock market," *PLoS ONE*, 15, 1–11.

Brown, S. J. and Warner, J. B. (1980), "Measuring security price performance," *Journal of Financial Economics*, 8, 205–258.

— (1985), "Using daily stock returns. The case of event studies," *Journal of Financial Economics*, 14, 3–31.

Buera, F. J. and Moll, B. (2015), "Aggregate implications of a credit crunch: The importance of heterogeneity," *American Economic Journal: Macroeconomics*, 7, 1–42.

Buera, F. J. and Shin, Y. (2013), "Financial frictions and the persistence of history: A quantitative exploration," *Journal of Political Economy*, 121, 221–272.

Burnside, C. (1998), "Solving asset pricing models with Gaussian shocks," *Journal of Economic Dynamics and control*, 22, 329–340.

Cai, Y., Judd, K. L., and Steinbuks, J. (2017), "A nonlinear certainty equivalent approximation method for dynamic stochastic problems," *Quantitative Economics*, 8, 117–147.

Caldara, D., Fernández-Villaverde, J., Rubio-Ramírez, J. F., and Yao, W. (2012), "Computing DSGE models with recursive preferences and stochastic volatility," *Review of Economic Dynamics*, 15, 188–206.

Campbell, C. J., Cowan, A. R., and Salotti, V. (2010), "Multi-country event-study methods," *Journal of Banking and Finance*, 34, 3078–3090.

Chan, W. C. (2003), "Stock price reaction to news and no-news: Drift and reversal after headlines," *Journal of Financial Economics*, 70, 223–260.

Collard, F. and Juillard, M. (2001), "Accuracy of stochastic perturbation methods: The case of asset pricing models," *Journal of Economic Dynamics and Control*, 25, 979–999.

Cooper, R. and Johri, A. (2002), "Learning-by-doing and aggregate fluctuations," *Journal of Monetary Economics 49*, 49, 1539–1566.

De Nardi, M. and Fella, G. (2017), "Saving and wealth inequality," *Review of Economic Dynamics*, 26, 280–300.

Den Haan, W. J. and Marcet, A. (1994), "Accuracy in Simulations," *The Review of Economic Studies*, 61, 3–17.

Den Haan, W. J., RenDahl, P., Allais, O., and Algan, Y. (2010), "Solving and Simulating Models with Heterogeneous Agents and Aggregate Uncertainty," *Fothcoming, Handbook of Computational Economics*.

Epstein, L. G. and Zin, S. E. (1989), "Substitution , Risk Aversion , and the Temporal Behavior of Consumption and Asset Returns : A Theoretical Framework," *Econometrica*, 57, 937–969.

Fernández-Villaverde, J., Rubio-Ramírez, J., and Schorfheide, F. (2016), "Solution and

Estimation Methods for DSGE Models," in *Handbook of Macroeconomics*, Elsevier B.V., vol. 2A, chap. 9, pp. 527–724.

Fernández-Villaverde, J. and Rubio-Ramírez, J. F. (2006), "Solving DSGE models with perturbation methods and a change of variables," *Journal of Economic Dynamics and Control*, 30, 2509–2531.

Gaspar, J. and Judd, K. L. (1997), "Solving Large-Scale Rational-Expectations Models," *Macroeconomic Dynamics*, 1.

Ge, Q. and Wolfe, M. H. (2017), "Stock Market Reactions to Presidential Social Media Usage: Evidence from Company-Specific Tweets," *SSRN Electronic Journal*.

Gourio, F., Messer, T., and Siemer, M. (2016), "Firm entry and macroeconomic dynamics: A state-level analysis," *American Economic Review*, 106, 214–218.

Greenwood, J., Hercowitz, Z., and Krusell, P. (1997), "Long-Run Implications of Investment-Specific Technological Change," *The American Economic Review*, 87, 342–362.

Hall, R. E. (2018), "New Evidence on the Markup of Prices over Marginal Costs and the Role of Mega-Firms in the US Economy," *NBER Working Paper Series*, 21.

Jermann, U. J. (1998), "Asset Pricing in Production Networks," *Journal of Monetary Economics*, 41, 257–275.

Judd, K. L. (1992), "Projection methods for solving aggregate growth models," *Journal of Economic Theory*, 58, 410–452.

— (1996), "Chapter 12 Approximation, perturbation, and projection methods in economic analysis," in *Handbook of Computational Economics*, vol. 1, pp. 509–585.

— (1998), *Numerical Methods in Economics Optimization Problems*, MIT Press, Cambridge.

— (2003), "Perturbation methods with nonlinear changes of variables," *Mimeo, Hoover Institution. Judd, K.L., Guu, S.M*, 21, 1025–1042.

Judd, K. L. and Guu, S.-M. (1993), "Perturbation Solution Methods for Economic Growth Models," in *Economic and Financial Modeling with Mathematica*, Springer, New York, NY, chap. 4, pp. 80–103.

Judd, K. L. and Guu, S. M. (2001), "Asymptotic methods for asset market equilibrium analysis," *Economic Theory*, 18, 127–157.

Judd, K. L. and Jin, H.-h. (2002), "Perturbation methods for general dynamic stochastic models," .

Judd, K. L., Maliar, L., Maliar, S., and Valero, R. (2014), "Smolyak method for solving dynamic economic models: Lagrange interpolation, anisotropic grid and adaptive domain," *Journal of Economic Dynamics and Control*, 44, 92–123.

Juma'h, A. H. and Alnsour, Y. (2018), "Using social media analytics: The effect of President Trump's tweets on companies' performance," *Journal of Accounting and Management Information Systems*, 17, 100–121.

Kaltenbrunner, G. and Lochstoer, L. A. (2010), "Long-run risk through consumption smoothing," *Review of Financial Studies*, 23, 3190–3224.

Karabarbounis, L. and Neiman, B. (2014), "The global decline of the labor share," *Quarterly Journal of Economics*, 129, 61–103.

Khan, A. and Thomas, J. K. (2008), "Idiosyncratic shocks and the role of nonconvexities in plant and aggregate investment dynamics," *Econometrica*, 76, 395–436.

— (2013), "Credit shocks and aggregate fluctuations in an economy with production heterogeneity," *Journal of Political Economy*, 121, 1055–1107.

Krusell, P. and Smith, A. A. (1998), "Income and wealth heterogeneity in the macroeconomy," *Journal of Political Economy*, 106, 867–896.

Mackinlay, A. C. (1997), "Event Studies in Economics and Finance," *Journal of Economic Literature*, 35, 13–39.

Marco, C. and Mariacristina, D. N. (2009), "Estate Taxation, Entrepreneurship, and Wealth," *American Economic Review*, 99, 85–111.

Moll, B. (2014), "Productivity Losses from Financial Frictions: Can Self-Financing Undo Capital Misallocation?" *American Economic Review*.

Petrosky-Nadeau, N. and Zhang, L. (2017), "Solving the Diamond-Mortensen-Pissarides model accurately," *Quantitative Economics*, 8, 611–650.

Santos, M. S. (2000), "Accuracy of numerical solutions using the Euler equation residuals," *Econometrica*, 68, 1377–1402.

Schneider, C. and Spalt, O. (2016), "Conglomerate Investment, Skewness, and the CEO Long-Shot Bias," *Journal of Finance*, 71, 635–672.

Schumacher, M. D. and Nikolai Graber (2019), "When Local Approximations Fail," .

S.P. Kothari and Warner, J. B. (2006), "Econometrics of Event Studies," in *Handbook of Corporate Finance: Empirical Corporate Finance*, vol. A.

Swanson, E., Anderson, G., and Levin, A. (2006), "Higher-Order Perturbation Solutions to Dynamic , Discrete-Time Rational Expectations Models," .

Swanson, E. T. (2012), "Risk aversion and the labor margin in dynamic equilibrium models," *American Economic Review*, 102, 1663–1691.

Tauchen, G. (1986), "Finite state markov-chain approximations to univariate and vector autoregressions," *Economics Letters*, 20, 177–181.

Thelwall, M., Buckley, K., and Paltoglou, G. (2011), "Sentiment In Twitter Events (preprint)," *Journal of the American Society for Information Science and Technology*, 62, 406–418.

Thelwall, M., Buckley, K., Paltoglou, G., and Di, C. (2010), "Sentiment Strength Detection in Short Informal Text Mike," *Journal of the American Society for Information Science and Technology*, 61, 2544–2558.

Van Binsbergen, J. H., Fernández-Villaverde, J., Koijen, R. S., and Rubio-Ramírez, J. (2012), "The term structure of interest rates in a DSGE model with recursive preferences," *Journal of Monetary Economics*, 59, 634–648.

Weil, P. (1990), "Nonexpected Utility in Macroeconomics," *The Quarterly Journal of Economics*, 105, 29–42.

Winberry, T. (2018), "A method for solving and estimating heterogeneous agent macro models," *Quantitative Economics*, 9, 1123–1151.

Wolff, E. (2017), "Household Wealth Trends in the United States, 1962 to 2016: Has Middle Class Wealth Recovered?" *National Bureau of Economic Research*.

Zhang, L. (2018), "Credit crunches , individual heterogeneity and the labor wedge," *Journal of Macroeconomics*, 56, 65–88.

Appendix A

Chapter 1

A.1 Proofs of the 2S-Inter-ld algorithm in Section 1.2

This section provides all necessary proofs and illustrations of Section 1.2 of the paper. This includes Lemma 1-2, Proposition 1-3. (They are all provided right after the statement in the main text of the paper for this version)

A.2 Examples on other univariate functions

I pick three univariate functions and use the analytical result from the ratio test, root test, and complex plane approach as my benchmark result to test the performance of Algorithm 1 on ROC approximation. This section exposits two examples other than the square root function showed in Section 1.2.

A.2.1 $f(x) = \sin x$ and the root test

I decide to use function $f(x) = \sin x$ to test the performance of our algorithm on the case with oscillating coefficients. At $c = 0$, the Taylor expansion can be written as

$$\sin x = \sum_{n=1}^{\infty} (-1)^{n-1} \frac{x^{2n-1}}{(2n-1)!} \tag{A.1}$$

The root test approach delivers the ROC value as,

$$R^c = \frac{1}{\limsup_{n\to\infty} \sqrt[n]{|t_n^c|}} = \frac{1}{\limsup_{n\to\infty} \sqrt[n]{\left|\frac{(-1)^{n-1}}{(2n-1)!}\right|}} = \infty \tag{A.2}$$

Equation (A.2) suggests that the ROC of $f(x) = \sin x$ at $c = 0$ is infinite.

Figure A.1: Algorithm 1 on $f(x) = \sin x$ at $c = 0$

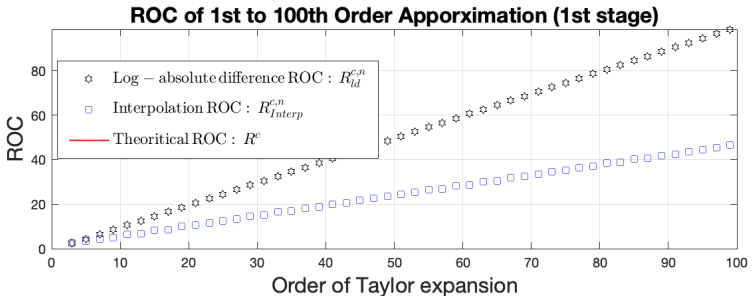

Figure A.1 plots the first-stage sequence solved by both polynomial interpolation and the log-absolute difference method. There are two points I want to point put using this case. First, the sequence only has 50 elements. Hence, the approximation is bi-coefficient (meaning only odd terms are used for the 2S-Inter-ld algorithm). The reason for this is that the Taylor coefficients of $\sin x$ oscillate between $(-1)^{n-1} \frac{x^{2n-1}}{(2n-1)!}$ for n odd and zero for n even. To make the CLS and log-absolute difference well defined after taking the log-absolute value, we need to remove the zero terms. Further, knowing the ROC is infinite in this case, we only need the first-stage approximation, as no penalty is needed (i.e., conservative is not necessary for an infinite ROC case).

The sequence of approximated ROC values monotonically increases in Figure A.1. Conceptually, it will approach infinity as the order of the Taylor polynomial continues to increase. Given a finite Taylor polynomial in realistic practice, such a sequence can be considered as evidence (or indication) of an infinite ROC. This practice gives some insight into how essential the active set (the none zero subset) of Taylor coefficients are to this algorithm. It also shows some potential in dealing with infinite ROC cases using the 2S-Inter-ld algorithm.

A.2.2 $f(x) = \frac{1}{(9802-198x+x^2)}$ and the complex plane approach

For the last one-dimensional function practice, we decide to use $f(x) = \frac{1}{(9802-198x+x^2)}$ from Judd (1998) to show how our algorithm can overcome the limitations of analytical approaches in computing ROC. It is easy to identify the singularity of this function is located at $x = 99 \pm \sqrt{-1}$, hence the complex plane approach implies the $R^c = 1$ when $c = 99$. Notice this is the only way we can get an analytical answer for the ROC (both the ratio and root test are not helpful) in this case.

Similar to $f(x) = \sin x$, Figure A.2 shows there are zero and periodically oscillating coefficients in this case. Hence, the original Taylor coefficient set does not coincide with the active set. However, by dropping zero coefficients and taking log-absolute values, the approximation on even terms implies the linear trend does exist for the active set. One may notice the log-absolute difference solution perfectly approximates the true ROC (the black hexagram sequence in the first stage perfectly coincides with the horizontal red line). This is because the objective function is well behaved in this case. Hence, the log-absolute Taylor coefficients lie perfectly on a linear curve; therefore, the log-absolute difference approach is efficient.

However, as the ROC, in this case, is a finite number, and suppose we do not know the true limit, a conservative approximation after the second stage (the blue hexagram sequence) still leads us to the true value. Till this practice, we used three types of objective functions

Figure A.2: Algorithm 1 on $f(x) = \frac{1}{(9802-198x+x^2)}$ at $c = 99$

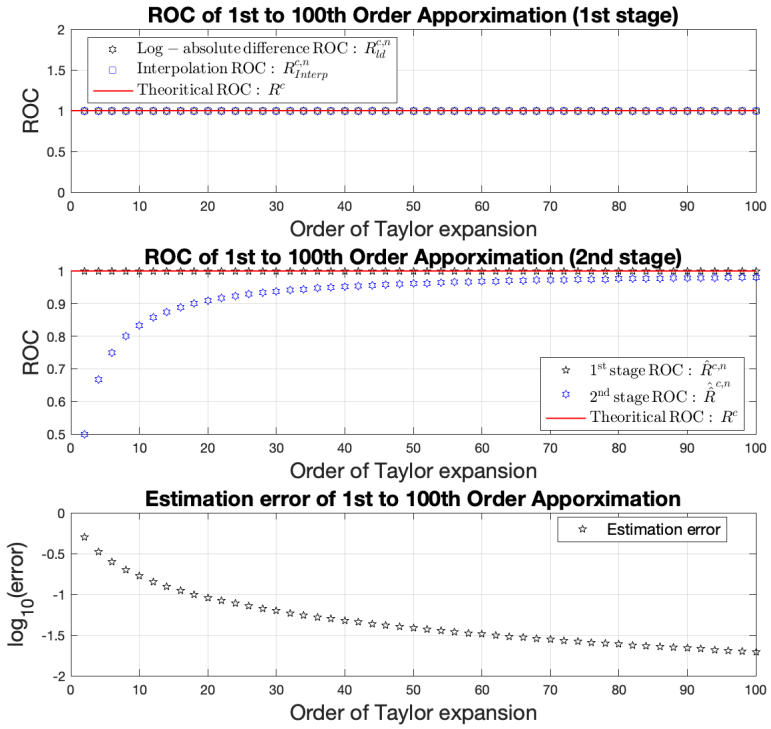

to test Algorithm 1's performance using three analytical methods for computing ROC. Overall, the toy examples in this subsection verify that Algorithm 1 is a solid numerical foundation for attacking multi-dimensional functions or models with unknown ROC.

A.3 Proof of ROC of $k_{t+1}(\cdot)$ in closed-form Neoclassical growth model

Given the solution from the neoclassical growth model with closed-form formula

$$k_{t+1} = \alpha\beta e^{z_t} k_t^{\alpha}$$

The Taylor expansion (perturbation solution) of this solution at deterministic steady state $(k, z; \chi) = (k_{ss}, 0; 0)$ on the capital direction will be

$$\begin{aligned}
k_{t+1} =& \sum_{n=0}^{\infty} \frac{F^{(n)}(k_{ss}, 0; 0)}{n!}(k - k_{ss})^n \\
=& \alpha\beta k_{ss}^{\alpha} + \alpha^2\beta k_{ss}^{\alpha-1}(k - k_{ss}) + \frac{1}{2}(\alpha - 1)\alpha^2\beta k_{ss}^{\alpha-2}(k - k_{ss})^2 \\
=& + \frac{1}{6}(\alpha - 2)(\alpha - 1)\alpha^2\beta k_{ss}^{\alpha-3}(k - k_{ss})^3 + \cdots \\
& + \frac{1}{n!}(\alpha - n + 1)\cdots(\alpha - 1)\alpha^2\beta k_{ss}^{\alpha-n}(k - k_{ss})^n + \cdots
\end{aligned}$$

We can use the ratio test to derive the theoretical ROC in this case, as we have the analytical expression for t_n and t_{n+1}. This suggests

$$\begin{aligned}
R^c &= \lim_{n\to\infty} \left| \frac{t_n}{t_{n+1}} \right| \\
&= \lim_{n\to\infty} \left| \frac{\frac{1}{n!}(\alpha - n + 1)\cdots(\alpha - 1)\alpha^2\beta k_{ss}^{\alpha-n}}{\frac{1}{(n+1)!}(\alpha - n)\cdots(\alpha - 1)\alpha^2\beta k_{ss}^{\alpha-n-1}} \right| \\
&= \lim_{n\to\infty} \left| \frac{(n+1)}{(\alpha - n)k_{ss}} \right|
\end{aligned}$$

Using L' Hospital's rule, we get

$$R^c = \lim_{n\to\infty} \left| \frac{(n+1)}{(\alpha - n)} k_{ss} \right| = \lim_{n\to\infty} \left| \frac{1}{-1} k_{ss} \right| = |k_{ss}|$$

This implies the ROC of the neoclassical model on capital direction is $|k_{ss}|$. Now let's look at the ROC of another state variable z_t. To see this, the Taylor expansion of this solution at the deterministic steady state $(k, z; \chi) = (k_{ss}, 0; 0)$ on the TFP shock direction will be

$$\begin{aligned}
k_{t+1} &= \sum_{n=0}^{\infty} \frac{F^{(n)}(k_{ss}, 0; 0)}{n!}(z)^n \\
&= \alpha\beta k_{ss}^{\alpha} + \alpha\beta k_{ss}^{\alpha} z + \frac{1}{2}\alpha\beta k_{ss}^{\alpha} z^2 + \frac{1}{6}\alpha\beta k_{ss}^{\alpha} z^3 + \cdots + \frac{1}{n!}\alpha\beta k_{ss}^{\alpha} z^n + \cdots
\end{aligned}$$

we can also use the ratio test to derive the theoretical ROC in this case as we also have the analytical expression for t_n and t_{n+1}. This suggests

$$\begin{aligned} R^c &= \lim_{n\to\infty}\left|\frac{t_n}{t_{n+1}}\right| \\ &= \lim_{n\to\infty}\left|\frac{\frac{1}{n!}\alpha\beta k_{ss}^{\alpha}}{\frac{1}{(n+1)!}\alpha\beta k_{ss}^{\alpha}}\right| = \lim_{n\to\infty}|n+1| = \infty \end{aligned}$$

This implies the ROC of the neoclassical model on TFP direction is infinite.

A.4 ROC of Burnside's asset pricing model

A.4.1 Model set up and numerical result

In this section, we consider another simple macro model with closed form solution used by Burnside. In this model, agents decide consumption, c_t, and equity holding, e_t, at every period to maximize their lifetime utility on

$$\max_{\{c_t,e_t\}_{t=0}^{\infty}} \mathbb{E}_0 \sum_{t=0}^{\infty} \beta^t \frac{c_t^{\theta}}{\theta}, \quad \theta \leq 0 \,\text{and}\, \theta \neq 0$$

where θ is the elasticity of consumption and $\beta \in (0,1)$ is the discount factor. Defining p_t as the price of equity and d_t as corresponding dividend in period t, which grow at rate x_t so

$$d_{t+1} = e^{x_{t+1}} d_t$$

and the growth rate x_t follows the $AR(1)$ process with $|\rho| < 1$

$$x_{t+1} = (1-\rho)\, x_{ss} + \rho x_t + \chi \epsilon_{t+1}, \quad \epsilon_{t+1} \sim \mathcal{N}\left(0, \sigma^2\right)$$

the budget constraint can be written as

$$p_t e_{t+1} + c_t = (p_t + d_t)\, e_t$$

Defining the price-dividend ratio $y_t = p_t/d_t$, Burnside (1998) showed the solution of this model is given by

$$y_t = \sum_{i=1}^{\infty} \beta^i \exp\left[a_i + b_i\left(x_i - x_{ss}\right)\right] \tag{A.3}$$

where

$$a_i = \theta x_{ss} i + \frac{\theta^2\sigma^2}{2(1-\rho)^2}\left[i - \frac{2\rho\left(1-\rho^i\right)}{1-\rho} + \frac{\rho^2\left(1-\rho^{2i}\right)}{1-\rho^2}\right]$$

and

$$b_i = \frac{\theta\rho(1-\rho^i)}{1-\rho}$$

Again, because of the analytical solution, we can use the Taylor polynomial as a shortcut to denote the perturbation solution. As we can reduce the model's state space to one dimension, the range of convergence of this model is the ROC of the perturbation polynomial of the policy function (A.3)

$$y_t\left(x_t;\chi=0\right) \approx \sum_{n=0}^{k} \frac{F^{(n)}(x_{ss};0)}{n!}(x_t - x_{ss})^n$$
$$F(x_t;\chi) = \sum_{i=1}^{\infty} \beta^i \exp\left[a_i + b_i\left(x_i - x_{ss}\right)\right]$$

We proved the ROC of the policy function in this model is defined by $(-\infty,\infty) \subseteq \mathbb{R}^1$ in this next subsection.

Figure A.3 plots the ROC approximation process on Burnside's asset-pricing model. Notice that because we have a well behaved active set, the linear trend is clear and the approximated value increases monotonically . This result also provides another explanation on one of the main conclusions in Collard and Juillard (2001). The paper states the perturbation method captures the distribution of shocks much more precisely than Chebychev polynomials in the Burnside asset-pricing model. From a numerical perspective, our results confirm their conclusion. Our results also suggest the dominance of the perturbation method is as a result of the state variable of Burnside asset-pricing model having an infinite ROC.

Figure A.3: Burnside asset pricing model (ROC approximation on z_t dimension)

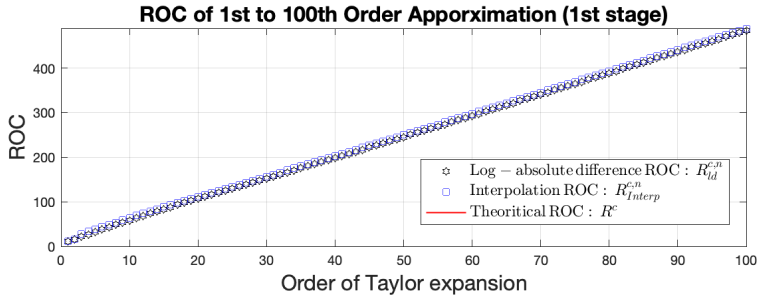

A.4.2 Proof of ROC of price-dividend ratio in policy function

Proof. Given the solution of Burnside asset-pricing model (A.3), the Taylor expansion of this solution at the deterministic steady state $x = x_{ss}$ on the state space of rate of growth of dividends will be

$$\begin{aligned} y_t &= \sum_{n=0}^{\infty} \frac{F^{(n)}(x_{ss};0)}{n!}(z)^n \\ &= \sum_{i=1}^{\infty} \beta^i \exp\left[\alpha_i\right] + \sum_{i=1}^{\infty} \beta^i b_i \exp\left[a_i\right](x_i - x_{ss}) + \frac{1}{2}\sum_{i=1}^{\infty} \beta^i b_i^2 \exp\left[a_i\right](x_i - x_{ss})^2 \\ &+ \frac{1}{6}\sum_{i=1}^{\infty} \beta^i b_i^3 \exp\left[a_i\right](x_i - x_{ss})^3 + \cdots + \frac{1}{n!}\sum_{i=1}^{\infty} \beta^i b_i^n \exp\left[a_i\right](x_i - x_{ss})^n + \cdots \end{aligned}$$

Using the ratio test, we have

$$\begin{aligned} R^c &= \lim_{n\to\infty} \left| \frac{t_n}{t_{n+1}} \right| \\ &= \lim_{n\to\infty} \left| \frac{\frac{1}{n!}\sum_{i=1}^{\infty} \beta^i b_i^n \exp\left[a_i\right]}{\frac{1}{(n+1)!}\sum_{i=1}^{\infty} \beta^i b_i^{n+1} \exp\left[a_i\right]} \right| \\ &= \lim_{n\to\infty} |n+1| \left| \frac{\sum_{i=1}^{\infty} \beta^i b_i^n \exp\left[a_i\right]}{\sum_{i=1}^{\infty} \beta^i b_i^{n+1} \exp\left[a_i\right]} \right| \\ &= \lim_{n\to\infty} |n+1| \left| \frac{\sum_{i=1}^{\infty} \beta^i \left(\frac{\theta\rho(1-\rho^i)}{1-\rho}\right)^n \exp\left[a_i\right]}{\sum_{i=1}^{\infty} \beta^i \left(\frac{\theta\rho(1-\rho^i)}{1-\rho}\right)^{n+1} \exp\left[a_i\right]} \right| \\ &= \lim_{n\to\infty} |n+1| \left| \frac{1-\rho}{\theta\rho} \right| \left| \frac{\sum_{i=1}^{\infty} \beta^i \left(1-\rho^i\right)^n \exp\left[a_i\right]}{\sum_{i=1}^{\infty} \beta^i \left(1-\rho^i\right)^{n+1} \exp\left[a_i\right]} \right| \end{aligned}$$

because of the calibration we always have $|\rho| < 1$, let's discuss the possible outcome by cases.

Case 1: $0 \leq \rho < 1$

In this case we always have $(1-\rho^i) < 1$. Therefore we have

$$\begin{aligned}
&\beta^i(1-\rho^i)^n \exp[\alpha_i] \geq \beta^i(1-\rho^i)^{n+1} \exp[\alpha_i] \\
&\qquad \Rightarrow \sum_{i=1}^{\infty} \beta^i \left(1-\rho^i\right)^n \exp[a_i] \geq \sum_{i=1}^{\infty} \beta^i \left(1-\rho^i\right)^{n+1} \exp[a_i] \\
&\qquad \Leftrightarrow \left| \frac{\sum_{i=1}^{\infty} \beta^i \left(1-\rho^i\right)^n \exp[a_i]}{\sum_{i=1}^{\infty} \beta^i \left(1-\rho^i\right)^{n+1} \exp[a_i]} \right| \geq 1
\end{aligned}$$

Using this result we can say

$$R^c = \lim_{n\to\infty} \left| \frac{t_n}{t_{n+1}} \right| = \infty$$

Case 2: $-1 < \rho < 0$

In this case, we have

$$\begin{cases} (1-\rho^i) < 1 & if\ i\ even \\ (1-\rho^i) > 1 & if\ i\ odd \end{cases}$$

Therefore we split the summation of even terms and odd terms by

$$\left| \frac{\sum_{i=1}^{\infty} \beta^i \left(1-\rho^i\right)^n \exp[a_i]}{\sum_{i=1}^{\infty} \beta^i \left(1-\rho^i\right)^{n+1} \exp[a_i]} \right| = \left| \frac{\sum_{j=1}^{\infty} \beta^{2j-1} \left(1-\rho^{2j-1}\right)^n \exp[a_{2j-1}] + \sum_{j=1}^{\infty} \beta^{2j} \left(1-\rho^{2j}\right)^n \exp[a_{2j}]}{\sum_{j=1}^{\infty} \beta^{2j-1} \left(1-\rho^{2j-1}\right)^{n+1} \exp[a_{2j-1}] + \sum_{j=1}^{\infty} \beta^{2j} \left(1-\rho^{2j}\right)^{n+1} \exp[a_{2j}]} \right|$$

Note that for summation of odd terms, the denominator is larger than the numerator, while for summation of even terms, it is the another way around. Hence, to compare the ratio, we first compute the gap between the denominator and numerator for the summation of odd terms as

$$\begin{aligned}
&\sum_{j=1}^{\infty} \left[\beta^{2j-1} \left(1-\rho^{2j-1}\right)^{n+1} \exp[a_{2j-1}] - \beta^{2j-1} \left(1-\rho^{2j-1}\right)^n \exp[a_{2j-1}] \right] \\
&\qquad = \sum_{j=1}^{\infty} \beta^{2j-1} \left(1-\rho^{2j-1}\right)^n \exp[a_{2j-1}] \left(-\rho^{2j-1}\right) \\
&\qquad \Leftrightarrow C - A = E
\end{aligned}$$

and for summation of even terms as

$$\sum_{j=1}^{\infty}\left[\beta^{2j}\left(1-\rho^{2j}\right)^{n}\exp\left[a_{2j}\right]-\beta^{2j}\left(1-\rho^{2j}\right)^{n+1}\exp\left[a_{2j}\right]\right]$$

$$=\sum_{j=1}^{\infty}\beta^{2j}\left(1-\rho^{2j}\right)^{n}\exp\left[a_{2j}\right]\left(\rho^{2j}\right)$$

$$\Leftrightarrow B-D=-F$$

Where we define

$$A=\sum_{j=1}^{\infty}\beta^{2j-1}\left(1-\rho^{2j-1}\right)^{n}\exp\left[a_{2j-1}\right]$$

$$B=\sum_{j=1}^{\infty}\beta^{2j}\left(1-\rho^{2j}\right)^{n}\exp\left[a_{2j}\right]$$

$$C=\sum_{j=1}^{\infty}\beta^{2j-1}\left(1-\rho^{2j-1}\right)^{n+1}\exp\left[a_{2j-1}\right]$$

$$D=\sum_{j=1}^{\infty}\beta^{2j}\left(1-\rho^{2j}\right)^{n+1}\exp\left[a_{2j}\right]$$

$$E=\sum_{j=1}^{\infty}\beta^{2j-1}\left(1-\rho^{2j-1}\right)^{n}\exp\left[a_{2j-1}\right]\left(-\rho^{2j-1}\right)$$

$$F=\sum_{j=1}^{\infty}\beta^{2j}\left(1-\rho^{2j}\right)^{n}\exp\left[a_{2j}\right]\left(-\rho^{2j}\right)$$

Then the ratio can be simplified to

$$\left|\frac{\sum_{i=1}^{\infty}\beta^{i}\left(1-\rho^{i}\right)^{n}\exp\left[a_{i}\right]}{\sum_{i=1}^{\infty}\beta^{i}\left(1-\rho^{i}\right)^{n+1}\exp\left[a_{i}\right]}\right|=\left|\frac{A+B}{C+D}\right|=\left|\frac{A+B}{A+E+B+F}\right|$$

which can be bounded by

$$\left|\frac{A+B}{A+E+B+F}\right|\geq\frac{|A+B|}{|A+B|+|E+F|}$$

on the other hand, we can bound $|E+F|$ by

$$\begin{aligned}
|E+F| &= \left| \sum_{j=1}^{\infty} \beta^{2j-1} \left(1-\rho^{2j-1}\right)^n \exp\left[a_{2j-1}\right] \left(-\rho^{2j-1}\right) + \sum_{j=1}^{\infty} \beta^{2j} \left(1-\rho^{2j}\right)^n \exp\left[a_{2j}\right] \left(-\rho^{2j}\right) \right| \\
&= \left| - \left[\sum_{j=1}^{\infty} \left(\beta^{2j-1} \left(1-\rho^{2j-1}\right)^n \exp\left[a_{2j-1}\right] \left(\rho^{2j-1}\right) \right) + \sum_{j=1}^{\infty} \beta^{2j} \left(1-\rho^{2j}\right)^n \exp\left[a_{2j}\right] \left(\rho^{2j}\right) \right] \right| \\
&= \left| \sum_{i=1}^{\infty} (\rho\beta)^i \left(1-\rho^i\right)^n \exp\left[a_i\right] \right| \\
&\leq \left| \sum_{i=1}^{\infty} \beta^i \left(1-\rho^i\right)^n \exp\left[a_i\right] \right| = |A+B|
\end{aligned}$$

Therefore

$$\left| \frac{A+B}{A+E+B+F} \right| \geq \frac{|A+B|}{|A+B|+|E+F|} \geq \frac{|A+B|}{|A+B|+|A+B|} = \frac{1}{2}$$

back to equation of R^c, we get

$$\begin{aligned}
R^c &= \lim_{n\to\infty} |n+1| \left| \frac{1-\rho}{\theta\rho} \right| \left| \frac{\sum_{i=1}^{\infty} \beta^i \left(1-\rho^i\right)^n \exp\left[a_i\right]}{\sum_{i=1}^{\infty} \beta^i \left(1-\rho^i\right)^{n+1} \exp\left[a_i\right]} \right| \\
&\geq \frac{1}{2} \left| \frac{1-\rho}{\theta\rho} \right| \lim_{n\to\infty} |n+1| = \infty
\end{aligned}$$

Combining these, we see the ROC of the perturbation solution of the Burnside asset pricing model is $(-\infty, \infty) \subseteq \mathbb{R}^1$. □

A.5 Numerical specification of RBC model with Epstein-Zin-Weil utility and adjustment costs

To avoid the convergence issue of the perturbation solution of the system, (1.23) following the notation of Judd et al. (2014) we normalized the value function, consumption, and TFP by their deterministic steady state level. In addition, to solve the model for larger γ, we defined households' resolved deviation of welfare as $\widehat{RDV}_t$. Combining these, the equilibrium

system (1.23) can be equivalently written as

$$\widehat{RDV}_t = \mathbb{E}_t \left[\left(\frac{\hat{Z}_{t+1}}{Z_{dss}} \widehat{DV}_{t+1} \right)^{1-\gamma} \right] \tag{A.4a}$$

$$1 = \mathbb{E}_t \left[M_{t+1} \phi' \left(\frac{\hat{I}_t}{\hat{K}_t} \right) \left(\frac{(\alpha - 1)\hat{Y}_{t+1} + \hat{C}_{t+1}}{\hat{K}_{t+1}} \right) + \frac{\phi\left(\frac{\hat{I}_{t+1}}{\hat{K}_{t+1}}\right) + 1 - \delta}{\phi'\left(\frac{\hat{I}_{t+1}}{\hat{K}_{t+1}}\right)} \right] \tag{A.4b}$$

$$\hat{K}_{t+1} = \frac{\hat{K}_t}{\hat{Z}_{t+1}} \left((1-\delta) + \phi\left(\frac{\hat{I}_t}{\hat{K}_t} \right) \right) \tag{A.4c}$$

$$\hat{Z}_t = \exp\left(\mu + \chi \sigma_z \epsilon_t\right), \quad \epsilon_t \sim \mathcal{N}(0,1) \tag{A.4d}$$

where we define

$$\widehat{DV}_t = \frac{\hat{V}_t}{\hat{V}_{dss}}$$

$$M_{t+1} = \beta \hat{Z}_{t+1}^{-\gamma} \left(\frac{\hat{C}_{t+1}}{\hat{C}_t} \right)^{-\frac{1}{\psi}} \frac{\widehat{DV}_{t+1}^{\frac{1}{\psi}-\gamma}}{\exp\left(\left(\frac{1}{\psi} - \gamma\right)\mu\right) \widehat{RDV}_t^{1-\frac{1}{\theta}}}$$

$$\widehat{DV}_t^{\frac{1-\gamma}{\theta}} = (1-\beta) \left(\frac{\hat{C}_t}{\hat{C}_{dss}} \right)^{\frac{1-\gamma}{\theta}} \left(\frac{\hat{C}_{dss}}{\hat{V}_{dss}} \right)^{\frac{1-\gamma}{\theta}} + \beta \exp\left(\frac{1-\gamma}{\theta} \mu \right) \widehat{RDV}_t^{\frac{1}{\theta}}$$

$$\hat{Y}_t = \hat{K}_t^{\alpha}$$

$$\hat{I}_t = \hat{Y}_t - \hat{C}_t$$

The deterministic steady-states (DSS) are given by

$$\hat{K}_{dss} = \left[\frac{\alpha\beta}{\exp\left(\frac{1}{\psi}\mu\right) - \beta\left(1-\delta\right)}\right]^{\frac{1}{1-\alpha}},$$

$$\hat{Y}_{dss} = \hat{K}_{dss}^{\alpha},$$

$$\hat{I}_{dss} = \left(\exp\left(\mu\right) - 1 + \delta\right)\hat{K}_{dss},$$

$$\hat{Z}_{dss} = \exp\left(\mu\right),$$

$$\hat{C}_{dss} = \hat{Y}_{dss} - \hat{I}_{dss}, \hat{V}_{dss} = \left[\frac{\left(1-\beta\right)\hat{C}_{dss}^{1-\frac{1}{\psi}}}{\left(1-\beta\hat{Z}_{ss}^{1-\frac{1}{\psi}}\right)}\right]^{\frac{\theta}{1-\gamma}},$$

$$\widehat{DV}_{dss} = 1,$$

$$\widehat{RDV}_{dss} = \left(\frac{\left[1-\left(1-\beta\right)\left(\frac{\hat{C}_{dss}}{\hat{V}_{dss}}\right)^{\frac{1-\gamma}{\theta}}\right]}{\beta\exp\left(\frac{1-\gamma}{\theta}\mu\right)}\right)^{\theta}.$$

Appendix B

Chapter 2

B.1 Ten stylized facts on declining business dynamism summarized in Akcigit

Fact 1. Market concentration has risen.

Fact 2. Average markups have increased.

Fact 3. The profit share of GDP has increased.

Fact 4. The labor share of output has gone down.

Fact 5. The rise in market concentration and the fall in labor share are positively associated.

Fact 6. Productivity dispersion of firms has risen. Similarly, the labor productivity gap between frontier and laggard firms has widened.

Fact 7. Firm entry rate has declined.

Fact 8. The share of young firms in economic activity has declined.

Fact. 9. Job reallocation has slowed down.

Fact 10. The dispersion of firm growth has decreased.

Appendix C

Chapter 3

C.1 Sentiment analysis on tweet event study

Company	Date	Near Earnings Date	Response to announcement	Tweet	Sentiment
News Corp	May 1, 2012	Yes	Yes	@rupertmurdoch is a superb businessman and a world class CEO. He has built a tremendous empire and is certainly "fit" to run his corporation	Positive
Procter & Gamble Co	May 11, 2012	Yes	Yes	Procter and Gamble is relocating its beauty headquarters from Cincinnati to Asia–what are we doing?	Negative
JPMorgan Chase & Co.	May 16, 2012	No	Yes	Glad to see that Jamie Dimon passed yesterday's shareholder vote. The JP Morgan stock holders understand that a good CEO is worth keeping.	Positive
Facebook	May 17, 2012	No	No	@Facebook's Mark Zuckerberg is clearly a brilliant guy. My advice? Get a pre-nup!	Positive

Goldman Sachs Group	June 12, 2012	No	Yes	Welcome to the new reality. Goldman Sachs just based their new Asia Pacific chairman not in Tokyo, but Beijing.	Negative
Apple Inc	July 2, 2012	No	Yes	WRONG: A China court ordered @apple to pay $60M to a Chinese company that registered iPad before@apple	Neutral
JPMorgan Chase & Co.	July 18, 2012	No	Yes	What recovery? JP Morgan has readjusted Q2 growth down from 1.7% to 1.4% and Q3 to 1.5% with 2012 on a whole at 1.7%	Negative
Papa John's Int'l Inc.	Aug 9, 2012	No	Yes	@PapaJohns CEO John Schnatte hastold shareholders that ObamaCare will force him to raise pizza prices.	Neutral
⋮	⋮	⋮	⋮	⋮	⋮
Apple Inc	Apr 3, 2020	No	Yes	RT @WhiteHouse: Huge thanks to @Apple! Together with the White House, @CDCgov & @fema, Apple launched a COVID19 screening tool that guides	Positive
Bank of America	Apr 3, 2020	No	Yes	Great job being done by @BankofAmerica and many community banks throughout thecountry. Small businesses appreciate your work!	Positive
Bank of America	Apr 4, 2020	No	Yes	I will immediately ask Congress for more money to support small businesses under the #PPPloan if the allocated money runs out. So far, way ahead of schedule. @BankofAmerica & community banks are rocking! @SBAgov @USTreasuryI will immediately ask Congress for more money to support small businesses under the @ppploan if the allocated money runs out. So far, way ahead of schedule. @BankofAmerica & community banks are rocking! @SBAgov @USTreasury	Positive

Due to space limitation, the table above just provide a overview of the data set of sentiment analysis. For fully detailed data set, please check the link SentiData.